THE JOURNAL
OF
CHEMICAL PHYSICS

VOLUME 10 MAY, 1942 NUMBER 5

The Decomposition of Methane in Glow Discharge at Liquid-Air Temperature

LOURDU M. YEDDANAPALLI
Physical Chemistry Laboratory, Louvain University, Belgium, and Frick Chemical Laboratory, Princeton University, Princeton, New Jersey

(Received February 13, 1942)

The decomposition of methane in the glow discharge at liquid-air temperature has been investigated under different experimental conditions. Contrary to the earlier conclusion of Brewer and Kueck that the reaction products are only hydrogen and ethylene, they are invariably found to be hydrogen, a polymer of composition $(CH_2)_n$, and ethane, ethylene, and acetylene, the last three resulting presumably from the mutual interaction of the primary active species CH_4^+, CH_3^+, CH_2^+, CH^+ formed from methane. In the absence of hydrogen, ethane predominates; in its presence, ethylene and acetylene proportions increase due, it is suggested, to the dehydrogenating action of atomic hydrogen. In the negative glow, the rate of methane decomposition is directly proportional to the current, and the electronic efficiency, i.e., the number of methane molecules decomposed per electronic charge, is ~10 both for alternating and direct current. In the positive column, the rate is directly proportional to current only if pressure and field strength are constant; with constant current, the rate increases with pressure and field strength but in a manner which does not lend itself at present to a quantitative expression; the electronic efficiency is ~0.2 for alternating and ~0.6 for direct current. The results lead to the conclusion that a 60-cycle alternating current discharge approximates closely to that with direct current. These may be explained by considerations of the electrical energies involved. No marked difference in reaction rate or products is observed by substituting iron for aluminum electrodes, or by variation in current density. A certain chemical activity might be attributed to the Faraday dark space.

INTRODUCTION

THE original purpose of this research was to convert the heavy carbon methane, $C^{13}H_4$, that was being separated from ordinary methane in the physics laboratory of the University of Louvain[1] into the more reactive unsaturated hydrocarbons from which a series of halogen and deuterium compounds could be prepared for physico-chemical investigation. The published scientific literature on the decomposition of methane in electrical discharges of various kinds was concerned mainly with the production of the industrially important acetylene, though this was always found mixed with other unsaturated and saturated hydrocarbons.[2] The only investigation that seemed suited to the purpose was the work of Brewer and Kueck[3] who found that methane in glow discharge at liquid-air temperature was quantitatively converted into ethylene according to the reaction:

$$2CH_4 \rightarrow C_2H_4 + 2H_2.$$

Since the experimental evidence presented by these authors was meager and mostly of a physical character, it was thought advisable to

[1] Capron, Delfosse, de Hemptinne, and Taylor, J. Chem. Phys. **6**, 656 (1938).

[2] See the extensive bibliography: (a) Ellis, *Chemistry of Petroleum Derivatives* (Reinhold, New York, 1934); (b) Glockler and Lind, *Electrochemistry of Gases and Other Dielectrics* (Wiley, New York, 1939); (c) more recently, Thomas, Egloff, and Morrell, Chem. Rev. **28** (1), 1–70 (1941).

[3] Brewer and Kueck, J. Phys. Chem. **35**, 1293 (1931).

study the reaction in greater detail with ordinary methane, before adopting the method for our particular purpose.

Preliminary experiments indicated, however, that, although no appreciable pressure change occurred in the gas during discharge, the condensate did not cause, on removal of the liquid air, the theoretical 50 percent increase in the total gas pressure, as would be the case if the condensate consisted solely of ethylene, but only 30 percent to 35 percent. Moreover, part of the methane decomposed appeared in the form of a thin yellowish brown deposit on the electrode and the surrounding glass walls. Finally, the condensable gases were found, by chemical analysis, to consist not only of ethylene but also of acetylene and ethane. This cast serious doubt on the validity of the apparently simple conclusion of Brewer and Kueck and necessitated a thorough investigation of the whole reaction. A serious handicap in following the progress of the reaction during discharge was the absence of any pressure variation of the reaction system; attempts at following the reaction by thermal conductivity measurements of the gases were not successful; also, the hydrogen liberated during the reaction appeared to influence the nature of the reaction products.

The experimental technique was therefore modified so as to oxidize the hydrogen over heated copper oxide; the reaction could then be followed by measuring with McLeod gauge the change in pressure of methane. In this manner several series of experiments were conducted in the University of Louvain, with different electrode distances and pressures under varying electrical conditions, and with different electrode size and material, all only with alternating current. These results were, in part, repeated in Princeton and completed by measurements with direct current. It is, in the main, the work done at Princeton that is presented in this paper, except in one or two cases in which the Louvain data are adduced with due mention.

The zones of the glow discharge which we have selected for investigation are the negative glow (N.G.), by which is actually meant the region between the cathode and the anode end of the negative glow, and the positive column (P.C.) extending beyond the N.G. up to the anode. The

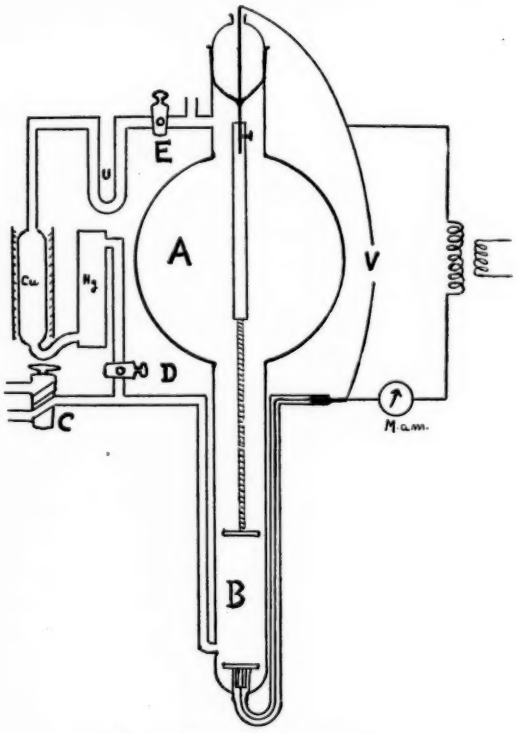

FIG. 1. Diagram of apparatus.

reason for this choice is that the physics of these two zones[4] is known fairly well and they seem to be by far the most important in effecting chemical change both from theoretical considerations,[2b] and from the available experimental material.[5] In the present research attempt has been made not only to evaluate the relative chemical activities of the N.G. and the P.C. but also to elucidate the mechanism of methane decomposition in the glow discharge, both in the absence and presence of hydrogen.

APPARATUS

The apparatus shown in Fig. 1 consists of a Pyrex glass bulb *A* of 2.5-liter capacity provided

[4] (a) J. J. and G. P. Thomson, *Conduction of Electricity Through Gases*, Volume 2 (Cambridge University Press, 1933); (b) K. Darrow, *Electrical Phenomena in Gases* (Williams and Wilkins Company, Baltimore, 1932); (c) L. B. Loeb, *Fundamental Processes of Electrical Discharge in Gases* (John Wiley and Sons, Inc., New York, 1939); (d) An excellent review article by M. J. Druyvesteyn and F. M. Penning, "Mechanism of electrical discharge in gases at low pressure," Rev. Mod. Phys. **12**, 87 (1940).

[5] (a) Kirkby, Phil. Mag. **13**, 289 (1907); Proc. Roy. Soc. **A85**, 151 (1911); (b) Guntherschultze, Zeits. f. Physik **21**, 50 (1924); (c) Linder, Phys. Rev. (2) **36**, 1375 (1930); **38**, 679 (1931); (d) Brewer and co-workers, a series of papers in J. Phys. Chem. between 1929–31; (e) Linder and Davis, J. Phys. Chem. **35**, 3649 (1931) etc.

with a ground glass neck and a close fitting hollow ground glass stopper in the center of which has been sealed a heavy tungsten wire. The bulb terminates below in a tube *B*, 35 cm in length and 4.2 cm in internal diameter, in which the discharge takes place. The lower electrode is slid by means of a short metallic stalk into a thick cylindrical brass socket, 2 cm in length, the lower end of which is soldered to a copper wire. This is then led out of the discharge tube through a bent glass tubing and is finally sealed into the latter with the help of a tungsten wire, the extremity of which serves as a terminal for electrical contact. The upper electrode is riveted to a long threaded brass wire capable of being screwed up and down the central groove of a stout brass rod which is fastened by a screw to the tungsten lead in the hollow glass stopper: in this manner the electrode distance could be adjusted to any desired length. Also, the electrodes could, after an experiment, be removed from the apparatus and cleaned for subsequent use.

At the lower end of the discharge tube *B* is sealed a side tube connecting the whole discharge vessel, on the one hand, with the vacuum pumps and the analysis apparatus by means of a three-way stopcock *C*, and on the other, with the circulatory system through the large bore stopcock *D*. A similar stopcock *E* leads the circulatory system back to the discharge vessel.

The circulatory system consists of a mercury diffusion pump Hg, a copper oxide tube Cu surrounded by an electrically heated furnace and a U-tube cooled in liquid air. The mixture of non-condensable gases, methane and hydrogen, is drawn by the mercury pump from the discharge zone into the copper oxide tube in which hydrogen is oxidized, the water vapor formed being retained by the liquid-air cooled U-tube so that the gas pumped back into the discharge vessel through the stopcock *E* is almost pure methane. Thus, a steady stream of pure methane can be maintained in the discharge zone.

The connections to methane and hydrogen reservoirs, and to McLeod gauge are indicated in the figure. The electrical setup is clear from the diagram. The use of a capacity has not been resorted to, for the reason that the presence of capacity gave a very unsteady and erratic discharge, and the combination of it with a surge resistance resulted in a discharge similar to the one obtained without their use.

Methane from a cylinder was purified by repeated fractionation with liquid air. Hydrogen employed in certain experiments was of electrolytic source.

Ordinary granulated copper oxide was subjected *in situ* to successive reductions at a higher, and oxidations at a lower temperature so as to render it active at about 265°C, at which it was used to oxidize the hydrogen liberated from methane during the discharge.

The electrodes employed in most of the experiments were aluminum disks. In certain cases, iron electrodes were employed.

The source of the alternating current was a 5000-volt transformer run on a primary of 110 volts of 60 cycles. The direct current was drawn from a high power transformer of 25,000 volts provided with kynetrons and worked with 110 volts. The current was measured by milliammeter and the voltage by a system of high resistances and micromilliammeters.

The micro-analysis apparatus, essentially of the type designed by Blacet and co-workers,[6] was used with a few minor modifications for the analysis of the reaction products.

EXPERIMENTAL PROCEDURE

The relative positions of the N.G. and the P.C. of the glow discharge were determined from a study of their electrical properties. The potential across the region between the cathode and the farther end of the N.G. is known to be just equal to the cathode drop characteristic of the electrode material and the gas, and independent of the current and the gas pressure within the limits obtaining in the ordinary glow discharge. By measuring, therefore, the voltage for different electrode distances with varying currents and gas pressures, an electrode distance of 0.7 to 0.8 cm was found to satisfy the above electrical criterion of the N.G. both in the case of alternating and direct current (cf. Fig. 2). Beyond this distance from the cathode, the P.C. including the

[6] Blacet and Leighton, Ind. Eng. Chem. Anal. Ed. **3**, 266 (1931); Blacet, MacDonald, and Leighton, *ibid.* **5**, 273 (1933).

Faraday dark space, F.D.S., was assumed to make its appearance.

With the knowledge of the relative position of the N.G. and the P.C., the electrodes could be so placed in the discharge tube as to confine between them the former zone alone or both. Before the experiment, the discharge vessel and the circulatory system were completely evacuated, the copper oxide being electrically heated in the meantime and maintained at 265°C. The mercury diffusion pump Hg was then brought into working condition. By means of the stopcocks, the circulatory system was cut off from the discharge vessel. Methane was admitted into the latter to a known pressure; after surrounding the discharge tube *B* with liquid air to a constant depth, the gas pressure was again measured, and finally the gas was expanded into the circulatory system with the U-tube in liquid air, the pressure being once more recorded. This procedure was adopted for each experiment in order to make the necessary pressure and temperature corrections in the final calculations.

In an actual experiment, a definite current of the order of milliamperes was passed through the discharge tube for a known period of time; the decrease in the methane pressure was measured a few minutes after cutting off the discharge to make sure that all the hydrogen liberated during the reaction was completely oxidized by copper oxide. This experimental precaution was found necessary, for, although most of the hydrogen was removed by copper oxide within the discharge time, there remained, due to hold-up in the circulation system, a small fraction of a mm of hydrogen which sometimes took two or three minutes for complete oxidation.

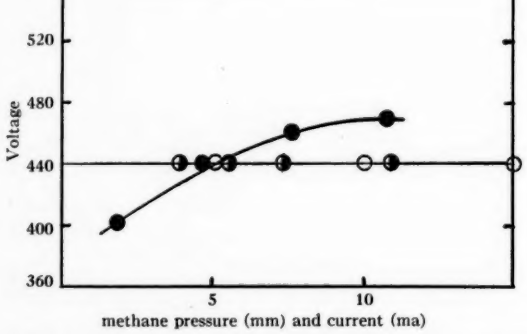

FIG. 2. Relation between current or methane pressure and voltage at different electrode distances. Voltage *versus* pressure at 0.95 cm (filled circles) and at 0.75 cm (half-filled). Voltage *versus* current (empty circles) at the latter distance.

With the discharge tube *B* still in liquid air, the unchanged methane was carefully pumped off, the circulatory system shut off from the reaction vessel and the pressure of the condensed gases, allowed to expand into the reaction vessel by removal of liquid air, was measured. They were then recondensed in a small trap in liquid air by means of the stopcock *C*, next drawn into a Töpler pump and finally transferred into small gas holders over mercury for analysis.

From a known volume of the mixture of gases, acetylene was determined by absorption on an alkaline cuprous chloride bead. From the remaining volume, ethylene was absorbed by a porous glass bead moistened with fuming sulfuric acid, followed by a potassium hydroxide bead to remove the acid fumes; the remaining gas was assumed to be ethane.

Concerning the time of discharge, it is to be remarked that, in a given experiment, several runs of discharge were made. Depending on the strength of the current employed, the discharge was passed for a few minutes at a time, the corresponding decrease in methane pressure for each run being noted until the reaction was near completion. This procedure had the double advantage of bringing out the effect of pressure on the reaction rate under otherwise identical experimental conditions, and of yielding, with different currents and electrode distances, comparable data of rate of reaction over approximately equal ranges of pressure.

After each experiment the electrodes were cleared of the polymer deposit and polished in a uniform manner before subsequent use; also, the polymer on the glass wall, close to the discharge zone, was removed before the succeeding experiment.

EXPERIMENTAL RESULTS

The chemical activity of the N.G. and the P.C. is expressed, according to the method indicated by Kirkby[5a] and adopted by Emeleus and Lunt[7] *et al.* in terms of the electron efficiency η referred, not to the reaction product which

[7] Emeleus and Lunt, Trans. Faraday Soc. **32**, 1504 (1936).

TABLE I.

Expt.	Elect. dist. cm	Av. CH_4 press. mm	Discharge time min.	ΔP/min.	η_N	I in ma	V volts	Cond. gases %	C_2H_2 %	C_2H_4 %	C_2H_6 %
				Negative glow with alternating current							
2	0.75	9.57	5	0.554	10.4	15	425	66.2			
		6.80	5	0.554	10.4	15	425				
		4.03	5	0.554	10.4	15	415				
				Negative glow with direct current							
11	0.70	9.54	7.5	0.36	10.2	10	440	64.8	[37.	13.5	49.5]
		6.84	7.5	0.36	10.2	10	440		[29.3	32.	38.7]
		3.26	11.25	0.4	11.2	10	440				
12	0.70	8.95	5	0.686	9.7	20	440	62.8	[34.	13.2	52.8]
		5.53	5	0.681	9.6	20	440		[26.3	33.0	40.7]
		2.11	5	0.686	9.7	20	440				
13	0.70	8.68	4	1.08	10.2	30	440	60.4	[37.8	13.4	48.8]
		3.88	5	1.05	9.9	30	400*		[28.5	34.8	36.7]
19	0.3–0.35	9.51	7.6	0.31	8.8	10	420	60.4	[40.5	17.8	41.7]
		7.29	7.5	0.29	8.1	10	420				
		4.40	11.25	0.32	8.9	10	420		[30.6	38.2	31.2]
			7.5	0.31	8.8	10	420				

N.B. The lower of the 2 series of the bracketed analytical data represent the values corrected for ethylene polymerization.

consists, in our case, of a mixture of gases but to the reactant molecules of methane. η is, therefore, defined as the number of methane molecules decomposed per electron charge carried by the current and is given by the expression:

$$\eta = V \cdot n \cdot \Delta P / e \cdot I \cdot \Delta t$$

where V is the volume in cc of the reaction vessel and accessories, n the number of molecules in 1 cc of gas at 1 mm Hg at 0°C; e the number of electronic charges conveyed by 1 milliampere per second, and I the current in ma measured in the external circuit; ΔP and Δt are the pressure decrease of methane in mm and the corresponding time of discharge in sec., respectively. Since $n = 3.55 \times 10^{16}$, $e = 6.3 \times 10^{15}$ and $V = 3000$,

$$\eta = (3000 \times 3.55 \times 10^{16})/6.3 \times 10^{15}) \cdot \Delta P / I \times \Delta t.$$

n was not corrected for room temperature since the correction is a small constant factor affecting all the results uniformly. The electron efficiency of the N.G. is denoted by η_N; the total efficiency due to the N.G. and the P.C. by η_{NP} and that of the P.C. which is defined as the number of methane molecules decomposed per electron per cm length of the P.C. is given by

$$\eta_P = (\eta_{NP} - \eta_N)/l$$

where l is the length of the P.C. alone and equal to the total electrode distance minus the length of the N.G.

The Negative Glow

Table I represents the data on the activity of the N.G. for both alternating and direct currents for an electrode distance of 0.7–0.75 cm; the results of several runs in a given experiment are included, as they bring out the effect of pressure on the rate and the voltage. It may be well to note that the percentage yield of condensable gases is in reference to the methane decomposed; the composition of these gases is given in the last three columns.

Several conclusions may directly be drawn from the results. As would be expected for the N.G., the voltage is independent of the current and the gas pressure. The close similarity between the electron efficiencies for the alternating and the direct current, demonstrates clearly that the 60-cycle alternating current discharge approximates closely to that of the direct current. The rate of decomposition of methane is directly proportional to the current and independent of the pressure. The electron efficiency is ~10, a value which can be shown to be equivalent to that found by Brewer and Kueck who obtained 3.1 supposedly ethylene molecules synthesized per electron. Now, as we

TABLE II.

Expt.	Elect. dist. cm	Av. CH_4 press. mm	Discharge time min.	ΔP/min.	η_{NP}	I in ma	V volts	Cond. gases %	C_2H_2 %	C_2H_4 %	C_2H_6 %	η_P	X	X/P
						A. Positive column with alternating current.								
3	0.95	9.43	5	0.59	11.0	15	448–440	72.				3.0	95	10.
		6.66	5	0.52	9.8	15	440–436							
		3.94	5	0.57	10.7	15	422*							
4	1.5	9.6	5	0.59	11.2	15	475–465	48.5				1.0	60	6.3
		6.64	5	0.59	11.1	15	440–420							
		3.78	5	0.55	10.4	15	420–400							
5	3.5	9.41	5	0.61	11.5	15	666–642	66.0	[33.8	18.6	47.6]	0.4	83	8.8
		6.34	5	0.61	11.5	15	573–549		[26.9	35.3	37.8]	0.4	50	7.9
		3.56	4	0.62	11.6	15	493							
6	10.	9.27	5	0.69	12.9	15	1250–1116	73.	[30.3	19.7	50.]	0.3	82	8.9
		6.01	5	0.61	11.5	15	990–900		[25.6	32.1	42.3]	0.1	56	9.2
		2.94	5	0.61	11.5	15	823–738					0.1	38	13.
7	15.	9.40	5	0.71	13.3	15	2040–1296	75.	[30.5	15.5	54.]	0.2	87	9.3
		5.99	5	0.66	12.4	15	1164–1056		[26.2	27.6	46.2]	0.1	48	8.0
		2.82	5	0.61	11.5	15	960–684					0.1	28	9.9
						B. Positive column with direct current.								
21	0.95	9.21	7.5	0.41	11.6	10	470–60	66.8	[34.5	16.2	49.3]	5.8	100	10.8
		6.18	7.5	0.40	11.2	10	460		[27.6	32.9	39.5]			
		3.23	7.5	0.39	11.0	10	440–420							
49	2.	8.15	5	0.98	13.7	20	520–480					2.8	46	5.6
		3.70	5	0.81	11.3	20	440							
22	3.5	8.52	7.5	0.53	15.0	10	740–620	66.4	[35.8	13.1	51.1]	1.7	86	10.
		4.81	7.5	0.49	14.0	10	620–480		[28.6	30.6	40.8]	1.4	40	8.3
		1.80	7.5	0.40	11.2	10	440							
46	3.5	7.92	5	1.03	14.5	20	620–540	71.6	[31.9	18.3	49.8]	1.6	51	6.4
		3.10	5	0.90	12.6	20	510–436*		[26.6	31.8	41.6]			
14	7.0	8.57	7.5	0.55	15.4	10	980–860	69.0	[38.3	14.4	47.3]	0.8	76	8.9
		4.60	7.5	0.51	14.5	10	800–600		[31.3	30.0	38.7]	0.7	41	9.0
		1.62	5.0	0.42	11.8	10	600–460					0.3	14	8.8
47	7.0	7.80	5	1.08	15.2	20	830–670	71.4	[32.0	17.0	51.0]	0.8	49	6.3
		3.31	5	0.92	12.9	20	590–470*		[26.6	30.8	42.6]	0.4	14	4.3
17	10.0	7.90	5	1.12	15.7	20	960–800	73.4	[29.8	14.0	56.2]	0.6	47	6.0
		2.86	5	0.90	12.7	20	720–560		[25.2	27.3	47.5]	0.3	22	7.5
18	10.0	7.91	6.5	0.85	15.9	15	1080–880	69.0	[32.0	13.2	54.8]	0.6	58	7.3
		2.92	6.5	0.69	13.0	15	720–560		[26.2	29.0	44.8]	0.3	22	7.3
48	15.0	7.61	5	1.19	16.8	20	1230–870	67.0	[28.4	13.3	58.3]	0.5	43	5.6
		2.67	5	0.98	13.8	20	770–630		[22.6	30.6	46.8]	0.3	18	6.7

* Abnormal.
N.B. The lower of the 2 series of the bracketed analytical data represent the values corrected for the ethylene polymerization.

shall see later in the section on reaction products, only about two thirds of the methane decomposed is recovered in the form of condensable gases; the rest is lost as a polymer deposit. Consequently, if the computation is made on the basis that all the methane decomposed appears as ethylene, as was assumed by Brewer and Kueck, the number of ethylene molecules per electron will be 4.7 which will correspond to 9.4 methane molecules decomposed, a value quite similar to the 10 we have obtained.

Experiment 19, listed at the end of the table, was conducted at an electrode distance of 0.3 to 0.35 cm, almost half the normal length of the N.G. The electron efficiency drops, however, by only one unit as compared with that of the full

N.G. and all the characteristics of the latter are equally verified.

The Positive Column

The results of the series of experiments with electrode distance gradually extending beyond the N.G. up to 15 cm are presented in Table II, *A* and *B*; *A* for alternating, and *B* for direct current. The notation of Table II is similar to that of Table I; the significance of the few added columns is clear from the indicated notation, if it is remembered that η_{NP} represents the total electronic efficiency of the N.G. and P.C. from which η_P due to P.C. alone is evaluated according to the method already described. X is the field strength in volts per cm length of the P.C. and P is the average working pressure in mm of the given run.

It is of importance to note the approximate nature of the η_P values, as they are obtained by subtracting a relatively large quantity η_N from only a little larger quantity η_{NP} and dividing the difference by a small, in the case of short electrode distance, and by a relatively large number, in the case of longer electrode distances. Consequently, precise quantitative relations between the electron efficiency and the electrical factors cannot be derived, though definite conclusions of a qualitative nature can certainly be deduced.

The average value of η_P in the case of direct current as evaluated from experiments 47, 17, and 48 is $\sim$0.6, and in the case of alternating current, from experiments 6 and 7, it is $\sim$0.2. In either case it is a much smaller quantity than the value of 10 for η_N as is to be expected from the relatively low density of space charge of the P.C., as compared with the N.G., as is known from the physics of the glow discharge.[4] The rate of methane decomposition and the electron efficiency η_P decrease with decreasing average working pressure and decreasing field strengths, as is evident from the different runs of a given experiment.

TABLE III. Influence of current density.

Expt.	Elect. surface in cm sq.	Init. CH_4 press. mm	ΔP/min.	Cond. gas %	C_2H_2	C_2H_4	C_2H_6
38	12.6	5.44	0.42	61.7	37.4	16.1	46.5
44	4.9	5.39	0.46	66.0	30.6	16.3	53.1
45	1.8	5.39	0.42	63.0	28.5	18.0	53.5

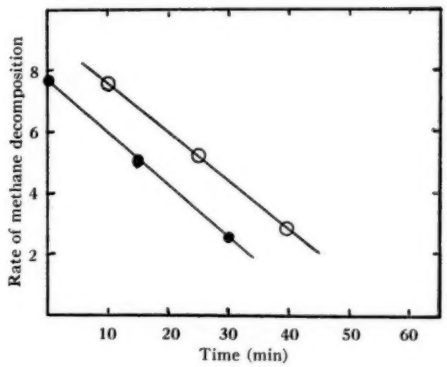

FIG. 3. Influence of electrode material on the rate of methane decomposition. Aluminum (filled-circles), iron (empty).

From Table IIB, it is obvious that, for a given electrode distance and an approximately same average pressure, the rate of decomposition is directly proportional to the current strength.

There is no evidence of an absence or of a marked lowering of activity in the region between the N.G. and the P.C. On the contrary, the indication is that at about a distance of 2 cm from the cathode, well within the region where the F.D.S. would be expected to lie, the calculated electron efficiency is decidedly greater than at 3.5 cm and beyond. This is true for both direct and alternating currents. It would seem that the F.D.S. is not totally devoid of chemical activity; this will be more fully examined in the discussion section.

Current Density

The size of the electrodes was varied from 12.6 to 4.9 and then to 1.8 sq. cm, and the current and all other experimental conditions were kept constant. From the results recorded in Table III current density seems to have little influence on the reaction rate or the nature of the reaction products. This may be due to the fact that with smaller size electrodes, the glow spreads out radially beyond the boundaries of the electrode surface toward the surrounding walls of the discharge tube.

Electrode Material

The effect of electrode material on the methane decomposition under otherwise identical experi-

TABLE IVA. Effect of hydrogen on methane decomposition.

Expt.	Init. CH_4 mm	H_2 add. mm	H_2 ave. mm	H_2 from reaction	CH_4 decomposed	Cond. gas %	C_2H_2 %	C_2H_4 %	C_2H_6 %	H_2 of cond. gases	H_2 in polymer	C in polymer
38	5.44	—	—	4.19	4.19	61.7	37.4	16.1	46.5	2.72	1.47	1.59
40	5.4	—	1.54	3.07	2.95	48.5	48.0	14.4	37.6	1.36	1.47	1.52
37	5.29	1.72	2.97	2.50	2.38	50.4	48.3	15.0	36.7	1.13	1.13	1.18
36	5.39	3.39	4.37	1.96	1.84	53.4	47.9	14.4	37.7	0.93	0.79	0.85
35	5.41	5.17	6.03	1.71	1.56	54.0	56.4	8.5	35.1	0.73	0.68	0.71

mental conditions is shown by the curves in Fig. 3, with the velocity plotted against time. The curves for aluminum and iron disk electrodes of 1.2-cm diameter are practically parallel, indicating the rate to be the same in either case. Also, given the similarity in the yield of condensable gases and their composition, the discharge with aluminum electrodes is practically identical with that for iron electrodes.

Composition and Reaction Products

The products of the decomposition of methane by the discharge were the non-condensable hydrogen equal in amount to the methane decomposed and the condensable gases retained on the walls of the discharge tube *B* cooled in liquid air. The analyses of these condensable gases are presented in Tables I, II, and III. In these experiments, the hydrogen was removed during the discharge by oxidation over heated copper oxide. The percentage yield of condensable gases was calculated in reference to the methane decomposed. In general, the yields are approximately 65 percent, since the rest of the methane is lost as a polymer, of composition $(CH_2)_n$ as will later be shown, deposited partly on the glass walls and partly on the surface of the cathode in the case of direct current, and on both electrode surfaces in the case of alternating current.

The reaction products in each case, under different experimental conditions, consist of a mixture of ethane, ethylene, and acetylene. The ethylene content appears to be much smaller than that of the other two components, because part of it has gone to form, as can reasonably be assumed, the polymer deposit of composition $(CH_2)_n$. Recalculation, on this assumption, of the analytical data leads, in every case, to percentage values of composition which decrease regularly down the series ethane, ethylene, and acetylene, as can be verified from the second lines of the bracketed analytical data in Tables I and II, which give the analytical results when so recalculated.

TABLE IVB. Analytical data corrected for ethylene polymerization

Expt.	C_2H_2 %	C_2H_4 %	C_2H_6 %
38	30.4	31.7	37.9
40	31.5	43.8	24.7
37	32.4	43.0	24.6
36	33.4	40.4	26.2
35	39.5	35.9	24.4

Influence of Hydrogen

In Table IV are recorded the results of experiments designed to bring out the effect of hydrogen on the nature of the reaction products of methane decomposition and to supply further evidence for the reaction mechanism. All these experiments were conducted in the negative glow with identical conditions of initial methane pressure ~5.3 mm, of current 10 ma, and of discharge time 10 min. In experiment 38, the hydrogen liberated during the discharge was prevented from taking part in the reaction by being oxidized over heated copper oxide. In all the other experiments, the hydrogen coming from the decomposition of methane and that added initially in some cases was allowed to take part in the reaction by keeping the copper oxide at room temperature. It may be noted that, when copper oxide was not active during the discharge, there was only a very slight variation in the initial and final gas pressure, which has been taken into account in the calculations.

Column 1 of Table IV gives the serial number of the experiment; column 2, the initial pressure of methane in mm; column 3, the pressure of added hydrogen; column 4, the average pressure

of hydrogen taking part in the reaction, obtained by adding to the initial hydrogen the mean, namely, half of the hydrogen coming from the methane decomposed; column 5, the total amount of hydrogen just mentioned as coming from the decomposed methane; column 6, the methane decomposed; column 7, the percentage yield of condensable gas in terms of methane decomposed; columns 8, 9, 10, the percentages, respectively, of acetylene, ethylene, and ethane in the condensable gases; column 11, the hydrogen content of these latter gases; column 12, the hydrogen to be accounted for in the polymer deposit, obtained by subtracting from the total hydrogen of the methane transformed the amount in column 5 and that in column 11; column 13 gives the amount of carbon in the polymer deposit, evaluated from the yield of condensable gases.

The effect of hydrogen on the decomposition rate of methane is shown in Fig. 4 plotted against $P_{H_2}/(P_{H_2}+P_{CH_4})$ as abscissae. The straight line relationship indicates that the rate is inversely proportional to the partial pressure of hydrogen. In other words the rate of decomposition is simply proportional to the partial pressure of methane, the reason being that the electrical energy available for methane decomposition is in direct proportion to its partial pressure.

Before examining the influence of hydrogen on the reaction products, it is well first to determine the nature of the polymer deposit. The data of the last two columns of Table IVA lead to the conclusion that, since the ratio of carbon

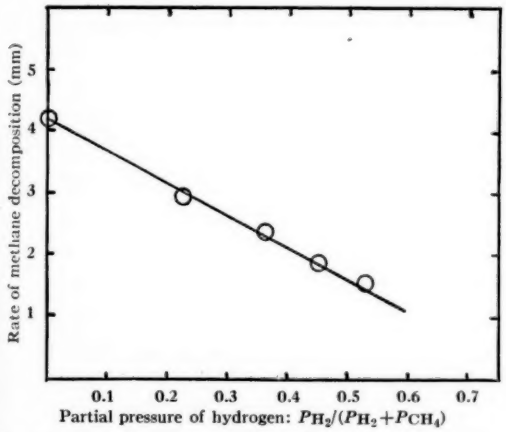

FIG. 4. Effect of hydrogen on the rate of methane decomposition in the negative glow.

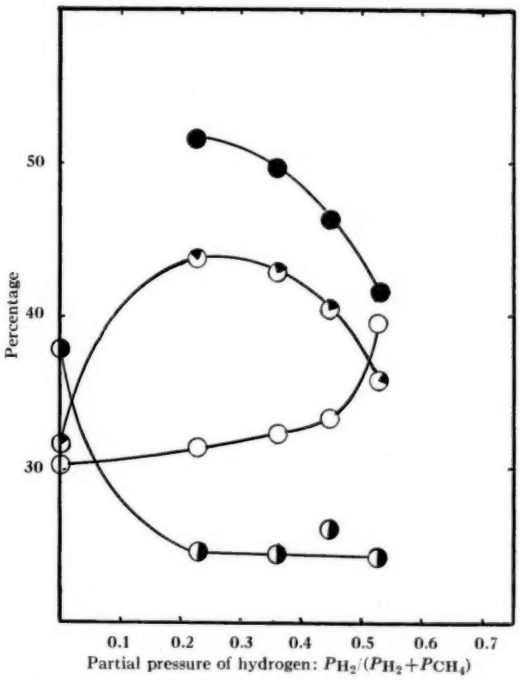

FIG. 5. Influence of hydrogen on the percentage composition of products of methane decomposition in the negative glow. Polymer (filled circles), ethane (half-filled), ethylene (quarter-filled), and acetylene (empty circles).

to hydrogen in the polymer is 1 : 2, its composition must be $(CH_2)_n$. Further, as the hydrogen content is slightly less than the theoretical amount corresponding to the above composition, the polymer may safely be assumed to be an unsaturated ethylene polymer, resulting from the ethylene which would otherwise have been recovered as condensable gas. It is for this reason that the actual percentage of ethylene in the condensable gases is found to be low, as can be seen from the analytical results in Table IVA.

On adding, however, to the ethylene actually recovered the amount lost as polymer and recalculating the analytical data, we obtain the corrected percentage compositions of the gases as recorded in Table IVB. Figure 5 gives the plot of the percentage of each component against the partial pressure of hydrogen. From the nature of the curves it is evident that the percentage of ethane drops rather sharply at a certain critical pressure of hydrogen and then remains constant with further increases in hydrogen. Ethylene, too, shows, at the same

critical hydrogen pressure, a marked increase and then diminishes gradually with increasing amount of hydrogen. On the other hand, acetylene content increases steadily with increase in hydrogen pressure. The general conclusion seems obvious that hydrogen in glow discharge being in atomic form dehydrogenates ethane or the radical fragments from which it results to give ethylene, and reacts further with the latter or its component fragments to yield acetylene.

Atomic hydrogen induces, at the same time, polymerization of ethylene which is seen first to increase with hydrogen concentration, as is shown by the polymerization curve in Fig. 5, and then decrease as the acetylene yield begins rapidly to rise.

DISCUSSION OF RESULTS

Kinetics of Reaction in the N.G. and the P.C.

A careful examination of the results on the rate of decomposition of methane in the N.G. and the P.C. reveals certain general relationships between reaction rate and pressure, voltage and current, which must be considered in any theoretical explanation of the kinetics of the glow discharge.

In the N.G. the rate of decomposition of methane is directly proportional to the current and independent of pressure, the voltage being an invariable factor equal to the cathode drop of the electrode material and the gas.

In the P.C. also, the rate is directly proportional to current provided that the average working pressure of methane is approximately the same, as is evident from the first runs of experiments 14 and 47, also of experiments 22 and 46, and from the first and second runs of experiments 17 and 18. In the absence of the latter condition, however, the linear dependence does not hold, as can be seen from the second runs of experiments 14 and 47, and of 22 and 46. An interesting confirmatory evidence is presented by the following consideration. The average working pressure of methane of the second and third runs of experiment 14 is 3.1 mm closely similar to the 3.3 mm pressure of the second run of experiment 47. A similar averaging gives for the reaction rates of the two experiments 0.467 and 0.915, the ratio of which is 1 to 2 in agreement with a current of 10 ma in the one and 20 ma in the other case, as would be demanded by the linear dependence of rate on current.

With constant current, the rate decreases with decreasing methane pressure, as is clear from all the experiments on the P.C.

Similar general relationships hold for the dependence of rate on voltage, though only in a qualitative manner. A quantitative evaluation of this does not seem feasible, as the voltage is a complex function of both pressure and current, which is not known clearly. Moreover, the measurements of voltage across the P.C. could not be made accurately, for, during a run, the voltage decreased continually with the decrease in pressure of methane due to reaction, so that the initial and final voltages of a run differed rather widely, especially in the case of long electrode distances as can be seen from Table IIA–B. The averages of such widely differing values lose therefore much of their quantitative significance. Nevertheless, in a qualitative manner at least, the general dependence of rate on voltage is quite similar to that existing between rate and pressure.

As a quantitative expression of the above characteristics of the kinetics of the glow discharge, the simple electrochemical equivalence law proposed by Brewer and co-workers[5d] is definitely inadequate; at best it holds only for the N.G. but breaks down completely in the case of the P.C. Linder's[8] interpretation of his results on the dissociation of water vapor in glow discharge from energy relationships involving current, voltage and pressure, deals only with the N.G. A more satisfactory explanation seems to be the one suggested by Kirkby's work[5a] on water synthesis in the P.C. and later taken up and developed by Emeleus and Lunt[7] from statistical consideration of the electron collision processes occurring in glow discharge. These authors conclude that, in the case of N.G. with normal cathode drop, the rate of reaction must be proportional to the current, whereas in the P.C. it will be also proportional to the current provided the field strength is constant. These conclusions seem to be substantiated to some extent

[8] Linder, Phys. Rev. **38**, 679 (1931).

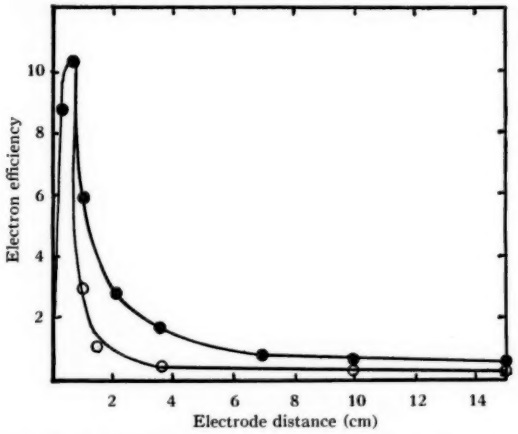

FIG. 6. Electron efficiency, i.e., number of methane molecules decomposed per electron charge, *versus* electrode distance. Filled circles for direct and empty for alternating current.

by our results. But no explanation is offered for what happens when the field strength changes. The complete elucidation, based on energetic considerations, of the kinetics in the P.C. would require a better knowledge, than is at present available, of the quantiative relationships between voltage, pressure and current in the P.C.

The relative chemical activities (cf. Fig. 6) expressed in electron efficiencies of the N.G. and the P.C. are consistent with the general physics of the two zones, for the density of space charge in the former zone is known to be much higher than in the latter. This is also substantiated by the experimental fact that, on removing the liquid air from the discharge tube after reaction, a thick deposit of condensable gases is clearly visible on the glass walls enclosing the N.G., which fades off rapidly towards the anode. The large value of ten molecules of methane per electron in the N.G. is not surprising when one remembers that every electron leaving the cathode surface is known[8,9] to give rise to 50 to 100 by successive electron collisions with the gas molecules, of which only a certain fraction may be effective in activating sufficiently the gas molecules.

Regarding the F.D.S., as already remarked in the section on experimental results, the absence of any sudden drop of reaction rate or electron efficiency, in the zone between the N.G. and the P.C., may be accounted for either by the fact that the anode end of the N.G. is not sharp, but rather diffuse, or, better, by the activity due to the presence in the F.D.S. of active atoms and molecules as has been postulated by some workers.[10]

[9] Compton and Morse, Phys. Rev. (2) **30**, 305 (1928).

Reaction Mechanism

The primary active species resulting from the electron collisions with methane molecules in the glow discharge are the series of ions CH_4^+, CH_3^+, CH_2^+, CH^+, and C^+ and the corresponding series of neutral radicals. The presence of the former is demonstrated by the abundant mass-spectroscopic data on methane.[11] In fact, as long as the energy of the colliding electron is well above that corresponding to the ionization potential of methane, there is no reason why the latter cannot be successively stripped of its hydrogen atoms to give the above series of ionized radicals. In our case, the cathode drop is 440 volts of which only one sixth, i.e., 73 volts, is generally recognized as effective in accelerating the electrons in the negative zone, so that the electron can collide with an average energy of 73 ev, a value greater than is needed for the process $CH_4 \rightarrow CH^+ + 3H$ for which the energy required, evaluated from mass-spectroscopic measurements,[2b] is 23.3 ev. The positively charged radicals will easily become neutralized by the sourrounding electrons. Further, given the variety of collisions occurring in glow discharge between electrons of different speeds and the gas molecules,[2b] the possibility of neutral radicals CH_3, CH_2, etc., resulting from such collisions is easily understood. Bimolecular combinations of these radicals in the gas phase and on the walls of the discharge vessel will then lead to the formation of ethane, ethylene, and acetylene, in agreement with the analytical data of the reaction products obtained by the decomposition of methane in glow discharge.

Moreover, according to this explanation, the relative proportions of ethane, ethylene, and acetylene in the reaction products would be expected to be in decreasing order of magnitude, for the difficulty of stripping methane of hydro-

[10] M. J. Druyvesteyn, Physica **11**, 9 (1931); Emeleus and Duffendack, Phys. Rev. **44**, 322 (1933).

[11] Eisenhut and Conrad, Zeits. f. Elektrochem. **36**, 654 (1930); Hipple and Bleakney, Phys. Rev. **67**, 802 (A) (1935); Smith, *ibid.* (2) **51**, 263 (1937).

gen atoms increases down the series CH_3^+, CH_2^+, CH^+. This is clearly substantiated by the corrected analytical data for the reaction products in Tables I and II. The amounts of ethylene and acetylene would, in fact, have been smaller but for some dehydrogenating action, as will presently be seen, of hydrogen before it was removed completely from the reaction zone.

There is, consequently, neither theoretical nor experimental evidence for the conclusion that the only product of the decomposition of methane in glow discharge is ethylene. On the basis of this erroneous statement various authors[2c] have been misled trying to interpret the complex hydrocarbon mixtures generally obtained from the decomposition of methane in electrical discharge as the result of the secondary reactions of hydrogen and methane with the supposed primary product, ethylene.

Influence of Hydrogen

The effect of hydrogen on the decomposition of methane appears to be twofold, as can be judged from the results in Table III. In the first place, it acts as a diluent taking up a part of the electrical energy proportional to its partial pressure so that the rate of decomposition of methane decreases in direct proportion to the partial pressure of hydrogen. Secondly, it acts as a dehydrogenating agent increasing the percentage of the unsaturated hydrocarbons in the reaction products.

This dehydrogenating effect of hydrogen is to be ascribed to the high concentration of the atomic hydrogen into which molecular hydrogen is converted by the absorption of electrical energy in the glow discharge. Bonhoeffer and Harteck[12] found that atomic hydrogen acted both as hydrogenating and dehydrogenating agent for hydrocarbons. A more specific conclusion was drawn by Jungers and Taylor[13] from their work on the mercury photosensitized reaction of hydrogen and ethylene that atomic hydrogen whose concentration is necessarily low in such conditions caused predominantly the hydrogenation to take place. More recently, Taylor[14] suggested that, in general, atomic hydrogen in low concentrations behaves as a hydrogenating and in high concentrations as a dehydrogenating agent for ethylene. With low hydrogen atom concentrations, such as are obtained in the mercury photosensitized reaction, the system of hydrogen and ethylene behaves as though the atomic hydrogen concentration was negligible due to rapid interaction of atoms and ethylene to form ethyl radicals which yield butane. On the other hand, with high atom concentration, such as is obtained in the glow discharge tube, the hydrocarbon molecule is both stripped of hydrogen and is ruptured to give CH fragments. We find, in our experiments, that the system behaves like systems of high atomic hydrogen concentrations and that in place of ethane, ethylene and acetylene are increasingly important reaction products with increase of hydrogen (cf. Fig. 5). This may arise both by interaction of the atomic hydrogen with the molecules of hydrocarbon and with the radical fragments from which the molecules are ultimately formed.

ACKNOWLEDGMENTS

This research, started in the University of Louvain and interrupted owing to the sudden invasion of Belgium, was completed at Princeton. The author wishes, therefore, to express his thanks to Professor J. C. Jungers at whose suggestion and in whose laboratory the research was undertaken, and also to Professors J. Verhulst and M. de Hemptinne for the supply of a variety of experimental material. To Dr. R. W. Lunt of London University he is indebted for much useful information and discussion on electrical discharge reactions. He deeply appreciates the favor granted him by the authorities of Princeton University to complete the research in the Frick Chemical Laboratory, and thanks Professor H. S. Taylor for many helpful suggestions and for his continued interest.

[12] Bonhoeffer and Harteck, Zeits. f. physik. Chemie **139**, 75 (1928); Zeits. f. Elektrochemie, **34**, 652 (1928).

[13] Jungers and Taylor, J. Chem. Phys. **6**, 325 (1938).

[14] Taylor, Ann. N. Y. Acad. Sci. **41**, 202 (1941).

Zinc Photosensitized Reactions of Ethylene

H. Habeeb, D. J. LeRoy, and E. W. R. Steacie
Physical Chemistry Laboratory, McGill University, Montreal, Canada

and

National Research Laboratories, Ottawa, Canada

(Received March 16, 1942)

An investigation has been made of the polymerization of ethylene photosensitized by zinc, both resonance lines, 2139A and 3076A, being used. With λ3076 the rate of the reaction is very small, and it is concluded that this is probably due to inefficient quenching. With λ2139 a rapid polymerization occurs. The products of the reaction are propylene, butene, and small amounts of higher hydrocarbons. Acetylene formation is negligible. The rate of polymerization increases rapidly with increasing ethylene pressure. While there is some doubt about the mechanism, the most plausible suggestion seems to be that the initial step is

$$Zn(4^1P_1)+C_2H_4=ZnH+C_2H_3,$$

and that this is followed by an atom and free radical sensitized polymerization of ethylene.

INTRODUCTION

In a number of recent papers we have described investigations of cadmium photosensitized reactions.[1-4] The present paper is concerned with photosensitization by zinc, both resonance lines 2139A and 3076A being employed. The excitation energies of the states involved are 133.4 and 92.5 kcal. for Zn (4^1P_1) and Zn(4^3P_1), respectively, as compared with 124.4 and 87.3 kcal. for Cd(5^1P_1) and Cd(5^3P_1), and 112.2 for Hg(6^3P_1). In addition the heat of formation of ZnH is considerably higher than that of the other hydrides (23.1 kcal. for ZnH, 15.5 kcal. for CdH, and 8.5 kcal. for HgH). As a result processes of the type

$$Zn^*+HX=ZnH+X$$

will be possible provided that the strength of the H−X bond is lower than 156.5 kcal. for Zn$(^1P_1)$ and 115.6 kcal. for Zn $(^3P_1)$.

Much previous work has been done by other methods on the photochemistry of ethylene. In the case of the mercury photosensitized reaction, at least at low temperatures, it seems to be definitely established that the primary step is:[5]

$$Hg(6^3P_1)+C_2H_4=Hg(6^1S_0)+C_2H_4^* \quad (1)$$

followed by

$$C_2H_4^*+C_2H_4=2C_2H_4, \quad (2)$$

$$C_2H_4^* \quad =C_2H_2+H_2. \quad (3)$$

With cadmium $(^1P_1)$ atoms the evidence favors[1] a primary step which is at least in part

$$Cd(5^1P_1)+C_2H_4=CdH+C_2H_3, \quad (4)$$

although the possibility of a reaction analogous to (1) is not excluded. The reaction photosensitized by Cd(5^3P_1) atoms has a relatively low quantum yield, and hence not much definite information exists, but it appears probable that what reaction does occur involves a direct polymerization, by a mechanism such as (1) and (2) together with

$$C_2H_4^*+C_2H_4=C_4H_8. \quad (5)$$

This is not unexpected since the excitation energy of Cd(5^3P_1) atoms is probably too small to permit reactions analogous to either (3) or (4) to occur. (See (3) for a discussion of this point.)

EXPERIMENTAL

The Light Source

The zinc resonance lamp was of the high voltage, low pressure type, with neon as a carrier. It was similar in all essential details to

[1] E. W. R. Steacie and D. J. LeRoy, J. Chem. Phys. **10**, 22 (1942).
[2] E. W. R. Steacie, D. J. LeRoy, and R. Potvin, J. Chem. Phys. **9**, 306 (1941).
[3] E. W. R. Steacie, Ann. N. Y. Acad. Sci. **41**, 187 (1941).
[4] E. W. R. Steacie and R. Potvin, Can. J. Research **B18**, 47 (1940); J. Chem. Phys. **7**, 782 (1939).
[5] D. J. LeRoy and E. W. R. Steacie, J. Chem. Phys. **9**, 829 (1941).

the cadmium lamps which we have previously described,[1] except that it was necessary to operate at a somewhat higher temperature on account of the lower vapor pressure of zinc.

A set of spectrograms of the lamp is shown in Fig. 1. These were taken with an Eastman 40 U.V. sensitized plate. Actually λ2139 is more intense than λ3076, but this is masked by the falling off in plate sensitivity in the short ultraviolet. It is evident that the lamps are a highly efficient source of the two zinc resonance lines. The cadmium resonance lines, 3261A and 2288A, and the mercury line at 2537A appear also, but are much too weak to have any appreciable effect.

The behavior of the lamps was by no means as satisfactory as that of cadmium lamps. We have had several of the latter with lives of over 1000 hours. With zinc the average life was quite short, less than 50 hours. Failure occurred either at the lead-in wires or at the graded seal, usually the former. It appears probable from an examination of broken lamps that the zinc vapor destroys the "coating" on the electrodes. This decreases their effective surface, and the electrodes run continually hotter until failure occurs by cracking at the lead-in wire. This suggests that the life might be much longer at lower currents, and in the last lamp used a current of 40 ma was used instead of 120 as formerly. This appeared to give much more satisfactory operation. It appears likely that where high intensities are not so essential very much longer life could be obtained by operating at 15 ma.

As a result of difficulties with the lamps it was not possible to obtain as reproducible results as would have been desired, although the output of any given lamp was satisfactorily constant up to very shortly before its failure. Also the short life of the lamps made it impracticable to carry out a succession of long runs for the purpose of accumulating products. This was especially true in the case of runs with λ3076 since the reaction in this case was very slow.

In experiments with the long-wave resonance line at 3076A a filter consisting of an 18-inch length of Corex D tubing with a wall thickness of approximately 2.3 mm was slipped over the entire lamp. This completely removed the lower resonance line. Since, as will appear subsequently, the effect of λ3076 was slight compared

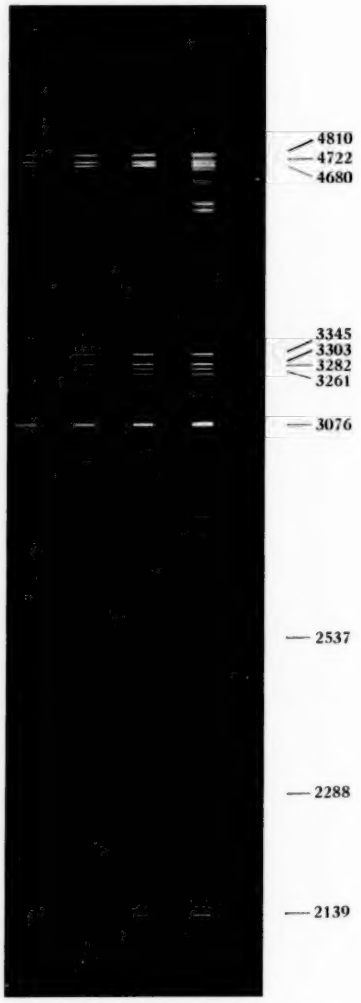

FIG. 1. Spectrogram of zinc lamp. Successive exposures 4, 12, 60, 300 sec.

with that of λ2139, the experiments with λ2139 were done with the full radiation from the lamp. The output of the lamp was determined only by a very rough geometrical estimate, and indications were that the amount of λ2139 entering the reaction system was of the order of 10^{-7} Einstein per sec.

Information on the quenching of zinc resonance radiation is entirely lacking. Failing this, some rough "absorption" measurements were made. Owing to difficulties associated with imprisonment of radiation and pressure broadening such measurements are difficult to interpret. They do, however, give a qualitative indication of the fraction of the incident energy which is

absorbed by the sensitizer and transferred to the reactant. The results obtained indicated a very strong absorption of λ2139 in the presence of ethylene, over 95 percent of the incident radiation being absorbed in the presence of 100 mm of ethylene, with a zinc vapor pressure corresponding to 310°C, and a light path of approximately 4 cm. The absorption of λ3076 by ethylene was comparatively slight, not over 4.5 percent being absorbed in the presence of 200 mm of ethylene. There thus appears to be a very strong decrease in the quenching efficiency of ethylene for $^3P_1$ atoms as we go down the series Hg, Cd, Zn, in spite of the increasing lifetime of the excited state. Absorption of λ3076 in the presence of hydrogen was also surprisingly small, and was not very much greater than that of ethylene under comparable conditions. This is unexpected in view of the fact that Bender[6] obtained resonance excitation of the ZnH bands when a mixture of zinc vapor and hydrogen was illuminated with the radiation from a zinc-hydrogen lamp containing λ3076. λ2139, however, did not give rise to ZnH bands under these conditions. Further discussion of this point will be deferred since it is planned to investigate the quenching in the near future.

The Reaction System

The reaction system was the same as that previously employed.[1] The lamp was contained in a cylindrical furnace which was heated electrically. It was surrounded by an annular fused quartz reaction vessel, 10-cm length, 8-cm diameter, with a 4-cm diameter hole through the middle. The reaction vessel was connected to a saturator containing zinc turnings, which was contained in a separate furnace. (In some preliminary runs a 1 : 1 zinc-tin alloy was used in the saturator. This is liquid at the temperatures employed. However, the turnings proved to be more efficient and convenient.)

For circulating runs a pump passed the gas through the saturator and then through the reaction vessel and traps to condense out higher boiling products. For static runs the tubing between the saturator and the reaction vessel was sealed off, and zinc turnings were placed directly in the reaction vessel. The total apparent volume of the circulating system at 310°C was about 2 liters, and that of the static system was 558 cc. In the circulating runs the rate of circulation was about 500 cc per minute.

[6] P. Bender, Phys. Rev. **36**, 1543 (1930).

Analysis

The gaseous products of the reaction were analysed by distillation in a small-capacity Podbielniak type still. Acetylene was determined as previously described.[5]

Materials

The zinc used was British Chemical Standard grade, and contained 99.95 percent zinc, and about 0.01 percent cadmium.

Ethylene was obtained in cylinders from the Ohio Chemical and Manufacturing Company. It was purified by bulb to bulb distillation, and the resulting gas contained no impurities detectable with the analytical methods used.

Hydrogen was taken from commercial cylinders and was purified by passage over platinized asbestos at 600°C, and through a liquid-air trap.

RESULTS

Most of the work reported here was done with the lower resonance line, 2139A. On account of the small quenching of the 3076A line it was not possible to make a very thorough investigation with it, and the results obtained may be regarded as only semiquantitative.

(A) Photosensitization by $^1P_1$ Atoms (λ2139)

The results of a typical series of static runs at 310°C without the Corex D filter are given in Fig. 2. As will be shown later, the effect produced by λ3076 is negligible compared with that due to λ2139, and hence the results given in Fig. 2 are, within the experimental error, due to λ2139 only. It will be seen that there are no indications of an initial pressure rise, as occurs with the mercury photosensitized reaction, and that the pressure decrease in the early stages of the reaction is a linear function of the time.

As shown by Fig. 2, and better by Fig. 3, the initial rate of pressure decrease increases rapidly with increasing pressure. In view of the efficient absorption of λ2139 in the presence of ethylene this effect cannot be ascribed to increased quenching at the higher pressures, and must be

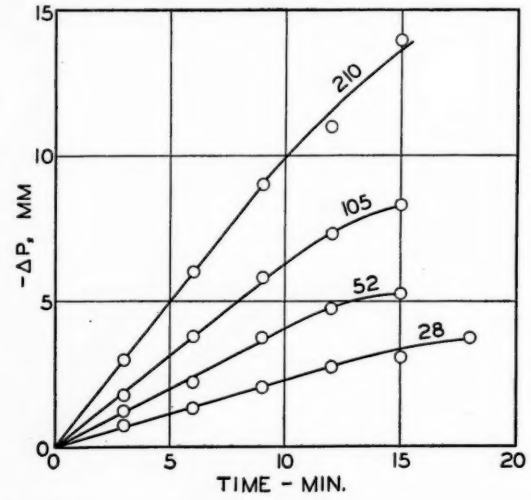

FIG. 2. Experiments with λ2139. Static system at 310°C. Ethylene pressures in mm, as indicated on the curves.

due to an increase in the rate of the polymerization itself.

Blank runs indicated no appreciable thermal reaction under the conditions used, and possible catalytic effects due to zinc or traces of zinc oxide are thus ruled out.

The Products of the Reaction
Acetylene

In view of the importance of acetylene as a product in the mercury photosensitized reaction, analyses for it were carried out in a number of cases by the method previously used.[5] The results indicated that acetylene formation is of even less importance here than in the case of the cadmium photosensitized reaction. Even in static runs which were carried to a pressure drop of 50 percent, analyses showed amounts of acetylene of the order of 0.1 percent or less. Acetylene formation is thus negligible compared with polymerization.

Hydrogen

A very small amount of non-condensable gas was observed. This was very roughly equal in amount to the acetylene formed, and it was assumed to be hydrogen.

Condensable Products

A number of circulating runs at 310°C were made for the purpose of collecting condensable

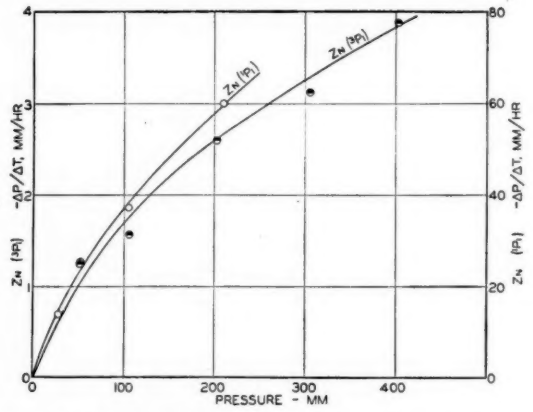

FIG. 3. Initial rates of reaction. Static system. Temperature 310°C for runs with λ2139, 320°C for runs with λ3076.

products for analysis. The gases in the reaction system were circulated during these runs through a trap which was maintained at −125° to −130°C. In these experiments the initial ethylene pressure was approximately 200 mm, but the pressure during the run with the trap cold was less than this owing to the condensation of ethylene in the trap, and the actual pressure was thus the vapor pressure of ethylene at the trap temperature, *viz.*, about 120 mm.

In a typical run the pressure decrease, after warming the trap to room temperature, was 78 mm in 7.2 hours. The products were analyzed by low temperature fractional distillation with the result shown below:

	cc at N.T.P.
H_2+CH_4	trace
C_3H_6	87
C_4H_8	31
Higher	~30

The distillation curve for this run is shown in Fig. 4. The production of propylene as a major product was established beyond doubt. The distillation curve was absolutely flat over a range of 72 cc, and this fraction was again distilled separately with the same result. It was then analyzed by combustion by the method of Marion and Ledingham.[7] The carbon-hydrogen ratio agreed with that of an olefin to within less than 1 percent. The molecular weight was found to be 39.2 as compared with 42 for propylene and 28 for ethylene. There seems to be no doubt, therefore, that the gas is mainly propylene.

[7] L. Marion and A. E. Ledingham, Ind. Eng. Chem. Anal. Ed. **13**, 260 (1941).

A number of other circulating runs gave results in agreement with the above, in every case propylene being a major product, together with butenes and small amounts of higher hydrocarbons.

Several blank runs were made in which ethylene was circulated in the apparatus with the lamp off for periods up to 24 hours. In all of these there was a negligible pressure change and no indication of either propylene or non-condensable gas.

(B) Photosensitization by $^3P_1$ Atoms (λ3076)

The results of a series of static runs at 320°C with λ3076 are shown in Fig. 5, and the initial rates, together with those for λ2139, are given in Fig. 3. The rates for the two resonance lines in Fig. 3 are not directly comparable since the two series of experiments were made with different lamps.

A series of runs at 200-mm pressure with the same lamp indicated that the relative rates of pressure decrease for λ2139 and λ3076, allowing for the decrease in intensity of λ3076 due to the transmission of the filter, were in the ratio of 8/1. An estimate of the relative intensities of the two lines was made using a sodium photo-tube of known wave-length sensitivity and various combinations of chlorine and Corex D filters of known transmission. This indicated that λ2139 was approximately twice as intense as λ3076. These measurements are somewhat uncertain since corrections must be made for other lines near those in question. However, photographic estimates indicated that the total intensity of 3261A, 3282A, 3303A, and 3345A was less than 10 percent that of 3076A, and that all other lines in the short ultraviolet were less than 0.5 percent of the intensity of λ2139. The ratio of the rates with λ2139 and λ3076 for equal intensities is thus approximately 4/1, or for equal numbers of quanta approximately 6/1. In view of the small absorption of λ3076 by ethylene, and the very high absorption of λ2139, the entire difference in rates could be accounted for on the basis of poor quenching of λ3076 by ethylene. In any case, it is apparent that the quantum yield for the $Zn(^3P_1)$ sensitized reaction is much higher than that for the $Cd(^3P_1)$ reaction.

(C) Ethylene-Hydrogen Mixtures

A number of static runs were made with ethylene-hydrogen mixtures at 320°C. With λ3076 the relative rates of pressure decrease with 20 cm C_2H_4 alone and with 20 cm of C_2H_4+20 cm of H_2 were in the ratio of 1 : 21. There is thus a much faster reaction in the presence of hydrogen, and at least part of the increase can be attributed to more efficient quenching by hydrogen. However, it seems certain that the whole effect cannot be explained in this way, and that the quantum yield for the reaction with ethylene-hydrogen mixtures must be considerably higher than that for ethylene alone. In view of Bender's work, the mechanism for the reaction in the presence of hydrogen is obviously

$$Zn(^3P_1)+H_2 \rightarrow ZnH+H,$$
$$H+C_2H_4 \rightarrow C_2H_5,$$

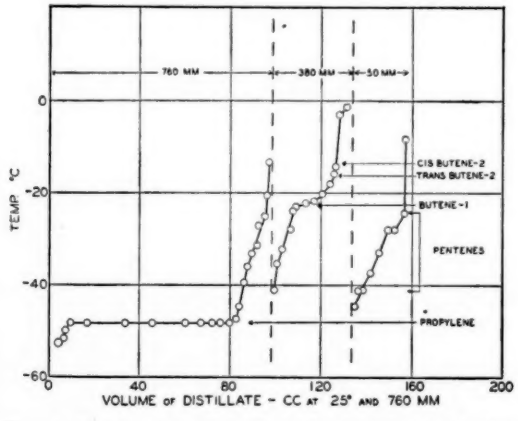

FIG. 4. Distillation curve of products from circulating run with λ2139.

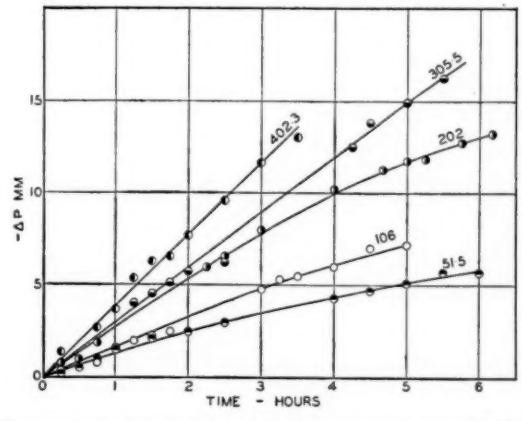

FIG. 5. Experiments with λ3076. Static system at 320°C. Ethylene pressures in mm, as indicated on the curves.

followed by a free radical sensitized polymerization of ethylene.

No acetylene could be detected in the products of these runs. A distillation analysis of the products of a typical circulating run is given below:

Temperature	320°C
Time	$10\frac{1}{4}$ hours.
Initial pressures (trap at room temp.)	$H_2 = 126.5$ mm
	$C_2H_4 = 126.0$ mm
	Total = 252.5 mm.
Final pressure (trap at room temp.)	= 215 mm.

Products, cc at N.T.P.	Initial	Final
H_2	407	376
C_2H_4	405	169
C_3H_6	—	54
"C_4"	—	14
Higher	—	14
CH_4	—	≤4

The products are thus very similar to those found with λ2139 and ethylene alone.

A few runs were also made with ethylene-hydrogen mixtures using the full radiation from the lamp. From Bender's work it appears that the quenching of the 2139A line by hydrogen is very small. Since the indications from our absorption measurements are that 3076A is only slightly quenched by ethylene while 2139A is very strongly quenched, it follows that in an ethylene-hydrogen mixture illuminated with both resonance lines the hydrogen should quench λ3076 and the ethylene λ2139. Hence the rate would be expected to be approximately the sum of the rates for an ethylene-hydrogen mixture illuminated with λ3076 and for ethylene alone illuminated with the full radiation of the lamp.

The relative rates obtained in a typical series of runs are given below in arbitrary units.

Line	Reactant	Relative Rate
3076	C_2H_4	0.048
3076+2139	C_2H_4	0.28
3076	$C_2H_4+H_2$	1.00
3076+2139	$C_2H_4+H_2$	1.20

It will be seen that the sum of the rates in lines 2 and 3 is 1.28, as compared with 1.20 for line 4.

DISCUSSION

(A) $Zn(4^1P_1)+C_2H_4$

In a general way the reaction resembles that with $Cd(5^1P_1)$ atoms. The main difference in the results with zinc is the fact that propylene is a major product of the reaction. Since, in the circulating system, the trap would quite efficiently remove butenes and all products of higher molecular weight, it appears that propylene cannot arise by secondary reactions of the stable products. It can, of course, arise by secondary reactions of short-lived substances. The main possibilities for the mechanism of its formation appear to be the following:

(a) $Zn(4^1P_1)+C_2H_4=Zn(4^1S_0)+2CH_2$

$CH_2+C_2H_4=C_3H_6$

(b) $Zn(4^1P_1)+C_2H_4=ZnCH_2+CH_2$

$ZnCH_2 = Zn(4^1S_0)+CH_2$

$CH_2+C_2H_4=C_3H_6$

(c) $Zn(4^1P_1)+C_2H_4=ZnH+C_2H_3$

or $= Zn(4^1S_0)+H+C_2H_3$

$ZnH = Zn(4^1S_0)+H$

$H+C_2H_4=C_2H_5,$

followed by the building up of larger alkyl radicals by successive additions of ethylene, and their ultimate breakdown by

$$R = R^1+C_3H_6.$$

The main difficulty with (a) is the energy requirement. The excitation energy of $Zn(4^1P_1)$ is 133.4 kcal. While there is considerable doubt about the strength of the C=C bond in ethylene, it appears unlikely that it is less than 145 kcal. and it may be somewhat higher than this. There is, however, the possibility that one or both of the methylenes should be formed as a molecule and not a radical, as has been suggested in other cases.[8] It appears probable that the change

$$>CH_2=CH_2$$

is exothermic to the extent of about 37 kcal.,[9] and the over-all process (a) would thus become energetically possible.

As far as (b) is concerned, there appears to be no information about the existence of compounds such as $ZnCH_2$. If such a compound exists with a heat of formation of 10–20 kcal. then (b) would be energetically possible. Such a process

[8] R. G. W. Norrish, H. G. Crone, and O. D. Saltmarsh, J. Chem. Soc. **1933**, 1533; J. E. Lennard-Jones, Trans. Faraday Soc. **30**, 70 (1934); R. G. W. Norrish, *ibid.* **35**, 191 (1939).

[9] W. Heitler and G. Herzberg, Zeits. f. Physik **53**, 52 (1929).

might occur with a high efficiency since the energy balance would be relatively exact. (The non-occurrence of the corresponding process[6]

$$Zn(4^1P_1)+H_2=ZnH+H$$

is probably to be ascribed to the large energy discrepancy, approximately 45 kcal. being available in excess of the energy required.)

It seems probable that the real explanation is (c). The most significant evidence in this connection is the comparison of the products of the reaction of ethylene photosensitized by λ2139 with those of ethylene-hydrogen mixtures photosensitized by λ3076. It will be seen that the products are very similar, and that propylene is a major product in the latter case as well. Now there is no question that there is insufficient energy to break the C=C bond in the case of λ3076. Further, in the case of λ3076 the reaction is very much faster with $C_2H_4-H_2$ mixtures than it is with ethylene alone. Hence it must be assumed that the primary step is almost exclusively

$$Zn(4^3P_1)+H_2=ZnH+H.$$

Propylene must therefore ultimately arise from reactions initiated by hydrogen atoms. It therefore seems reasonable to assume that it arises in a similar manner in the case of λ2139 with ethylene alone, i.e., by mechanism (c).

The only difficulty with this mechanism is the fact that propylene is not formed in appreciable amounts in the reaction photosensitized by $Cd(5^1P_1)$ atoms,[1] where the evidence points to a primary step analogous to (c). However, it has been pointed out that the results on the cadmium photosensitized reaction are also explainable in terms of a primary step involving the formation of an excited molecule.

The fact that the rate of polymerization increases with increasing ethylene pressure is in line with other investigations in which polymerization of ethylene proceeds by a free radical mechanism. Examples of this behavior are the cadmium photosensitized reaction,[1] the acetone photosensitized reaction,[10,11] the reaction photosensitized by aldehydes,[11] and the reaction induced by the thermal decomposition of azomethane.[12] It is significant that in the case of the mercury photosensitized reaction at room temperature, where free radicals are not involved, at least in the early stages,[5] the initial rate of the reaction *decreases* with increasing ethylene pressure.

(B) $Zn(4^3P_1)+C_2H_4$

In view of the semiquantitative nature of the results, and the absence of information about the products, speculation about the mechanism of the reaction is hardly justified. It may, however, be pointed out that there is ample energy available for the reaction

$$Zn(4^3P_1)+C_2H_4=ZnH+C_2H_3.$$

The low reaction rate is apparently due to inefficient quenching of λ3076 by ethylene, and further discussion will be deferred until information on quenching is available.

(C) $Zn(4^3P_1)+C_2H_4+H_2$

As pointed out above, there is little doubt that the primary process in this case is

$$Zn(4^3P_1)+H_2=ZnH+H,$$

and that this is followed by a hydrogen atom sensitized polymerization of ethylene, i.e.,

$$\begin{aligned} H+C_2H_4&=C_2H_5\\ C_2H_4+C_2H_5&=C_4H_9\\ C_4H_9&=CH_3+C_3H_6, \text{ etc.}\end{aligned}$$

The authors wish to express their indebtedness to Professor C. A. Winkler for his advice and assistance, to Mr. A. Van Winckel for assistance in carrying out the experiments, and to Mr. A. E. Ledingham for making the micro-analyses. One of them (H.H.) is indebted to the National Research Council of Canada for a Studentship, during the tenure of which part of this work was performed.

[10] H. S. Taylor and J. C. Jungers, Trans. Faraday Soc. **33**, 1353 (1937).

[11] C. J. Danby and C. N. Hinshelwood, Proc. Roy. Soc. **A179**, 169 (1941).

[12] O. K. Rice and D. V. Sickman, J. Am. Chem. Soc. **57**, 1384 (1935).

Energy Relations of the Surface of Solids

I. Surface Energy of the Diamond

WILLIAM D. HARKINS
George Herbert Jones Chemistry Laboratory, University of Chicago, and the Universal Oil Products Company, Chicago, Illinois

(Received February 12, 1942)

From the known structure of the diamond the total surface energy of the crystal has been calculated in terms of the energy of the carbon-carbon bond, and is found to be: $1.50\times10^{-9}E_B$ erg cm^{-2} for the 111 face, and $2.10\times10^{-9}E_B$ erg cm^{-2} for the 100 face, where E_B is the energy in ergs per bond. If the bond energy is assumed to be 90 kcal. mole^{-1} the values become 5650 erg cm^{-2} for the 111 face, and 9820 erg cm^{-2} for the 100 face. The corresponding free surface energies are found to be: 111 face at 25°=5400 erg cm^{-2} 100 face at 25°=9400 erg cm^{-2}. One uncertain feature in the calculation is that involved in the calculation of the decrease in energy caused by the long range binding of the valence bonds in the surfaces. In the 111 face the bonds are 2.517A apart, and are perpendicular to the surface. Thus the bond directions are parallel, while inside the diamond the carbon-carbon distance is only 1.54A, and the bonds meet head on. While in the 111 face there is only one bond per carbon atom, in the 100 face there are two bonds per atom. In the 111 face there are 1.825×10^{15} bonds per sq. cm^{-2}, with an area of 5.48A^2 each, while in the 100 face the corresponding values are 3.158×10^{15} bonds per cm^2 and 3.167A^2 per bond. It is concluded that in the 111 face the interaction energy of the type described above is less than one percent and is negligible. Even in the 100 face the interaction should be small. No account was taken of any adjustment of the energy of the unsevered bonds in the surface region. This should cause a greater decrease of energy than the long range binding of the severed bonds. Thus the values of the surface energy calculated in this paper should be considered as maximum values.

I. INTRODUCTION AND ELEMENTARY THEORY OF SURFACE ENERGY

EXTREMELY little is known concerning the magnitude of the surface energy of solids and there are no values for those solids which have high surface energies. From this point of view it is important to obtain a knowledge of at least one solid of this class. Presumably the diamond has one of the highest, and probably the highest, of the surface energies of all the known solids, and, partly for this reason, this solid has been chosen as the subject of investigation.

Since either the free or total surface energy of a liquid or solid is equal to approximately half the respective energy of cohesion involved in pulling the material apart to form two plane surfaces, the calculation of the surface energy and of the cohesion involve the same theory. If a solid is split in a plane which gives two unlike surfaces, then the factor is no longer one-half. Furthermore a correction for the "distortion" of the electrical fields in the surface is involved, and this in general reduces the value calculated from the cohesion obtained without an allowance for this distortion.

For homogeneous binding the total energy of a solid (E) is given by the relation

$$E=-aV+b\Sigma, \qquad (1)$$

where V is the volume of the material and Σ is the area of the surface. The second term on the right has a sign opposite to the preceding term on account of the fact that the molecules are bound toward the inside, but not toward the outside, of the surface.

In the formation of surfaces the London dispersion forces must be taken into account, since they add to the surface energy ($+b\Sigma$) of all surfaces, but they are relatively small in all of the solids considered here. The dispersion energy is additive, and decreases as the sixth power of the distance, so at the surface its contribution to the surface energy is almost altogether restricted to the adjacent molecules. The magnitude of the term $+b\Sigma$ may be obtained by a calculation of the binding energy for those molecules which would be present adjacent to the plane of the surface if the solid or liquid were to extend beyond it, but which, on account of the existence of the surface, are not there. This is

a general method of calculation applicable to all types of molecular, atomic, and ionic forces.

It is customary in surface chemistry to express the energy (ϵ) of a surface as that per unit area, so

$$\epsilon = b\Sigma/\Sigma = b. \qquad (2)$$

II. THE TOTAL SURFACE ENERGY OF SODIUM CHLORIDE AND OTHER CRYSTALS

Only one determination has ever been made of the surface energy of a solid. It is evident that a mole of fine crystals of any substance has a greater surface energy than the same mass of coarse crystals. This difference should appear in the heat of solution of the substance if the same final concentration in the same solvent is obtained in the solution. This idea has been utilized by Lipsett, Johnson, and Mass.[1]

The principal difficulty at that time was in the determination of the superficial area of the fine powder, which was formed by sublimation, and the segregation of the crystals according to size by floating in a current of air. The diameters were determined (1) from photomicrographs, and also (2) from the weight of a given number of particles.

The total surface energy (h) found in three experiments varied from 356 to 406 ergs per sq. cm, and is therefore about five times higher than that calculated for the free energy at 0°K by Lennard-Jones and Dent, as cited later. This is a surprisingly large difference. In the experimental work it was assumed that the salt crystals have smooth faces. The total amount of heat liberated as heat of solution in some of the experiments was about 900 cal. while the surface energy is only about 13 cal. per mole. The experimental work was repeated in a preliminary way by Boyd and Harkins, who also obtained about 400 erg cm^{-2}, but the fine crystals used were coarser than they should have been to give good accuracy, so much finer crystals are being prepared and calorimetric measurements are being made by J. E. Wertz.

If the values of Lipsett, Johnson, and Mass are too high, the error is presumably in the methods used for the determination of the area of the fine salt, which would seem to be much too small. It is obvious that the calorimetric work must be of an excessively high order of accuracy, unless a finer salt can be prepared, since the surface energy is only about 1.5 percent of the energy which they measure in the calorimeter.

On the basis of the assumption that certain halide and other crystals are ionic, and that the repulsive force constants are similar to those for neon and argon, theoretical values for the surface energy have been calculated by Lennard-Jones and Taylor, and by Miss Dent,[2] and these are collected in Table I. Unfortunately there are no entirely reliable data for the surface tension of molten sodium chloride. Jaeger,[3] by the use of the bubble pressure method found surface tensions of 113.8 dyne cm^{-1} at 803°C and 88 erg cm^{-1} at 1172°C. If it is considered that a linear extrapolation is justified, then at 0°K both the surface tension and the total surface energy would be 190 dyne cm^{-1}. Since Jaeger's value for the surface tension, even at the high temperature of 803°, is higher than that calculated by Miss Dent, it is evident that there is a serious disagreement between the calculated and the experimental values.

III. THE SURFACE ENERGY OF THE DIAMOND

The diamond crystal is the hardest of known substances, and has an extremely high melting point (for graphite m.p. = 3800°K). Blom[4] considers the cohesion in elementary solids to be

TABLE IA. The surface energies of alkali halides and alkaline earth oxides and sulfides (erg cm^{-2}). (100 planes.) (Lennard-Jones, Taylor, and Miss Dent.)

F	Cl	Br	*I*		*O*	*S*
Na (304)	(96)			Mg	1362	357
265	77	76	79			
K (180)	(76.6)			Ca	1032	356
149	56	54	58			

Values in parentheses are uncorrected for distortion of the surface.

TABLE IB. Surface energies of certain salts (0, 1, 1 plane).

011	*F*	Cl	011	*O*	*S*
Na	784	350	Mg	3940	1730
K	489	260	Ca	2850	1440

[1] S. G. Lipsett, F. M. G. Johnson, and O. Mass, J. Am. Chem. Soc. **49**, 925, 1940 (1927). See also *ibid.*, **50**, 2701 (1928).

[2] J. E. Lennard-Jones and P. A. Taylor, Proc. Roy. Soc. **109**, 476 (1925); B. E. Dent, Phil. Mag. (7) **8**, 530 (1929).

[3] Jaeger, Int. Crit. Tab. **4**, p. 443.

[4] Blom, Ann. d. Physik (4) **42**, 1397 (1913).

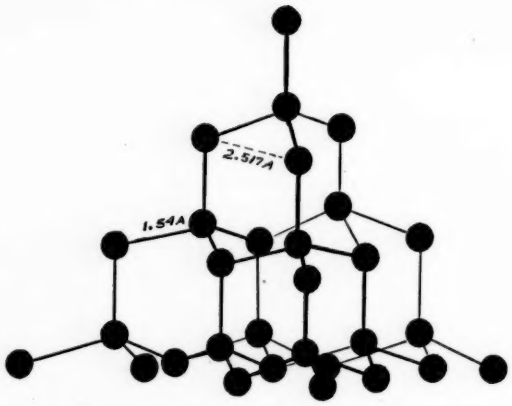

FIG. 1. Structure of the diamond, with the 111 plane horizontal. To obtain 111 faces the single vertical carbon-carbon bonds are broken.

proportional to T_m/V, where V is the atomic volume. The diamond has both an excessively high melting point and the lowest of all atomic volumes. From these relations it is evident that the cohesion in the diamond should be excessively high, which indicates that the related surface energy should also be extremely high. A method which may be applied in order to determine the cohesional energy is to calculate the energy utilized in splitting a diamond crystal along some definite plane to give two surfaces. Since for each cm² of the plane two cm² of surface are formed the surface energy is one-half the cohesional energy, or

$$\epsilon_S = \epsilon_C/2.$$

Cohesional and Surface Energy in the 111 Plane

If the diamond crystal is split in the 111 plane, in a position equidistant from the carbon atoms on the two sides of the plane, only one carbon-carbon bond is ruptured for each carbon atom on one of the sides of the plane. Furthermore the bonds, before rupture, are perpendicular to the plane. The well-known arrangement of the bonds is represented in Fig. 1. The rupture may be assumed to occur in a plane parallel to the base of the figure. The arrangement of the atoms in the layer just above or just below the plane, is shown in Fig. 2. The length of the carbon-carbon bond is 1.54A, but the edge (a_0) of the cubic lattice cell is 3.560A in length. The distance d between adjacent atoms in the 111 plane is given by

$$d = 3.560/\sqrt{2} = 2.517\text{A},$$

from which the area per atom (σ) in the plane, or per bond projecting perpendicularly from the plane, may be obtained as follows:

$$\sigma = (2.517)^2 \sin 60° = (2.517)^2\sqrt{3}/2 = 5.48\text{A}^2.$$

The density (ρ) of atoms (or bonds) of the above type is:

$$\rho = 10^{16}/5.48 = 1.825\times10^{15} \text{ bonds cm}^{-2}.$$

If the energy required to break one mole of bonds is E_B ergs, the energy per bond is $E_B/6.06\times10^{2}$ ergs, and the cohesional energy is given by:

$$\epsilon_C = 3.00\times10^{-9}E_B \text{ erg cm}^{-2}$$

or

$$\epsilon_S = 1.50\times10^{-9}E_B \text{ erg cm}^{-2}.$$

Cohesional and Surface Energy Parallel to the Cubic Face

If the diamond crystal is pulled apart in a plane parallel to the cubic face (Fig. 3), the area of this face, $\langle 3.560\rangle_{Av} = 12.56\text{A}^2$, represents two atoms, and two bonds per atom are broken. Thus

$$\sigma = 12.67/4 = 3.167\text{A}^2 \text{ per bond}$$

and

$$\rho = 10^{16}/3.167 = 3.158\times10^{15} \text{ bonds cm}^{-2}$$
$$\epsilon_C = 5.21\times10^{-9}E_B \text{ erg cm}^{-2}$$
$$\epsilon_S = 2.10_5\times10^{-9}E_B \text{ erg cm}^{-2}.$$

The energy required to rupture a mole of bonds may be assumed to be 90 kcal. which seems to be as close to the correct value as is known at present. This gives E_B as 3.77×10^{12} ergs per mole of bonds. On this basis

$$\epsilon_C(111 \text{ plane}) = 3.00\times3.77\times10^{3} = 11310 \text{ erg cm}^{-2}$$
$$\epsilon_S(111 \text{ plane}) = E_C/2 = 5650 \text{ erg cm}^{-2}$$
$$\epsilon_C(100) = 5.21\times3.77\times10 = 19640 \text{ erg cm}^{-2}$$
$$\epsilon_S(100) = E_C/2 = 9820 \text{ erg cm}^{-2}.$$

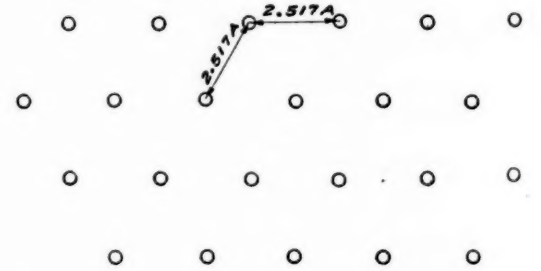

FIG. 2. Arrangement of bonds in the 111 plane of the diamond; also the arrangement of the atoms at the ends of the bonds.

Decrease of Surface Energy Due to Long Range Binding

The arrangement of the atoms in a 111 face of the diamond is exhibited in Fig. 2. Before the crystal is pulled apart parallel to this plane, all of the bonds which are to be broken are oriented perpendicular to the plane shown in the figure. There are no bonds between the atoms in this plane, but each atom is held by three bonds to adjacent carbon atoms which lie just below the plane.

It is evident that these bonds are not only very far apart, (2.517A, or 62 percent above the normal distance, 1.54A), but also they are not directed toward each other, since they are initially parallel. Both the large C–C distance and the direction of the bonds lower the interaction due to any overlapping of fields associated with two adjacent bonds to such an extent that it is probably not greater than one percent.

In the 100 plane, which is a face of the cube in Fig. 3, the distances are the same, but the two valence bonds from each carbon atom which are broken are not perpendicular to the plane in which they lie, which allows them to get closer together. Thus the correction for long range binding should be greater than with the 111 plane, but is presumably negligible in comparison with the uncertainty in the energy of the carbon-carbon bond itself.

The breaking of the bonds which become a part of the surface, causes some adjustment of the energy of the unbroken bonds adjacent to the surface, in such a direction as to decrease the surface energy, but no attempt has been made to estimate the magnitude of the decrease, although it is probably greater than that due to long range binding of the broken bonds.

Thus the magnitudes of the surface energy given in this paper may be considered as maximum values.

Free Surface Energy of the Diamond

The relation between the free (γ) and total (ϵ) surface energies is as follows:

$$\epsilon=\gamma-T(\partial\gamma/\partial T)_p=\gamma+Ts=\gamma+q,$$

in which the entropy s is positive. At 0°K the free energy is equal to the total energy. At the critical temperature ($\theta=1$) both become zero. Except near the critical temperature the free surface energy is in general a nearly linear function of the temperature.

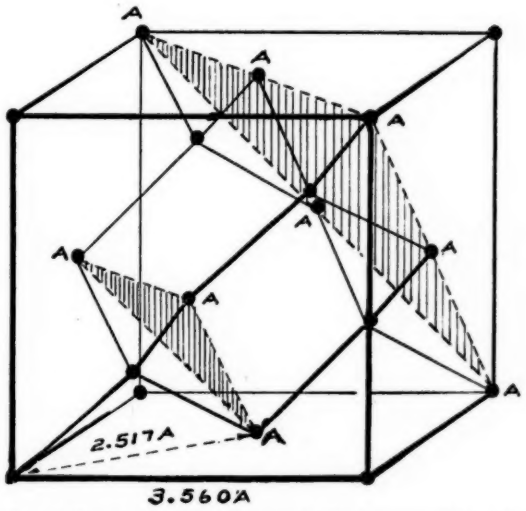

FIG. 3. Structure of the diamond. (If the crystal is pulled apart at a horizontal plane just above the base of the cube, four bonds are broken for the area $(3.560)^2$ A^2 or 12.67A^2.) The planes designated by AAA—are 111 planes.

Since there are no experimental data for the surface energy of the diamond, it is necessary to draw any desired conclusions from extremely general relations. The boiling point of carbon is given by *International Critical Tables* as 4200°K (Volume 3, p. 205). An empirical relation found by Guldberg and by P. A. Guye, independently, in 1890 gives the boiling point as 0.6 times the critical temperature, but the average value is closer to 0.63. For carbon this would give $T_C=6700$°K. Obviously it is not known how this rule applies to carbon, but at least the critical temperature must be extremely high. With a linear dependence of the free surface energy upon the temperature this would mean that the values of the free energy at 25°C should be 4.5 percent less than those of the total energy given in the last section. Since the three-dimensional entropy of the diamond is abnormally low, even at 25°C, it is not improbable that the surface entropy may also be low, which would mean that the difference would be less than 4.5 percent, but on the assumption that this is the correct value, the values obtained are:

Free energy of the 111 face of the diamond at 25°C = 5400 erg cm^{-2}.

Free energy of the 100 face of the diamond at 25°C = 9400 erg cm^{-2}.

It is difficult at present to estimate the limits of error of these values.

In general the maximum value of the heat absorbed (q) is exhibited not very greatly below the critical temperature (θ) of the material (e.g., at about 0.9θ).[5]

The highest value found for the surface energy of any solid in the calculations of Lennard-Jones and Taylor is 3940 erg cm^{-2} for the 011 face of magnesium oxide. This face does not occur, but the 100 face, with an energy of 1362 erg cm^{-2} is found in nature. These values are not corrected for distortion. All that can be added here is to state that, on account of the high critical temperature of magnesium oxide, its free surface energies should be only slightly below the total surface energies. The values of the total surface energy for the diamond are higher in comparison with those for magnesium oxide than would be expected from a comparison of the melting and boiling points of the materials. Since the free surface energy of the 100 face of the diamond is 4000 erg cm^{-2} greater than that of the 111 face, it is not to be expected that the 100 face will be found in nature (unless formed under extremely abnormal conditions).

[5] W. D. Harkins and L. E. Roberts, J. Am. Chem. Soc. **44**, 662 (1922).

MAY, 1942 JOURNAL OF CHEMICAL PHYSICS VOLUME 10

A Superliquid in Two Dimensions and a First-Order Change in a Condensed Monolayer

I. Energy, Compressibility, and Order of Phase Transformations

WILLIAM D. HARKINS AND L. E. COPELAND
George Herbert Jones Chemistry Laboratory, University of Chicago, Chicago Illinois

(Received February 20, 1942)

The transition from a liquid to a vapor in a two-dimensional system (monolayer) may exhibit the characteristics of a first- or of a second-order change. However, all transitions (as e.g., fusion) in liquid and solid monolayers found heretofore have been of the second or third order. Thus the change from three to two dimensions, or a decrease of one dimension, gives an increase of one in the order of the phase transitions. The most condensed two-dimensional phases thus far recognized are the liquid condensed L_2, or low pressure condensed phase, and the solid (S) or high pressure condensed phase. The L_2 phase is characterized by a compressibility of about 0.004 to 0.010 while that of the S phase is only about a tenth as large (0.0005 to 0.001). The fusion of the S phase to form the L_2 phase involves no absorption of heat and is a true second-order change. An attempt was made to discover a first-order transition from an L_2 to an S phase, with apparent success with monolayers of the n long paraffin chain alcohols. However, the relations were extremely peculiar in that with octadecanol the transition was first order in only the narrow temperature range of about 7.5 to 11°C, and was second order both below and above this narrow interval. Further investigation revealed that the S or solid phase exists only below 7.5°C, while above this temperature a new phase, which exhibits extremely peculiar properties, is the stable high pressure phase. This exhibits the low compressibility of the solid phase, but is about ten times more fluid than is the liquid phase at low pressures. This is designated as the LS phase. The compressibilities and the energy and entropy of expansion of the monolayers were determined. The heat absorbed in the expansion of the S and LS films in certain regions of temperature, pressure, and area, was extremely large. The entropy of extension of such a monolayer was found in one instance to be forty times higher than that of the surface of water, which for a pure liquid has a very high entropy of extension. The heat of transition of the high pressure LS phase to the low pressure liquid L_2 phase is zero above about 11°C, but between 11°C and 7.5°C heat is given off in the transition. This is analogous to the case of water in three dimensions, for which the high pressure phase is liquid and the low pressure phase is solid (ice). Since the increase of area is small the heat of transition is small (e.g., 40 cal. $mole^{-1}$). The small magnitude of the energy change is not surprising when it is considered that the transition is from one liquid phase to another. In a second paper it will be shown that in the first-order region the viscosity increases tenfold in the change from LS to L_2. One of the most remarkable features revealed by this work is the extremely great change in the properties of these highly condensed monolayers, which is brought about by extremely small, previously undetectable changes of molecular area. Thus not only are the energy relations of a monolayer of octadecanol

at 19.98A very different from those of 19.96A, but, in addition, one of the phases (S) present at the smaller, is absent at the larger area. This is related to the fact that 19.96A is very nearly the transition area, at all pressures thus far investigated, for the second-order transition $S \rightleftharpoons LS$. A further increase of 0.22A gives an even greater change of properties, since the L_2 and the LS phases and the first-order transition between them become involved. The relations found in this work would not have been discovered if the methods usually used in work on monolayers had been employed. It was necessary to make both the accuracy and the precision of the determination of area much greater than has been attained before, and also to increase the precision in the regulation of temperature. A new type of thermostat has been built for the work on phase changes and energy relations. In this the very large trough and its film balances are inclosed on all sides by a thick wall of water, and only small openings, closed by insulating materials, are used for the rods employed in the mechanical operations. There is also a small window for the beam of light used to determine the position of the mirror on one of the film balances.

I. INTRODUCTION

TO those who are accustomed to consider only three-dimensional systems, the phase relations in two dimensions appear anomalous. Thus, a change from three to two dimensions, that is a *loss* of one dimension, results in an *increase* of one in the order of a phase change of a condensed system.

This would not be difficult to understand if a two-dimensional film or monolayer were suspended in space, since in such a case, molecular binding in the third direction would be absent, and this would be very likely to involve an increase in the order of a change of phase. The fact that this occurs, even when an aqueous subphase is present, indicates that the binding to the subphase is sufficiently loose to allow the increase of order which is observed.

A phase is of the second order in the terminology of Ehrenfest[1] if a latent heat is absent and there are discontinuities in the heat capacity and the coefficients of thermal expansion and compressibility. The relations, including the abnormalities, of transitions of the first and second orders, have been considered in detail by Mayer and Streeter.[2]

It should be mentioned, since it does not seem to have been pointed out earlier, that the vaporization of a monolayer may exhibit the characteristics of either a first- or a second-order transition. For example a liquid expanded film of pentadecylic acid at 20°C begins to vaporize at a molecular area of 44A² and a vapor pressure of about 0.2 mm. This pressure remains constant up to an area of the order of 1500A². The latent heat of vaporization has not been measured but is moderately large. At 14.5° the intermediate liquid film begins to vaporize at about 42A² and becomes completely vaporized at about 2300A². These are changes of the first order.

However, at 25°C and 38A² ethyl palmitate transforms from the *intermediate* liquid to the vapor state without a latent heat of phase change, so this is a second-order transformation.

The work of the present paper was begun in an attempt to discover a first-order two-dimensional change of phase in a *constricted* (i.e., condensed) system. Unfortunately the term "condensed" cannot be used with its ordinary connotation for surface films, since Adam has applied this term to distinguish a more condensed from a less condensed phase.

Earlier exploratory work by Harkins and Nutting failed to give evidence for any change of this order, but indicated certain abnormalities in the behavior of monolayers of the long chain n paraffin alcohols. The abnormalities were such as to suggest the possibility that the films might exhibit a change of the first order.

However, the exploratory work indicated that if such a change were to be discovered, the accuracy of the work would have to be increased considerably beyond that attained anywhere, with respect to the measurement of molecular area and especially with respect to the control of the temperature of monolayers.

In order to attain accuracy in the temperature control a thermostat, specially designed for work on monolayers, has been constructed, and is in use. With this it will be possible to investigate films on an aqueous subphase at temperatures from −30°C to 60°C or more. If the air is kept saturated with respect to the liquid subphase, the temperature of the surface may be kept very constant.

[1] P. Ehrenfest, Proc. Kgl. Akad. Amst. **36**, 115 (1933).
[2] J. E. Mayer and S. F. Streeter, J. Chem. Phys. **7**, 1017 (1939).

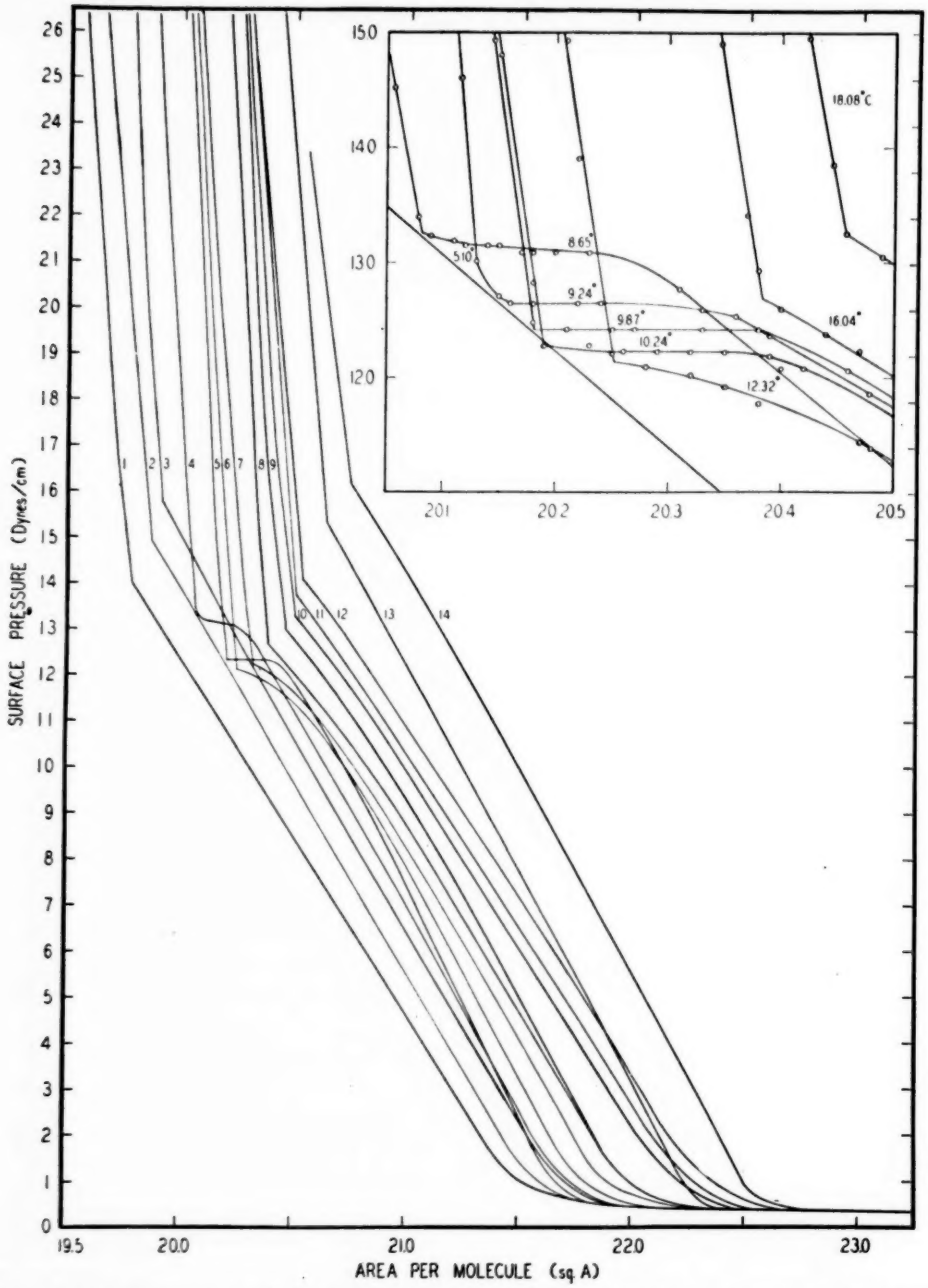

FIG. 1. Pressure-area-temperature relations of condensed monolayers of octadecanol on water. The insert gives an enlarged section in the region of the first-order transition. Outside of this region all of the transitions are second-order. The temperatures for the curves in the principal diagram are: 1, 2.85°; 2, 5.10°; 3, 7.10°; 4, 8.62°; 5, 9.90°; 6, 12.32°; 7, 14.06°; 8, 16.04°; 9, 18.08°; 10, 19.85°; 11, 22.95°; 12, 25.12°; 13, 30.30°; 14, 34.85°. Curves for four other temperatures are given in the insert.

II. A NEW SUPERLIQUID PHASE AND A FIRST-ORDER TRANSITION AS RELATED TO THE PRESSURE-AREA-TEMPERATURE DIAGRAM OF OCTADECANOL

Up to the time of the beginning of the work presented in this paper no first-order change of phase in a two-dimensional system, except that involved in the condensation of a gaseous film, had been discovered. However, such a change is now revealed in a highly condensed system by

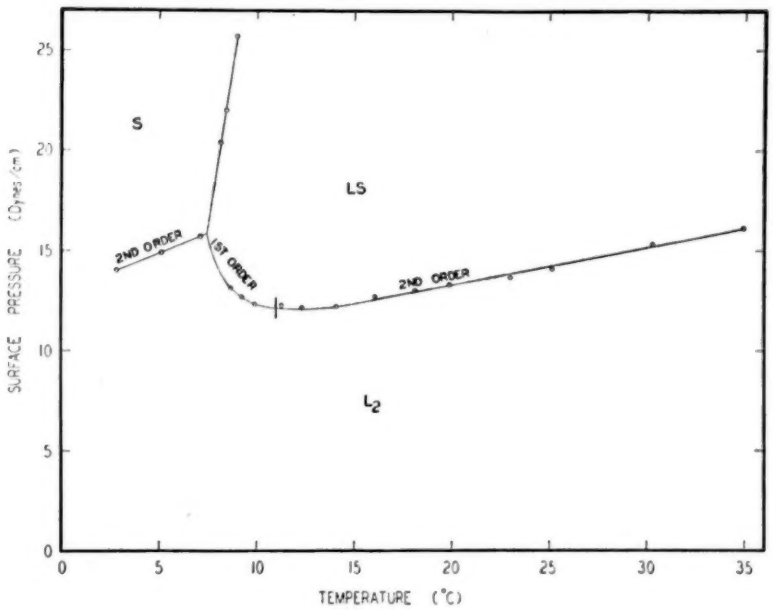

FIG. 2A. Pressure-temperature values for the phase boundaries of condensed monolayers of octadecanol. Transitions $L_2 \rightleftharpoons LS$ are *first-order* from the triple point at 7.5° on the descending curve to about 11°C, and become *second-order* above this. Transitions $L_2 \rightleftharpoons S$ are *second-order*.

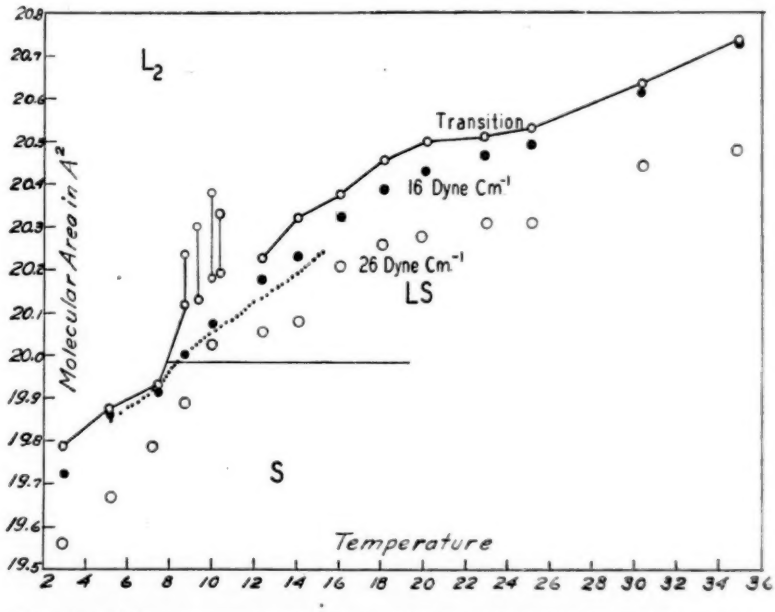

FIG. 2B. Molecular area-temperature values for the phase boundaries of condensed monolayers of octadecanol. In addition the molecular areas are given in the *S* and *LS* phases at pressures of 16 and 26 dyne cm^{-1}. The dotted line gives values at 16 dyne cm^{-1} as obtained by increase of the temperature of a monolayer. The black circles give values at the same pressure, but obtained from the isotherms.

TABLE I. Two-dimensional phases and probable order of changes between them.

Phases	Order of change between them
Classification A	
I. Gas, *G*. Includes compressed vapors such as the "vapor expanded" film of Adam Perfect gas: $\pi\sigma = kT$ Imperfect gas: minimum value of κ of same order as for L_1 films: e.g., 0.04 for ethyl palmitate at 25 C, 34A², and 14 dynes cm^{-1}	
	I and II: first (L_1G)
II. Liquid, L_1 (*BC*). "Liquid expanded" of Adam. Liquid of high compressibility $\kappa = 2$ to 7×10^{-2} $h_s = 50$ ergs cm^{-2}	
	II (or I) and III: second (*C*)
III. Intermediate (*I*) or transition (*CE*). Liquid of extremely high compressibility Intermediate, *I*. Maximum κ of order of 2 to 5×10^{-1} for normal long-chain acids 2.2×10^{-1} for normal long-chain esters Minimum same as κ of L_2 film: $h_s = 300$ ergs cm^{-2}, which is nearly constant at the higher areas, but decrease rapidly to a low value as transition to next phase is approached	
	III and IV: third (*D*)
IV. Liquid, L_2 (*DE*). "Liquid condensed" of Adam. Liquid of low compressibility $\kappa = 5$ to 10×10^{-3} $\log \eta = \log \eta_0 + k\pi$: h_s small	
	IV and V: first (perhaps anomalous) changing to second at higher temperatures. (See Fig. 1)
V. *LS*. Superliquid phase of extremely low compressibility $\kappa = 0.0005$ to 0.0017. Viscosity becomes high at temperatures far above that of first-order charge	
	IV and VI: second V and VI: second
VI. *S*. Previously classed as solid, may have the rigidity of a solid, or a non-Newtonian or a Newtonian viscosity. The most highly compressed phase. $\kappa = 0.0005$ to 0.001	

the pressure-area-temperature (π–σ–T) relations of long paraffin chain alcohols.

The most striking characteristic of the family of isotherms for any one long chain alcohol, as exhibited in those of octadecanol shown in Fig. 1, is the existence of a short flat region in the pressure-area curves at the transition between two condensed phases, one of which was heretofore unknown. This is all the more remarkable since this region, in which a first-order phase change seems to occur, exists only in a narrow temperature interval. With octadecanol at temperatures below 7.4° the isotherms show the second-order transitions which seem to be characteristic of the liquid condensed to solid ($L_2 \rightarrow S$) transitions. It is also seen (Fig. 2A) that from 2.85° to 7.10° the kink point pressures of the second-order change rise linearly with the temperature, but from 7.5°C to 11°C this trend is reversed, and the transition pressure falls with rising temperature. This is the region in which the first-order phase change takes place. Above 11°C the isotherms again show the usual second-order transition between the low pressure and high pressure phases, and it can be seen that there again the kink point pressure rises almost linearly with the temperature. Viscosity data, discussed later, show that *two high pressure phases exist*, while in all earlier work both of these have been classified as a single solid (*S*) phase. Of these two, one has so high a fluidity that it is considered as a new liquid (*LS*) phase.

This phase has remarkable properties:

(1) Although it is formed from the liquid condensed (L_2) phase by increase of pressure, it has at temperatures of the first-order change a very much smaller viscosity than that exhibited by the L_2 phase at low pressure. On this account it is designated as an *L* phase.

(2) It has the compressibility (0.0005 to 0.0017) of a monolayer in the *S* (usually designated as the solid) state. In the *S* state the three alcohols exhibit compressibilities from 0.0006 to 0.001.

(3) It, as well as the *S* state, is formed from the L_2 state by increase of pressure.

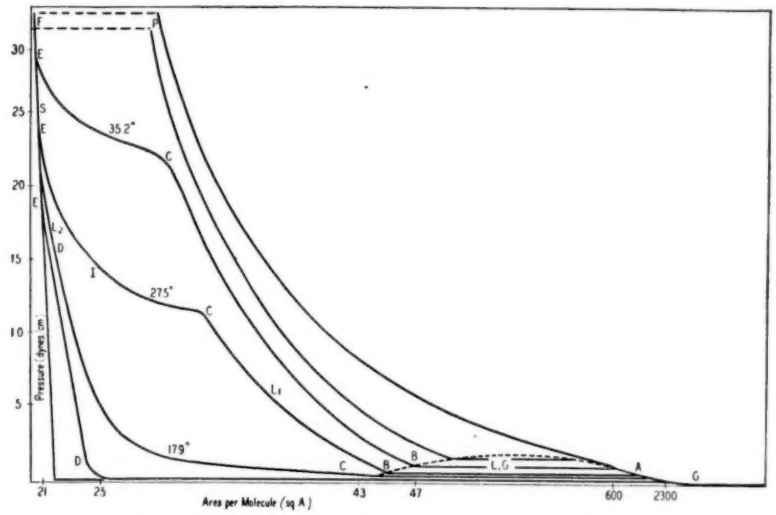

FIG. 3. General phase diagram for monolayers which exhibit a liquid expanded (L_1) phase: i.e., the temperature is below the critical temperature for the first-order transition $G \rightleftharpoons L_1$, where G represents the gaseous phase. The transitions at E and C are second-order, and L_1G is the region of the first-order change. The temperatures are correct for pentadecylic acid, but are different for other substances.

From 2 and 3 it is considered as similar an S state, and from 1, 2, and 3 it is given the designation LS phase.

The discovery of this new phase makes it essential to extend the classification of phases already adopted by Harkins, Young, and Boyd.[3] And this is done in Table I. (See also Fig. 3.)

The pressure-area curves for octadecyl alcohol were determined at 18 different temperatures between 3.85° and 34.85°C and these are exhibited in Fig. 1. The curves for a few temperatures are given on an enlarged scale in the upper right-hand corner of the diagram. To avoid confusion several of these curves have been omitted from the larger section of the figure. One of the principal characteristics of a first-order change is that it gives a "flat" in a p–v or a π–σ diagram. It is apparent that curve 5 exhibits such a flat at 9.90°C, while the smaller, but magnified, plot shows a flat at 9.87°, only 0.03°C lower than the other. However, this extends over an area range of only very slightly more than 0.2A², which is an indication that the latent heat of this phase transition is very small. To calculate this heat it is necessary to know the π–T relations at constant area in this region, and these have been determined. The π–σ curve at 10.24° is also almost flat, but it is apparent that if what is represented here is a true first-order change, the temperature range of this change is very small, and that it fades out into a second-order change if the temperature is either raised or lowered.

In order to make certain that these extremely abnormal relations are not due to an impurity the octadecyl alcohol was purified with extremely great care. In addition the work was repeated with the 19 and 20 carbon alcohols, which gave exactly the same set of curves, except that the longest flat found was raised from 9.90° to 14.88° and to about 20°, respectively, or an increase of 5° per carbon atom. Concurrently the film pressure of the flat increased from 12.0 to 14.0 to 16 dyne cm.

In the work of some other investigators it has been customary, when a π–σ curve as determined is apparently improperly placed in the diagram, due to the difficulty in the determination of the area (σ), to shift it to what appears to be its proper position.

This procedure was not followed in the determination of the correct positions of the curves exhibited here. The absolute areas were determined as accurately as possible, by the procedure given in the later section on methods. The rela-

[3] W. D. Harkins, T. F. Young, and G. Boyd, J. Chem. Phys. 8, 954 (1940).

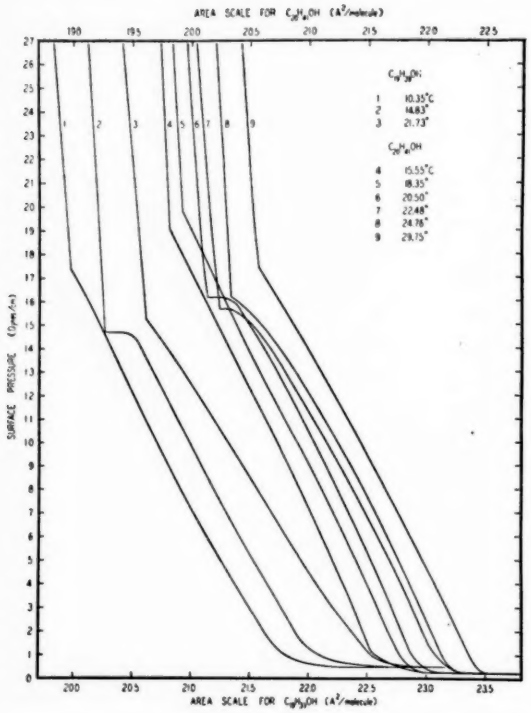

FIG. 4. Pressure-area-temperature relations for the normal long chain paraffin alcohols with 19 and 20 carbon atoms in the chain. The temperature of the first-order transition increases 5° while the pressure rises about 2 dyne cm^{-1} for each additional carbon atom (compare with Fig. 1).

tive positions were found by a measurement of the pressures obtained, at certain constant molecular areas, by increasing the temperature through the range, from 2.85° to 34.85°C, used in obtaining the $\pi-\sigma$ isothermals.

Phase Diagram for Octadecanol

Figure 2 shows the pressure-temperature regions for the existence of the low pressure liquid L_2 film, and of the high pressure liquid LS, and S films. The boundary between the LS and S films was determined from the viscosity relations, and will be considered in a paper on this subject. The other boundaries are taken from Fig. 1. The triple point is at a pressure of 16 dyne cm^{-1} and a temperature of 7.5°C. Bridgman[4] has given a geometrical relation for the slope of curves of the type given in Fig. 2, which show the course of a second-order transition:

$$dT_k/dp = -\Delta(\partial V/\partial p)_T/\Delta(\partial V/\partial T)_p. \quad (1)$$

In the application to films this equation becomes

$$dT_k/d\pi = -\Delta(\partial\sigma/\partial\pi)_T/\Delta(\partial\sigma/\partial T)_\pi, \quad (2)$$

which gives at 25.12° the value 4.3 degree cm $dyne^{-1}$, while the slope obtained from the experimental value plotted in Fig. 2 is 5.3 in the same units.

The existence of a first-order transition in only a limited range of temperature causes a crossing of the isotherms which exhibit this type of change with some of those which give a second-order transition. At 12.23 dyne cm^{-1}, which seemed to be just below this region it was found that there is no discontinuity, but the coefficient of thermal expansion (α) is negative. Now

$$(\partial\pi/\partial T)_\sigma = -(\partial\sigma/\partial T)_\pi/(\partial\sigma/\partial\pi)_T = \alpha/\kappa. \quad (3)$$

At $\pi = 11.23$ dyne cm^{-1}, $\sigma = 20.5A^2$ $molecule^{-1}$, and $T = 9$°C the calculated value of α/κ is 0.025 erg cm^{-2} $deg.^{-1}$ while the experimental value is 0.031, $\kappa = 0.055$ erg^{-1} cm^{-2}, and $\alpha = 0.0014$ deg^{-1}.

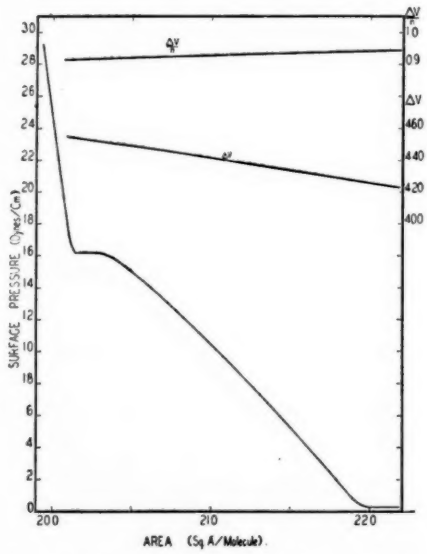

FIG. 5. Surface (contact) potential for monolayers of the 20 carbon alcohol on 0.01N HCl at 20°C. $\Delta V/n$, where n is the number of molecules of eicosanol per cm^2 is in volt cm^{-2} $molecule^{-1} \times 10^{-15}$, ΔV in millivolts. The contribution per molecule to the surface potential decreases slightly as the molecular area decreases.

[4] P. W. Bridgman, Rev. Mod. Phys. **7**, 21 (1935).

III. A FIRST-ORDER TRANSITION IN MONOLAYERS OF NONADECANOL (19C) EICOSANOL (20)

Figure 4 shows that the isotherms of films of the 19 and 20 C atom n alcohols[5,6] resemble those of octadecanol except for an increase of 5.0°, per carbon atom added, in the position of the "flat" of the first-order change, and an accompanying increase of about 2 dyne cm^{-1} in the film pressure.

Surface Potential and Homogeneity

The surface potential of the 20C alcohol (eicosanol) was determined at 20°C. The potential (ΔV) increases linearly (Fig. 5) with decrease of molecular area, and there is no indication of heterogeneity at the areas shown in the figure. Above 25A² the contact potential varied in such a way as to indicate the existence of islands of condensed, surrounded by gaseous, film. The value of $\Delta V/n$, where n is the number of molecules per cm^2 decreases very slowly with increase of packing (decrease of area). Although the potentials were determined at all areas above 20.07A², which includes all of the flat (20.14 to 20.3A), there is no perceptible change of slope in the $\sigma - V$ line. The potential increase is proportional to the decrease of area, that is to the increase in concentration of the molecules, and is independent otherwise, of the changes of pressure. The molecules are so tightly packed that their orientation is affected only slightly by the pressure. Schulman and Hughes[6] obtain a non-linear relation.

The film of eicosanol was examined at 20°C by the use of a dark field microscope, and no evidence of heterogeneity was detected.

The pressures of this monolayer were determined by the use of the vertical type of film balance, while in all of the earlier work the horizontal type was employed.

On account of the fact that, even if the electrode used to determine the surface potential has

TABLE II. Compressibility (κ) of monolayers of the normal long chain alcohols in different states.

Compound	t°C	A²/Molecule	Dyne/cm^{-1}	κ
		L_2 State		
Octadecanol	25.12°	22.6–20.54	1.5–14.05	0.0055–.008
Octadecanol	9.90	21.8–20.4	1.5–12.37	.004 –.016
Octadecanol	7.10	21.8–19.78	1.5–14.90	.0055–.008
Nonadecanol	21.73	22.7–20.71	1.5–15.27	.0055–.008
Nonadecanol	14.83	22.6–20.5	1.5–14.70	.0055–.008
Nonadecanol	10.35	22.3–19.97	1.5–17.40	.0047–.008
Eicosanol	24.76	22.3–20.33	1.5–16.20	.004 –.009
Eicosanol	22.48	22.3–20.30	1.5–15.70	.004 –.016
Eicosanol	18.34°	21.9–19.92	1.5–19.30	0.004 –.009
		LS State		
Octadecanol	25.12°	20.54–col.	14.05–col.	0.0014–.0017
Octadecanol	9.90	20.2 –col.	12.37–col.	.0007–.0009
Nonadecanol	21.73	20.71–col.	15.27–col.	.0008–.0009
Nonadecanol	14.83	20.36–col.	14.7 –col.	.0005–.0009
Eicosanol	24.76°	20.33–col.	16.20–col.	.0005–.0009
Eicosanol	22.48°	20.24–col.	15.70–col.	0.0008–.0011
		S State		
Octadecanol	7.10°	19.78–col.	14.90–col.	0.0006–.0008
Nonadecanol	10.35	19.97–col.	17.40–col.	.0007–.0009
Eicosanol	18.34°	19.92–col.	19.30–col.	0.0007–.001

Col. = Collapse.

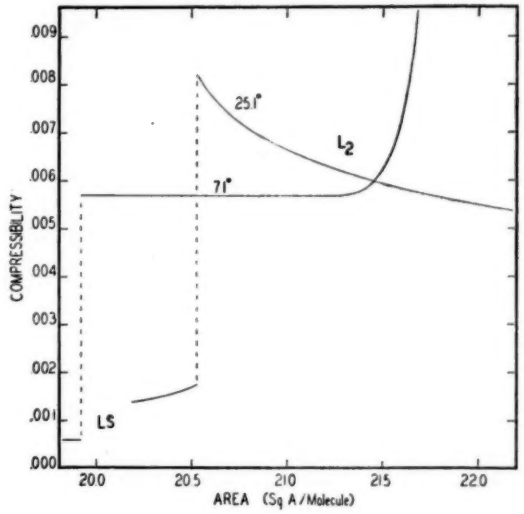

FIG. 6. Compressibility of the L_2, LS and S phases of octadecanol as a function of molecular area and temperature.

[5] N. K. Adam and J. W. W. Dyer, Proc. Roy. Soc. **A106**, 694 (1924). Adam and Dyer compared the pressure-area relations of tetradecanol and eicosanol. It was noted that the transition point between the high and low pressure phase occurred at a higher compression for the longer chain alcohol. Isotherms on subphases of $N/50$ HCl, and $N/10$ NaOH were identical. It was found in the course of the present work also that isotherms on acidic and basic subphases (pH[2] and pH[8]) are identical.

[6] J. H. Schulman and A. H. Hughes, Proc. Roy. Soc. **A138**, 430 (1932). Eicosanol was investigated at various temperatures ranging from 4° to 31°C. At 4°C the film was solid. Up to 16°C the same type of isotherm was found that was given by tetradecanol. At 20°C the isotherm showed a peculiar "arrest." The film acted normally upon compression to an area of 20.4A². At this area the compressibility suddenly increased, and between 20A² and 19.8A² the compressibility was about 0.2, which is very far from the infinity of a first-order change. At 19.8A² the compressibility again became very small, about the same as was found in the high pressure phase at lower temperatures. Above 22°C the film was found to be liquid throughout, and the isotherms were similar to those given by tetradecanol. The fluidity of the films was tested by blowing upon talc sprinkled upon the film.

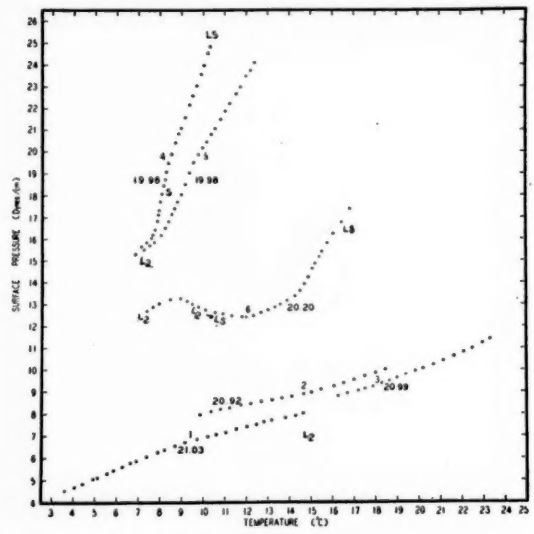

FIG. 7. Pressure-temperature relations of octadecanol monolayers at the molecular areas in A as indicated. 4 = L_2, S, and LS and 5 = L_2 and LS phases; 6 = transition from L_2 to LS phase; and 1, 2, and 3 = L_2 phase. The slope of these curves gives the entropy of spreading of the monolayer.

a small area, the area of the film which takes part in carrying the current from the electrode cannot be made minute, the contact potential is capable of revealing inhomogeneities only when they are moderately large scale.

IV. COMPRESSIBILITY OF MONOLAYERS OF THE *n* LONG CHAIN ALCOHOLS

The compressibility of monolayers of octadecanol at two temperatures is exhibited in Fig. 6. At 7.1°C (isotherm 3, Fig. 1) the compressibility is very low in the low area region of the S state (0.0006 to 0.0008). Immediately, on increase of area above that of the second-order transition, the value increases to 0.0055 in the L_2 state, and remains constant from a molecular area of 19.9A up to about 21.3A, above which it increases more and more rapidly. At 25°, at

TABLE III. ΔH_s for the transition $L_2 \rightarrow LS$.

Compound	t°C	$-d\pi/dT$	ΔA^2/ molecule	$\Delta H_s \times 10^{-16}$ ergs/ molecule	ΔH_s cal./mole
Octadecanol	8.6°	0.840	0.11	26.0	37.5
	9.2	.640	.12	21.7	31.2
	9.9	.394	.20	22.3	32.1
	10.2	.280	.19	15.1	21.7
Nonadecanol	14.8	.400	.17	19.6	28.2
Eicosanol	20.5°	0.790	0.12	27.5	39.6

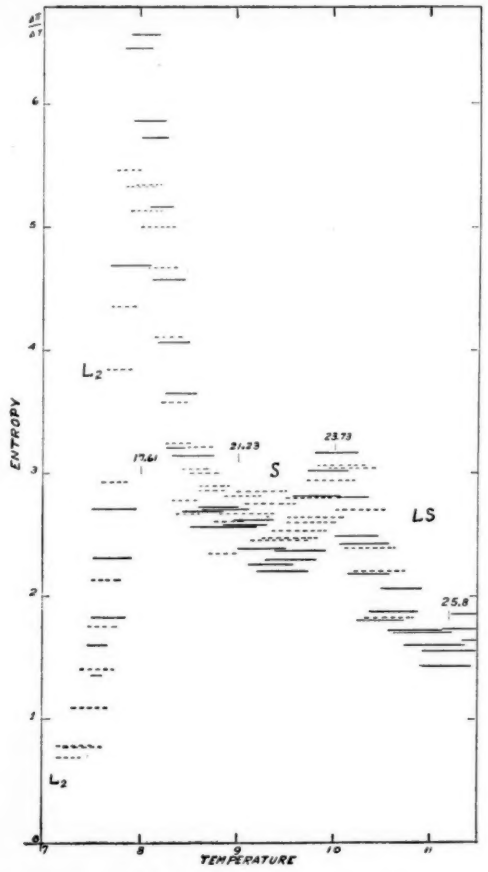

FIG. 8. Entropy of spreading of a monolayer of octadecanol at a molecular area of 19.96 A² as a function of temperature (chord plot). Reveals the presence of L_2, S, and LS phases, as confirmed by the viscosity relations.

areas from about 20.2 to 20.55 the film is in the LS state and has a compressibility of from 0.0014 to 0.0017. On transition to the L_2 state this rises abruptly to slightly above 0.008 and then decreases, at first rapidly, and then gradually to 0.0055. The values for all of the films are given in Table II.

V. THE LATENT HEAT OF THE FIRST-ORDER TRANSITION

The latent heat of the first-order transition (Table III) was calculated from the curves of Figs. 7 and 8 by the use of the Clapeyron equation. The change in area was obtained from the isotherms. Heat is absorbed in the change from the low pressure to the high pressure modification, as in the change from ice to water. The value of ΔH decreases as the temperature is

TABLE IV. The increase of free energy (f), enthalpy (h), and entropy (s), and heat absorbed (q) in the extension or spreading of monolayers on water. (Values for the extension of the surface of water for comparison. Values in erg cm^{-2} or erg cm^{-2} deg.$^{-1}$.)

Substance	Process	σ in A	f	ϵ or h	q	s
			L_2 film at 18°C			
Clean water	....	....	73.05	116.2	43.1	0.148
Octadecanol	extension	21.0	63.77	202	138	.473
Octadecanol	spreading		− 9.28	85.3	94.6	.325
Octadecanol	extension	20.9	61.21	213	150	.516
Octadecanol	spreading		− 9.84	97.3	107	.368
Octadecanol	extension	20.5	60.40	389	329	1.130
Octadecanol	spreading		−12.65	273	286	0.982
			L_2 film at 20°C			
Clean water	....	....	72.75	116	43.2	0.148
Octadecanol	extension	20.99	62.78	216	153	.523
Octadecanol	spreading		− 9.97	100	110	.375
Nonadecanol	extension	20.68	58.81	199	140	.479
Nonadecanol	spreading		−13.94	83	97	.331
Eicosanol	extension	21.01	62.73	276	213	.728
Eicosanol	spreading		−10.02	160	170	0.580
			LS film at 12°C			
Clean water	....	....	73.93	115.8	41.9	0.147
Octadecanol	extension	19.96	46.21	541	495	1.735
Octadecanol	spreading		−27.72	425	453	1.588
Octadecanol	extension	19.98	50.93	556	505	1.772
Octadecanol	spreading		−23.00	440	463	1.625
			LS film at 16°C			
Clean water	....	....	73.34	116.1	42.8	0.148
Octadecanol	extension	20.20	57.16	556	499	1.726
Octadecanol	spreading		−16.18	440	456	1.578
			LS film at 18°C			
Clean water	....	....	73.05	116.2	42.1	0.148
Nonadecanol	extension	20.25	53.92	738	684	2.348
Nonadecanol	spreading		−19.13	622	641	2.200
			LS film at 22°C			
Clean water	....	....	72.46	116.4	44.0	0.149
Eicosanol	extension	20.13	56.01	856	800	2.711
Eicosanol	spreading		−16.45	740	756	2.562
			S film at 9°C			
Clean water	....	....	74.37	115.5	41.2	0.146
Octadecanol	extension	19.96	53.14	826	772	2.746
Octadecanol	spreading		−21.23	710	731	2.600

raised. It must decrease to zero where the first-order transition changes to second-order. It is very small, since the transition is from one liquid state to another, and is also in a two-dimensional system, which usually involves no latent heat of phase change.

VI. ENERGY OF EXPANSION OF MONOLAYERS THE n LONG CHAIN ALCOHOLS

If the area of the clean surface of a body of water is extended by 1 cm² at 20°C the free energy (f or γ) of the system is increased, in erg cm², by 72.75; the enthalpy (h) by 116; the heat absorbed (q) is 43.2, and the entropy (s) is increased by 0.148 (Table IV). If the surface is covered by a monolayer of octadecanol, with a molecular area of 20.99A², the free energy increment is

TABLE V. The increase of entropy, and enthalpy, and the heat absorbed in the spreading of a monolayer of octadecanol as a function of the pressure, molecular area, temperature, and the phase. (h and q=erg cm^{-2} and s=erg cm^{-2} deg.$^{-1}$.)

Phase	π	t°C	s_π	q_π	h_π
		19.96 A²/molecule			
L_2	16.0	7.34°	1.00	280	264
S	17.0	7.88	5.5	1545	1528
	18.0	8.06	5.86	1648	1630
	19.0	8.28	3.840	1081	1062
	20.0	8.57	2.768	780	760
	21.0	8.92	2.593	731	710
	22.0	9.29	2.263	639	617
	23.0	9.68	2.838	803	780
	24.0	10.05	3.07	869	845
LS	25.0	10.38	2.212	627	602
	26.0	10.86	1.823	518	492
	27.0	11.66	1.625	463	436
	28.0	12.26	1.468	416	388
	29.0	12.95°	1.448	414	385
		19.98 A²/molecule			
L_2	15.3	6.98°	0.562	147	132
LS	16.0	7.86	1.570	441	425
	17.0	8.45	2.458	692	675
	18.0	8.93	2.582	728	710
	19.0	9.33	2.075	586	567
	20.0	9.86	1.802	510	490
	21.0	10.50	1.636	464	443
	22.0	11.08	1.618	460	438
	23.0	11.70	1.618	461	438
	24.0	12.32°	1.618	462	438
		20 A²/molecule			
L_2	12.5	7.00°	0.570	160	153
	13.0	7.94	.317	89	76
L_2-LS	13.0	9.50	−.514	−145	−158
	12.5	11.50	−.118	−34	−46
LS	12.5	12.42	.310	88	76
	13.0	13.65	.527	151	138
	14.0	14.62	1.578	454	440
	15.0	15.20	1.735	499	484
	16.0	15.79	1.630	471	455
	17.0	16.47°	1.440	417	400
		20.5A²			
L_2	8.5	2.85°	0.526	145	137
	9.0	3.83	.530	148	139
	10.0	5.80	.496	138	128
	11.0	7.96	.436	120	109
	11.8	9.74	.405	112	100
	11.3	12.35	.167	48	36
	12.0	15.80	.256	75	63
	13.0	19.05°	0.297	87	74
		20.9A²			
L_2	8.10	10.00°	0.272	77	69
	8.5	12.38	.175	50	42
	9.0	15.16	.232	65	56
	9.5	17.00	.316	92	82
	10.0	18.44°	0.388	104	94
	66				
		21.0A²			
L_2	4.5	3.58°	0.417	115	111
	6.1	7.40	.417	117	111
	7.0	10.32	.227	64	57
	8.0	14.60	.211	61	52
	9.0	17.06	.258	75	66
	10.0	20.09	.370	108	98
	11.0	22.47°	0.478	141	130

decreased to 62.78, the enthalpy (h) is nearly doubled and has the value 216; the heat absorbed is increased by 254 percent to 153, while, obviously, the percentage increase of entropy is also 254. If the monolayer spreads over the surface of the water the change of free energy becomes a decrease (−9.97), the increment of the enthalpy is 110, which is 154 percent above that for clean water, but below that for extension of the film.

TABLE VI. Effect of pressure (π) upon the energy of spreading of monolayers of the alcohols.

Phase	π	t°C	s_s	q_s	h_s
		Nonadecanol			
		20.25 A²/molecule			
L_2	14.5	10.90°	0.974	276	262
	15.0	11.55	.840	239	224
	16.0	13.06	.832	238	222
L_2-LS	16.0	13.60	−.754	−216	−232
	15.5	14.22	−.886	−254	−270
	15.0	15.50	−.198	−57	−72
LS	15.0	16.20	1.987	575	560
	16.0	16.64	2.374	688	672
	17.0	17.04	2.446	710	693
	18.0	17.45	2.358	685	667
	19.0	17.93	2.240	652	633
	20.0	18.40	2.065	602	582
	21.0	18.90	1.880	549	528
	22.0	19.45°	1.313	384	362
		20.68 A²/molecule			
L_2	10.0	10.15°	0.804	228	218
	11.0	11.47	.710	202	191
	12.0	13.08	.614	176	164
	13.0	15.72	.374	108	95
	14.0	20.18	.340	100	86
	15.0	22.20°	0.664	196	181
		Eicosanol			
		20.13 A²/molecule			
L_2	15.5	16.48°	0.603	175	159
	16.0	17.38	.658	191	175
	17.0	18.76	.346	101	84
E^c	16.5	19.40	−.949	−278	−294
	16.0	19.93	−.963	−282	−298
	15.5	20.52	−.836	−245	−261
	15.0	21.15	−.697	−205	−220
LS	15.0	21.47	2.562	755	740
	16.0	21.82	2.563	756	740
	17.0	22.20	2.562	757	740
	18.0	22.60	2.563	758	740
	19.0	22.98	2.563	759	740
	20.0	23.37	2.562	760	740
	21.0	23.73	2.563	761	740
	22.0	24.12	2.563	762	740
	23.0	24.52	2.564	763	740
	24.0	25.00°	2.562	764	740
		21.01 A²/molecule			
L_2	7.5	15.90°	0.770	222	214
	8.0	16.70	.614	178	170
	9.0	18.31	.614	179	170
	10.0	19.96	.614	180	170
	11.0	21.51	.459	135	124
	12.0	24.69°	0.326	97	85

A similar table, which exhibits the energy relations of a monolayer of hexadecyl alcohol in the L_2 and S states, has been presented in an earlier paper from this laboratory.[7]

Two processes by means of which a film expands may be considered. In *extension* the film covered surface increases in area, while the area of the clean part of the surface remains constant. In *spreading* the area of the film increases, while that of the clean surface decreases by the same amount. It is easily seen that any energy of spreading is smaller than the corresponding energy of extension by an amount equal to the value of that kind of energy for the surface of pure water. This is because in spreading the surface of the water disappears and this makes the energy of its surface available to help produce the monolayer-water surface which appears in its place.

The magnitude of any one of these energy quantities (f, h, q, or s) depends upon and in general increases with: 1. the length of the hydrocarbon chain, 2. the closeness of packing. However, it is affected very greatly by the *nature* of the two-dimensional phase.

Thus, although the molecules are less tightly packed in the intermediate (I) phase than in the liquid condensed (L_2) phase, the energy magnitudes are much larger in the former.

In agreement with (2) the values are very high in the LS phase, and even higher than in the S phase. Thus (Table V) 1650 ergs of heat is absorbed if the monolayer of octadecyl alcohol spreads over 1 cm^{-2} of a water surface at a pressure of 18 dyne cm^{-1}, a temperature of 8.06°C, and a molecular area of 19.96A² per molecule. The increase of entropy has the extremely large value of 5.86 erg cm^{-1} $deg.^{-1}$, which is *forty times larger* than the entropy of the clean surface water.

The energy and entropy of extension are even higher (1764 and 6.0). If a mole of the alcohol in the monolayer could double its area (1.2×10^9 cm^{-2}) without a change in the value of q, the heat absorbed would be 50 kcal. for the mole of

[7] W. D. Harkins, T. F. Young, and E. Boyd, J. Chem. Phys. 8, 961 (1940).

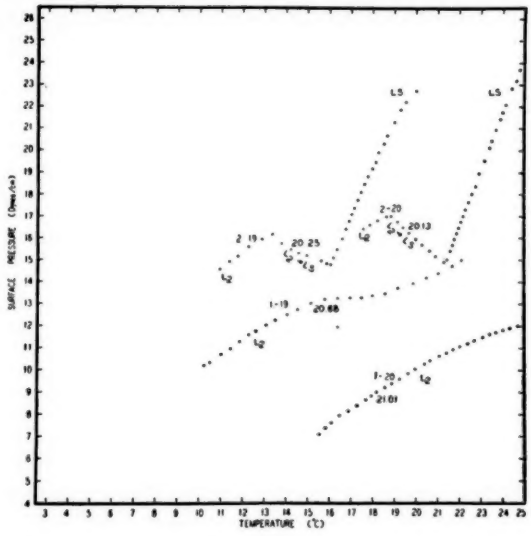

FIG. 9. Pressure-temperature relations for monolayers of the 19 and 20 carbon atom alcohols at the molecular areas in A as indicated. Curves $1 = L_2$ phase, curves $2 =$ transition from L_2 to LS. The slope of these curves gives the entropy of spreading of the monolayer.

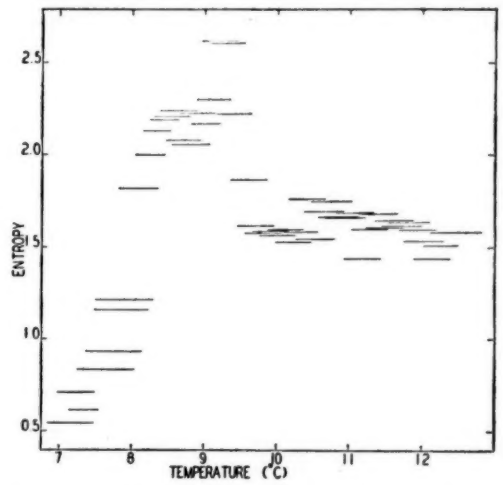

FIG. 10. Entropy of spreading of octadecanol at 19.18 A². The increase of 0.02 A² in molecular area has caused the S phase to disappear.

film. Actually, however, the value of q decreases rapidly as the film expands, usually with discontinuities at each change of phase.

If both the S phase and the L_2 phase are present together the energy of spreading becomes negative. Thus with eicosanol (Table VI) at 20.13A² molecule^{-1} $\pi = 16.50$ and $t = 19.40$, the values of q_s and h_s are, in erg cm^{-2}, -278 and -294, respectively. This is due to the fact, already mentioned, that the transformation of the high pressure to the low pressure phase is accompanied by the emission of heat.

VI. THE VARIATION OF SURFACE PRESSURE WITH TEMPERATURE AT CONSTANT AREA AS RELATED TO THE ENERGY OF EXPANSION

The two preceding sections have given a few examples of the energy magnitudes associated with the first-order transition between the two condensed liquid phases (L_2 and LS), which are very small, and those involved in the extension and spreading of alcohol films. In this section the energy relations are considered in more detail.

The first problem involved in obtaining the energy relations is to obtain the entropy of extension (s_e) and that of spreading (s_s) of the film. Equations which give these values are:

$$s_e = (\partial S/\partial \sigma_f)_{T,\sigma_w} = -(\partial \gamma_f/\partial T)_{\sigma_f}, \tag{4}$$

$$s_s = (\partial S/\partial \sigma_f)_{T,\Sigma} = -(\partial^2 F/\partial T \partial \sigma_f)_{\Sigma} = (\partial \pi/\partial T)_{\sigma_f,\Sigma}. \tag{5}$$

The heat absorbed is

$$q_e = Ts_e, \tag{6}$$

$$q_s = Ts_s \tag{7}$$

and the increase in heat content

$$h_e = (\partial H/\partial \sigma_f)_{T,\sigma_w} = [\partial(\gamma_f/T)/\partial(1/T)]_{\sigma_f},$$

$$h_s = (\partial H/\partial \sigma_f)_{T,\Sigma} = -[\partial(\pi/T)/\partial(1/T)]_{\sigma_f,\Sigma},$$

now π is defined by

$$\pi = \gamma_w - \gamma_f \tag{10}$$

and it can be shown that in Eqs. (4) to (9)

$$s_e = s_s + s_w, \tag{11}$$

$$h_e = h_s + h_w. \tag{12}$$

These equations were given in an earlier paper[8] but, unfortunately, some of the signs given there were incorrect, so it is essential to have them expressed correctly here.

[8] W. D. Harkins, T. F. Young, and E. Boyd J. Chem. Phys. **8**, 954 (1940).

The increase of internal energy on expansion or spreading (ϵ_e or ϵ_s) is almost equal to the increase of enthalpy, or

$$\epsilon_e \approx h_e, \tag{13}$$

$$\epsilon_s \approx h_s. \tag{14}$$

From these equations it is evident that the problem of obtaining the values of the different types of energy increments for the various types of expansion of a monolayer, reduces itself to the determination of the increment (s) in the entropy of the particular change. From Eqs. (4) and (5) it is apparent that this involves obtaining the slopes of curves which give the variation of surface pressure (π) with temperature at constant molecular area. Such curves may be obtained by experiments in which the film is kept at constant area between fixed barriers while the temperature is increased and the pressures are determined. The curves of Fig. 7 and 8 were obtained in this way. Another method is to determine $(\partial\pi/\partial T)_{\sigma f}$, Σ from a set of isotherms such as those of Fig. 1. Lines drawn on this plot at constant values of the molecular area give a set of points which represent the intersections with the isotherms. The values of the entropy are obtained from these points by the use of the chord method.

The values calculated from the data represented by Figs. 7 and 9 are also obtained by this method, and no use is made of the less accurate method of drawing tangents to the curves.

The lowest points in curve 4, Fig. 7, represent the liquid condensed (L_2) phase of octadecanol. As the temperature rises, with the molecular area constant at 19.96A^2, the pressure increases rapidly, while the monolayer passes first into the S state and then into the LS state. The data from two independent experiments at this area are presented more fully in Fig. 8, which gives a chord plot of the entropy $(\partial\pi/\partial T)_{\sigma f}$, Σ of spreading of the film at 19.96A^2, while Fig. 10 exhibits the great change in the entropy relations brought about by an increase in area of only 0.02A^2. The remarkable effect is that the S phase has been made to disappear by the increase of a tenth of one percent in area.

A few of the values thus obtained are listed in Table V, which shows that the heat absorbed (q_s) and the increase of internal energy (ϵ_s) on spreading of the S film are extremely high, with values as large as 1650 erg cm^{-2}, which corresponds to about 1770 erg cm^{-2} for extension.

Thus the increment of internal energy in the extension of the oil film in the S state is fifteen times larger than that for the extension of the clean surface of water, which was formerly considered to exhibit a very high value.

Curve 5, at 19.98A^2 seems somewhat similar but the corresponding chord plot (Fig. 10) shows that the minute increase of 0.02A^2 in the molecular area has eliminated entirely or almost entirely S phase. A few of the corresponding energy values are listed in Table V.

A very slight increase (0.22A^2) to 20.20A^2 in molecular area changes the relations very greatly since the area is getting into the range of the first-order transition $L_2 \rightleftharpoons LS$. According to Table V the heat of spreading in this transition region is -145 erg cm^{-2} at 13 dyne cm^{-1}. Here spreading involves a liberation of heat. The heat involved in the transition $L_2 \rightarrow LS$ is the heat of spreading multiplied by the change in area and, since the change in area is negative, heat is absorbed in the transition as written. This is similar to the case of water in three dimensions; the liquid phase is stable at high pressure, ice is the stable phase at low pressure, and heat is absorbed in the transition from the phase stable at low pressure to that stable at high pressure.

The four points on the left end of curve 6, Fig. 7, represent the liquid L_2, although the fourth point is just at the boundary which separates this from the region of the first-order transition (Fig. 2). The next eight or nine points exhibit a negative slope and represent the *first-order* transition described in the last paragraph. The ascending points on the right represent the LS phase. In this region the increase of internal energy of spreading of the film increases from 76 to 400 erg cm^{-2} (Table V) while each energy increment for *extension* is h_w (or about 116) erg cm^{-2} larger.

Curves 1, 2, and 3, Fig. 7 at 21.03, 20.99, and 20.92A^2 do not exhibit very large changes of slope and represent the liquid condensed phase. The values of ϵ_s vary from 36 to 139 erg cm^{-2}, as shown by the last three sections of Table V which includes values at 20.5A^2, which is a lower area than that represented by the curves.

The extremely remarkable feature revealed by Fig. 6 is the very great effect on the slope and position of the curves of an increase of $0.02A^2$ in molecular area between curves 4 and 5, and of $0.22A^2$ from 5 to 6.

Similar curves for the 18 and 20 carbon atom alcohols are given in Fig. 9. The first four points on the left of curve 2–20, for the 20 carbon atom alcohol, (eicosanol) at $20.13A^2$, represent the L_2 state with values of E_s from 159 to 84 erg cm^{-2}. The next nine points, with a negative slope, lie in the first-order transition region with values of ϵ_s from -294 to -220 erg cm^{-2} as shown in Table VI. These values are found at temperatures from 19.40 to 21.15°C.

The values of the heat of transition as given by $q=(\partial\pi/\partial T)_E(\Sigma_2-\Sigma_1)$ are very small (21.7 to 39.6 cal. $mole^{-1}$) on account of the smallness of the increment $(\Sigma_2-\Sigma_1)$ in area during the first-order change.

The sharpness of the minima and maxima of curves 2–20 and 2–19 of Fig. 9 as compared with those of curve 6 of Fig. 7 is due to the fact that the former curves are more nearly in the center of the region of the first-order change, so the change in the slope $d\pi/dT$, which is the entropy of spreading, is much more sudden. The maxima represent changes of entropy from positive to negative, and the minima from negative to positive.

It should not be forgotten in the consideration of the relations presented above that the transition $L_2 \rightleftharpoons LS$ is first-order and involves a latent heat of phase change only if the temperature is between about 7.5°C and 12°C, while at all higher temperatures the transition is second-order, as is the transition $L_2 \rightleftharpoons S$ at temperatures below 7.5°C.

VII. EXPERIMENTAL METHODS

The experimental methods employed in this work were, in general, the same as those used recently in this laboratory for the accurate determination of the relations between film pressure, molecular area, temperature, and surface potential. As usual the films were tested for homogeneity by the use of a dark field microscope.

However, it was necessary to improve the methods in two respects:

1. The control of the temperature of the film, which, by the use of a thermostat was regulated to ±0.01°C.
2. The determination of area.

In order to obtain the phase relations of the L_2, LS, and S phases it was necessary to have a much higher accuracy and precision in the determination of molecular area than had ever been obtained before. As is the usual procedure in this laboratory the volumes of the pentane-hexane solutions of the long chain alcohols were measured in the precision pipette designed by Harkins, and all weighings were made on a balance of very high accuracy and sensitivity. From three to seven independent determinations were made of the position of each $\pi-\sigma$ isotherm, and excellent agreement was obtained. The precision in the relative location of each set of curves was increased by obtaining $\pi-T$ curves at different constant molecular areas. The positions of the $\pi-\sigma$ isotherms were then shifted (very slightly) to fit the $\pi-T$ curves. It was quite remarkable that in no case did this make necessary a shift of any isotherm beyond the limits of the small mean error calculated for the individual isotherm from the various determinations of its position.

VIII. DISCUSSION

The experimental work shows that the liquid condensed (L_2) phase of an alcohol monolayer may, at constant temperature, be transformed by increase of pressure and a resultant decrease of area, into either an SL or an S phase, and that both of these have approximately the same compressibility. Either phase transition ($L_2 \rightleftharpoons LS$ or $L_2 \rightleftharpoons S$) usually occurs without the evolution or absorption of heat, and is therefore of the second order. However, an exception is found in that, if the temperature is decreased sufficiently the $L_2 \rightleftharpoons LS$ transition changes to a first-order transition.

If a three-dimensional organic solid is melted ($S \rightarrow L$) isothermally by an increase of pressure, there is an absorption of heat. In this transition the high pressure phase absorbs heat in its change to the low pressure phase. If ice is melted isothermally it absorbs heat, but changes from

the low pressure phase to the high pressure phase. If the low pressure phase (L_2) of the alcohol film is converted isothermally into the high pressure phase, along an isotherm which exhibits a first-order change, heat is absorbed. In this aspect of the transition the liquid condensed (L_2) liquid phase resembles ice, and the LS phase, water.

The investigation described here was undertaken in order to discover a first-order transition between the high and the low pressure phases of an alcohol film. It was considered possible that such a transition might enter on lowering the temperature to some unknown but definite value.

It was supposed, however, that such a transition, if found to exist at all, would persist to considerably lower temperatures (presumably with an increase of the latent heat of the transition with lowering of temperature as is found to be true). The isotherms of Fig. 1, when considered only casually seem to contradict this supposition that the transition persists to low temperatures, since the first-order transition which appears, on lowering the temperature, at about 11°, does not persist much below 9°. This disappearance of the first-order change is, however, associated with the metastability of the LS film at the lower temperatures. At temperatures below 7.5°C the transition $L_2 \rightarrow LS$ cannot occur, since below this temperature the S film becomes the more stable of the two. As soon as the transition becomes one between the L_2 and the S phases the order of the change immediately reverts to the customary second order.

It would be of interest to develop a plausible theory to account for the fact that in the region of the first-order change heat is absorbed in the isothermal change from the low pressure (L_2) to the high pressure (LS) phase. At present the experimental work is not sufficiently extensive to enable us to develop such a theory. If the analogy with the ice (low pressure) to water (high pressure) transition is used to suggest an hypothesis, it might be assumed that the liquid condensed (L_2) or low pressure phase possesses more structure, and more binding energy than the LS or high pressure phase. This would, by Eyring's theory, accord with the fact that the viscosity of the L_2 phase at a very low pressure, is about ten times greater than that of the high pressure LS phase. This would indicate the existence of some type of binding, in the L_2 film, which should disappear gradually as the intermolecular distance, in this phase, decreases. The nature of a binding of this type is unknown, but in later work an attempt will be made to see if hydrogen bond interactions between the monolayer (hydroxyl groups) and the water, offer the possibility of a decrease of bonding energy with decrease of area per hydroxyl group from about $22A^2$ to about $20.5A^2$.

One important property of the first-order change is that while each increase by one of the number of carbon atoms in the molecule increases the temperature of the transition by about 5°C, and the pressure, by about 2 dyne cm^{-1}, there is almost no change in the limits of the molecular area for the transition. However, this particular fact does not lead to any particular theory, since it would seem to accord with almost any plausible type of theory.

An interesting fact illustrates the complexity of the relations in the vicinity of the first-order change. While the temperature of the "flat" rises by about 5° per carbon atom, and the pressure by about 2 dyne cm^{-1}, the position in area and pressure of the second-order transition is almost the same in curve 13 of Fig. 1 for octadecanol, and curves 3 of Fig. 4 for nonadecanol. However the temperature is 30.3° with 18 carbon atoms but only 21.7° with 19 carbon atoms. Thus an increase of one carbon atom makes it necessary to *lower* the temperature by 8.6° to obtain the same pressure (15.3 dyne cm^{-1}) and area ($20.62A^2$) for the second-order transition.

. This publication was made possible by funds granted by the Carnegie Corporation of New York. That Corporation is not, however, the author, owner, publisher, or proprietor of this publication, and is not to be understood as approving by its grant any of the statements made or views expressed therein.

The Third Law of Classical Thermodynamics

PAUL C. CROSS AND HARTLEY C. ECKSTROM
Brown University, Providence, Rhode Island

(Received February 13, 1942)

The third law, or law of limits as $T\rightarrow 0°$K, is expressed as: "for any real phase

$$\operatorname{Lim}_{T\rightarrow 0}\left(\frac{\partial S}{\partial x_i}\right)_{x_j,\,n}=0,$$

and for any spontaneous isothermal process,

$$\operatorname{Lim}_{T\rightarrow 0}\Sigma_i\nu_i\left(\frac{\partial S}{\partial n_i}\right)_{T,\,y,\,n_j}\leq 0."$$

The equality sign applies to reversible processes and the inequality sign to irreversible processes. The n's represent composition variables, the x's (or T and the y's) a suitable set of state variables, and the ν's the number of moles of the components entering into the reaction (positive for products, negative for reactants). Alternative statements of the third law are given and derived from the above statement. The completeness of this statement as a usable postulate for the further development of classical thermodynamics is briefly discussed.

INTRODUCTION

LET us begin the discussion of the statement of the third law by a summary of the postulates necessary to form a basis for the development of a practical science of thermodynamics.

(1) There exist single valued functions of the state of the system which are: (a) The internal energy U; (b) the absolute temperature T; (c) the entropy S.

(2) These functions are such that: (a) For any infinitesimal change,

$$dU=dQ-dw,$$

where dU (a perfect differential) represents the change of the function U, dQ is the heat absorbed, and dw is the work done by the system during the change. (b) A temperature T may be assigned to any material system which is in thermal equilibrium, and this absolute temperature T is a function of the empirical temperature t only.[1] (c) For any infinitesimal change

$$dS\geqslant dQ/T,$$

where the equality sign applies to reversible processes and the inequality sign to irreversible processes. Furthermore, the entropy of an isolated system increases spontaneously until the isolated system reaches a state of equilibrium,[2] that is, $dS\geqslant 0$.

(3) The behavior of certain properties of a system as $T\rightarrow 0°$K may be expressed in terms of the following properties of the entropy function:

(a) For any real phase

$$\operatorname{Lim}_{T\rightarrow 0}\left(\frac{\partial S}{\partial x_i}\right)_{x_j,\,n}=0.$$

(b) For any spontaneous *isothermal* process

$$\operatorname{Lim}_{T\rightarrow 0}\sum_i \nu_i\left(\frac{\partial S}{\partial n_i}\right)_{T,\,y,\,n_j}\leqslant 0.$$

The equality sign applies to reversible processes and the inequality sign to irreversible processes. The n's represent composition variables, the x's (or T and the y's) a suitable set of state variables and the ν's the number of moles of the components entering into the reaction (positive for products and negative for the reactants).

The statements under (1) and (2) constitute a generally accepted set of postulates: sometimes referred to as the zeroth law, the definition of T; the first law, the definition of U; and the second law, the definition of S. We propose the state-

[1] The empirical temperature t is the temperature as measured on any scale determined only by the choice of the thermometer system. It may, for example, be the temperature as determined by a constant pressure air thermometer.

[2] This may be a state of stable, metastable, or neutral equilibrium.

ments under (3) as a formulation of the third law of thermodynamics[3] which has certain advantages over the formulations now commonly employed.

Fowler and Guggenheim[4] have discussed objections to the usual statements of the third law, which are essentially modifications of the Nernst heat theorem. Briefly, these objections are based upon the fact that certain reservations must be made in the interpretation of these statements which have the effect of limiting their applicability. One thus encounters the expressions, "exceptions to the third law" and the "so-called third law" which definitely place the third law in an inferior position relative to the other laws of thermodynamics. To avoid this, Fowler and Guggenheim propose the use of the *principle of the unattainability of the absolute zero of temperature* as the third law. Although this is accepted as universally valid, we wish to call attention to the fact that it is not generally useful until supplemented by further postulates. For example, the derivation of the Nernst heat theorem requires the additional postulate of the convergence of the heat capacity integral $\int_0^T C_{y,n} d \ln T$. Our above statement is the result of an attempt to express the third law in a form which is: (1) Universally valid; (2) complete as a postulatory basis for further development; (3) capable of yielding any of the other expressions formerly given as statements of the third law.

The expression "spontaneous isothermal process" includes chemical reactions, phase changes, or any change expressible in terms of variations of the amount of any component in any phase of the system. Note especially that in order to apply the third law in the form given above, these processes must be written *in the only direction in which they could possibly occur isothermally at temperatures approaching the absolute zero.*[5]

APPLICATIONS OF THE THIRD LAW

The Determination of Some Limits at $T \rightarrow 0°K$

From part (a) of the third law, it is possible to derive limits for a real phase of fixed composition which lend themselves to experimental verification and to useful application.

First consider only the usual type of thermodynamic system, for which $S = S(T, p, n_1, n_2, \cdots)$. It follows immediately that the third law requires

$$\lim_{T \rightarrow 0} \frac{C_p}{T} = 0, \quad \lim_{T \rightarrow 0} \left(\frac{\partial v}{\partial T} \right)_{p,n} = 0.$$

If S is given as $S(T, v, n_1, n_2, \cdots)$, then

$$\lim_{T \rightarrow 0} \frac{C_v}{T} = 0, \quad \lim_{T \rightarrow 0} \left(\frac{\partial p}{\partial T} \right)_{v,n} = 0.$$

To illustrate the application to other types of systems, consider one for which $S = S(T, p, \mathfrak{H}, n_1, \cdots)$, where $\mathfrak{H}$ represents the homogeneous magnetic field strength in the absence of the system. The third law then requires that

$$\lim_{T \rightarrow 0} \left(\frac{\partial S}{\partial \mathfrak{H}} \right)_{T,p,n} = 0.$$

The validity of these consequences of the third law and of other similar expressions is verified by experimental results insofar as the latter supply an adequate test, and may be further confirmed by arguments based upon quantum statistics.

It also follows from part (a) of the third law that for *a given amount of a single component, single phase system*

$$\lim_{T \rightarrow 0} S = S^\circ,$$

where S° *is finite and independent of all the variables which describe the state of the system.*

[3] An equivalent descriptive statement is: "(a) As $T \rightarrow 0°K$, the entropy of any real system becomes independent of all state variables, and: (b) As $T \rightarrow 0°K$, the entropy change for any spontaneous reversible isothermal process becomes equal to zero, and for any spontaneous irreversible isothermal process, becomes negative." The authors prefer the analytic form because its essential equivalent must be deduced from any descriptive form before the latter is of use in the formal development of thermodynamics. For the student of thermodynamics, it is easier to deduce physical behavior from mathematical statements than to formulate the latter from the former.

[4] R. H. Fowler and E. A. Guggenheim, *Statistical Thermodynamics* (Macmillan, New York, 1939), p. 224.

[5] The impossibility of a reaction, such as $Si + O_2 \rightarrow SiO_2$ (glass), leading to a metastable state, in the limit $T \rightarrow 0°K$ is implied by this statement. This, of course, cannot be confirmed *a priori*, but if such a reaction were possible, one could, in principle, use it to attain 0°K, in contradiction to the accepted principle of the unattainability of the absolute zero of temperature.

The Dependence of the Entropy upon Temperature

For any system, S may be taken as $S=S(T, y_1, y_2 \cdots n_1, n_2 \cdots)$. The following important result is readily derived from the above analytical form of the third law:

$$S=\int_0^T \left(\frac{\partial S}{\partial T}\right)_{y,n} dT+S^\circ(n) = \int_0^T \frac{C_{y,n}}{T} dT+S^\circ(n), \quad (1)$$

where $S^\circ(n)$ is a function of composition variables only.[6]

Since the conditions for stability of a thermodynamic system require $C_{y,n}$ always to be positive and not zero for any temperature $T \neq 0°\text{K}$, it follows that $\int_0^T C_{y,n} d \ln T$ approaches zero positively as $T \to 0°\text{K}$ and that $S-S^\circ(n) \gtrless 0$.

The Nernst Heat Theorem

From part (b) of the third law one may readily obtain the Nernst heat theorem. Let us introduce the notation

$$\left(\frac{\partial S}{\partial n_i}\right)_{T,y,n_j} = \bar{S}_i.$$

Where $y=p$ and no other external forces are acting, $\bar{S}_i$ is the usual *partial molal entropy* of the i-component. Hence

$$\sum_i \nu_i \left(\frac{\partial S}{\partial n_i}\right)_{T,y,n_j} = \sum_i \nu_i \bar{S}_i = \Delta S.$$

From the third law

$$\lim_{T \to 0} \sum_i \nu_i \bar{S}_i = \sum_i \nu_i \bar{S}_i^\circ \leqslant 0.$$

Now neglect the irreversible processes. For any *reversible* process, then

$$\sum_i \nu_i \bar{S}_i^\circ = \lim_{T \to 0} \Delta S = 0. \quad (2)$$

For a process to be reversible, the phases entering into the reaction at any given temperature must be in states of equilibrium at that temperature. If the state of equilibrium for any phase is one of frozen metastable equilibrium, then the process must not disturb this state of equilibrium. It can readily be seen that this statement (2) is equivalent to the statement of the Nernst heat theorem as given by Fowler and Guggenheim: "For any isothermal process involving only phases in internal equilibrium or, alternatively, if any phase is in frozen metastable equilibrium, provided the process does not disturb this frozen equilibrium $\lim_{T \to 0} \Delta S = 0$."

The So-Called Absolute Entropy

In any experimental determination of the entropy of a given substance only *entropy differences* can be determined. It follows that an entropy scale can be constructed for each substance by assigning an arbitrary value to S°. However, because of the requirement that $\Sigma_i \nu_i \bar{S}_i^\circ = 0$ (for reversible isothermal processes) the values of the S°'s are not all independent. For the construction of a useful scale upon which to represent entropies it is necessary to specify in some convenient way the arbitrary values of S° for a complete set of independent substances. As long as nuclear processes and isotopic separations are neglected, it is obvious that the chemical elements form such a complete independent set. By convention, therefore, the value zero is assigned to S° for each element in its state of stable equilibrium. This requires that $S^\circ = 0$ for all pure substances in their states of stable equilibrium, and that $S^\circ > 0$ for these substances in any other state. These conclusions were expressed by Lewis and Gibson in the following statement now commonly quoted as the third law. "If the entropy of each element in some crystalline state be taken as zero at the absolute zero of temperature, every substance has a finite positive entropy, but at the absolute zero of temperature the entropy may become zero,

---

[6] If $S=S(T, y, n)$ one obtains upon integration over the state variables

$$S=\int_0^T \left(\frac{\partial S}{\partial T}\right)_{y,n} dT+\int_{y_1^\circ}^{y_1} \left(\frac{\partial S}{\partial y_1}\right)_{T,y_2 \cdots n}\Bigg]_{T=0} dy_1 + \int_{y_2^\circ}^{y_2} \left(\frac{\partial S}{\partial y_2}\right)_{T,y_1,y_3 \cdots n}\Bigg]_{\substack{T=0 \\ y_1=y_1^\circ}} dy_2 \cdots + S^\circ(n).$$

The third law requires that

$$\left(\frac{\partial S}{\partial y_1}\right)_{T,y_2 \cdots n}\Bigg]_{T=0} = \left(\frac{\partial S}{\partial y_2}\right)_{T,y_1,y_3 \cdots n}\Bigg]_{\substack{T=0 \\ y_1=y_1^\circ}} = \cdots = 0$$

and the above relation (1) follows at once.

and does so become in the case of perfect crystalline substances."

It is to be noted that their expression "perfect crystalline substances" should be interpreted as the substance in its state of stable equilibrium as $T \rightarrow 0°K$.

It is obvious from the foregoing discussion that the values $S^\circ = 0$ for the elements and the resulting "absolute" entropy scale have no theoretical significance. In fact, this convention may indeed have to give way in the future to one which assigns $S^\circ = 0$ for pure isotopes of the elements in their stable states. The chemical elements would then have a finite positive entropy, the entropy of mixing of their isotopic constituents, at $T = 0°K$.

Apparent Exceptions to the Nernst Heat Theorem

The phenomena often discussed as "exceptions of the third law" should now more properly be described as "apparent exceptions to the Nernst heat theorem." Experimentally, the only means of studying the applicability of the Nernst heat theorem is to evaluate the heat capacity integrals $\int_0^T C_{y,n} d \ln T$ for the substances involved in the given process. This necessitates a knowledge of the heat capacity of these substances in states of stable equilibrium, or of undisturbed frozen metastable equilibrium, from 0°K to T°K. Part of this "knowledge" must be obtained by an extrapolation from the lowest available temperature to 0°K. The two main experimental causes of apparent exceptions to the Nernst heat theorem are: (1) Failure of the system to maintain the proper state of equilibrium (for the process in question) during the heat capacity measurements; (2) failure of the extrapolation of the heat capacity measurements to predict correctly the true heat capacity in the region of extrapolation.

The Unattainability of the Absolute Zero of Temperature

The limiting cases of the methods by which the temperature of a system may be lowered are: (1) The removal of heat from the system by transfer to a colder body; (2) the occurrence within the system of a spontaneous process yielding a state of lower temperature.

Obviously the first method cannot be used to lower the temperature of a system to 0°K because it would require the existence of an infinite heat reservoir at 0°K.

That the process of the second method must be spontaneous can be deduced from arguments concerning the stability of real systems. In general this method implies the occurrence of a process capable of decreasing the energy of the system by the performance of work, and such a process must necessarily be spontaneous.

Let any conceivable process for lowering the temperature of any conceivable system be represented by

$$A(T'y'n') \rightarrow B(T''y''n''),$$

where $T'y'n'$ are the values for the initial state of a set of variables capable of completely describing the system and $T''y''n''$ the corresponding values for the final state. T' is any temperature, however low, but not 0°K. Let us now show that T'' cannot be 0°K by showing that the assumption $T'' = 0°K$ leads to a contradiction of the third law.

Since the process must be spontaneous, the entropy change must be $\geqslant 0$.

$$\Delta S = S_B - S_A = \int_0^{T''} C_B d \ln T + S^\circ_B - \int_0^{T'} C_A d \ln T - S^\circ_A \geqslant 0.$$

From the third law

$$S^\circ_B - S^\circ_A = \operatorname*{Lim}_{T \rightarrow 0} \Delta S \leqslant 0.$$

If now we were to set $T'' = 0°K$

$$0 \geqslant S^\circ_B - S^\circ_A \geqslant \int_0^{T'} C_A d \ln T.$$

But the integral is always positive for any value of $T' \neq 0°K$, and we are forced to conclude that $T'' \neq 0°K$. This is true even for the most idealized case, that of an adiabatic reversible process, where the equality signs apply. Hence, "it is impossible by any procedure, no matter how idealized, to reduce the temperature of any system to the absolute zero in a finite number of operations." This is the principle of the unattainability of the absolute zero of temperature.

CONCLUSION

There are numerous ways, both descriptive and analytic, in which the basic principles of the third law may be satisfactorily expressed. The expression here advocated is favored because:

(1) Partial derivatives enter directly in most applications of the third law.

(2) The convergence of integrals of the type

$$\int_0^T \left(\frac{\partial S}{\partial T}\right)_{y,n} dT$$

becomes a part of the postulatory basis of classical thermodynamics.

(3) It includes the limiting behavior, as $T \rightarrow 0°K$, of the entropy as a function of both state and composition variables.

(4) It gives information relating to both reversible and irreversible isothermal processes for any real system.

(5) It is universally valid, thereby permitting it to rank as a *law* of thermodynamics.

(6) It leads naturally to the definition of an arbitrary zero of entropy such that (a) no system ever has a negative entropy, and (b) the zero of entropy could be obtained by a system only at the absolute zero of temperature.

MAY, 1942 JOURNAL OF CHEMICAL PHYSICS VOLUME 10

On the Strength of Carbon-Hydrogen and Carbon-Carbon Bonds

D. P. STEVENSON[1]
Westinghouse Research Laboratories, East Pittsburgh, Pennsylvania

(Received February 27, 1942)

Electron impact critical potentials are combined with thermochemical data to obtain values for the heats of the dissociation reactions, $CH_4 = CH_3 + H$, $C_2H_6 = C_2H_5 + H$, $C_2H_6 = 2CH_3$, and $nC_4H_{10} = 2C_2H_5$. The values found are: $D(CH_3-H) = 101$ kcal./mole, $D(C_2H_5-H) = 96$ kcal./mole, $D(CH_3-CH_3) = 82.6$ kcal./mole and $D(C_2H_5-C_2H_5) = 77.6$ kcal./mole. These values are compared with estimates based on kinetic and photochemical data.

VARIOUS estimates of the kinetically important energetic quantities, $D(CH_3-H)$ and $D(CH_3-CH_3)$, made by combining thermochemical data with either kinetic or photochemical data are not in good agreement. In this communication we shall discuss the application of still another source of energetic data, electron impact critical potentials, to this problem. It will be shown that certain reasonable assumptions as to the nature of the potential energy surfaces for the aliphatic ions, $C_nH_{2n+2}^+$, permit estimates of $D(CH_3-H)$ and $D(C_2H_5-H)$ to be made. In particular, data on ethane, propane, and the two isomeric butanes will be discussed.

The interpretation of electron impact data involves two difficulties. The first of these evolves from the necessity of correcting the voltage scale for contact potentials associated with the filament (source of bombarding electrons). The usual procedure is to compare the ionization efficiency curves for the processes of interest with that of a monatomic gas (usually argon), taken under similar conditions of sensitivity.[2] It is then assumed that the difference between the energies at which the first upward breaks of the two curves (process of interest and argon) occur gives the difference (δ) between the desired critical potential and the ionization potential (I^a) of argon. Since the latter quantity is known accurately from spectroscopic data, the critical potential is given by $I^a - \delta$. The assumption that the form of the ionization efficiency curves for the simple ionization of an atom and the ionization and dissociation of a complex molecule will be the same in the vicinity of the critical energy is without theoretical justification. Pronounced differences are to be noted in the experimental curves. It has been found, however, that the

[1] Westinghouse Research Fellow.

[2] L. G. Smith, Phys. Rev. **51**, 263 (1937).

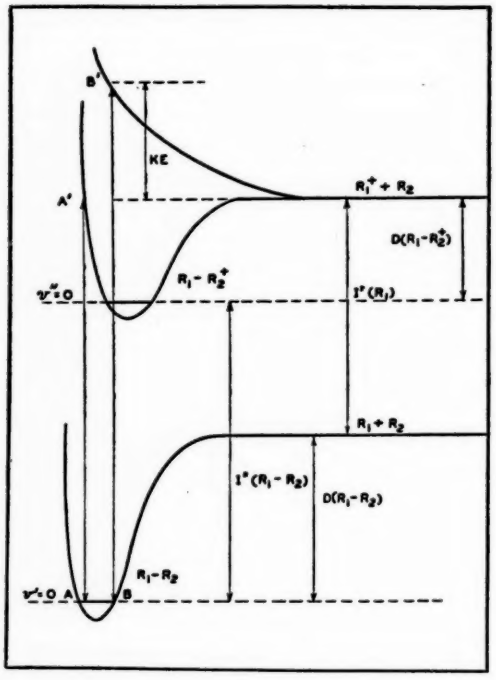

FIG. 1. Schematic cross section through the potential energy surfaces of the hydrocarbon molecule and molecular ion R_1-R_2 and $R_1-R_2^+$. The energy axis has not been drawn with a uniform scale. For orientation purposes the $I^z\sim 9$–13 ev while $D(R-R)\sim 4.0$ ev.The abscissa may be thought of as the R_1-R_2 distance.

ionization efficiency curves for similar process in related molecules are very much alike in form.[3] The data upon which the calculations in this article are based will involve only the differences in position of break of curves for such similar processes. This, it is to be hoped, will avoid or at least lessen considerably this objection.

Even after critical potentials (or apparent critical potentials) have been determined for the formation of ionic fragments from a molecule, the question of their relationship to the difference in energy between the molecule and its fragments remains open. Two of the possible correlations of the critical potential A_c for the formation of R_1^+ from R_1-R_2 are illustrated in the schematic energy diagram given in Fig. 1. The R's stand for aliphatic radicals or hydrogen atoms. If we correlate BB' with A_c, we write

$$A_c(R_1^+)=D(R_1-R_2)+I^z(R_1)+\text{K.E.} \quad (1)$$

[3] D. P. Stevenson and J. A. Hipple. To be published.

Since the repulsive energy of the antisymmetric state of H_2^+ increases very much more rapidly than the binding energy of the symmetric state with decreasing proton-proton distance,[4] we can probably assume the same would apply to the antibonding states of $R_1-R_2^+$. Under these conditions, K.E.>5 ev. Actually for many processes, where reasonable estimates of D and I^z can be made, K.E. is found to be <0.5 ev.

We will assume that the proper correlation is $A_c(R_1^+)\sim AA'$, or

$$A_c(R_1^+)\leq D(R_1-R_2)+I^z(R_1). \quad (2)$$

The inequality sign arises from the possibility that the transition is from a higher vibrational state than $V'=0$. Equation (2) has been written to conform with our curves, which assume no activation energy for the formation of the R_1-R_2 bond in $R_1-R_2^+$. This is in accord with the calculations of Gorin, Kauzmann, Walter, and Eyring.[5] It will be presumed that by taking differences between A_c's only, any errors due to vibrational excitation will cancel. The consequences of the failure of the assumption with respect to zero activitation energy for bond formation will be discussed later.

All the data pertinent to the calculations are summarized in Table I. The thermochemical quantities are from the review article by Rossini,[6] while the apparent (uncorrected) critical potentials are from unpublished work in this laboratory.[3] It should be mentioned that while our results on ethane are in excellent agreement with those of Hipple[7] the agreement with the work of Delfosse and Bleakney[8] on propane is not good. In order to avoid possible inconsistencies we use only data obtained in our instrument.

In the following calculations we assume A_c to be given by Eq. (2) with the equality sign, and that

$$D(R_1-R_2)=H^\circ(R_1)+H^\circ(R_2)-H^\circ(R_1-R_2). \quad (3)$$

[4] L. Pauling and E. B. Wilson, *Introduction to Quantum Mechanics* (McGraw-Hill Book Company, New York, 1935), p. 330.
[5] E. Gorin, W. Kauzmann, J. Walter, and H. Eyring, J. Chem. Phys. **7**, 633 (1939).
[6] F. D. Rossini, Chem. Rev. **27**, 1 (1940).
[7] J. A. Hipple, Jr., Phys. Rev. **53**, 530 (1938).
[8] J. Delfosse and W. Bleakney, Phys. Rev. **56**, 256 (1939).

From the data on H_2, CH_4, C_2H_6, and C_3H_8 we write:

$$\begin{aligned} &C_2H_6+CH_4=C_3H_8+2H \quad \Delta H°_{298.1}=5.08 \text{ ev} \\ &C_3H_8 \quad\quad =C_2H_5^++CH_3 \quad\quad A_c=14.5_0 \\ &H+C_2H_5^+=C_2H_6 \quad\quad -A_c=15.2_0, \end{aligned} \tag{a}$$

adding to

$$CH_4=CH_3+H \quad D(H_3C-H)=4.38 \text{ ev}.$$

Although we have the critical potentials for the formation of CH_3 from both normal and isobutane the unresolved ambiguity as to whether the $C_3H_7^+$ formed from propane is the normal, or iso-isomer reduces us to but one independent estimate. From the data on H_2, CH_4, C_3H_8, and C_4H_{10} we write, assuming the dissociation of the butanes involves no rearrangement, either b_1,

$$\begin{aligned} &C_3H_8+CH_4=nC_4H_{10}+2H \quad\quad \Delta H°_{298.1}=5.06 \text{ ev} \\ &nC_4H_{10}=nC_3H_7^++CH_3 \quad\quad A_c=13.5_0 \end{aligned}$$

(i or n)

$$C_3H_7^++H=C_3H_8 \quad\quad -A_c=13.9_5$$

which add to give

$$CH_4=CH_3+H \quad\quad D(CH_3-H)=4.61 \text{ ev}$$

or b_2,

$$\begin{aligned} &C_3H_8+CH_4=iC_4H_{10}+2H \quad\quad \Delta H°_{298.1}=4.99 \text{ ev} \\ &iC_4H_{10}=iC_3H_7^++CH_3 \quad\quad A_c=13.3_0 \end{aligned}$$

(i or n)

$$C_3H_7^++H=C_3H_8 \quad\quad -A_c=13.9_5$$

which add to

$$CH_4=CH_3+H \quad\quad D(CH_3-H)=4.34 \text{ ev}.$$

Data on propylene and isobutylene[3] may be similarly combined to give $D(CH_3-H)\leq 4.4_8$ ev. The values given by Cummings and Bleakney[9] for the appearance potentials of the ion CH_2OH^+ from methyl and ethyl alcohols,

$$CH_3OH\,;\, A_c(CH_2OH^+)=11.3 \text{ ev}$$

and

$$C_2H_5OH\,;\, A_c(CH_2OH^+)=11.8 \text{ ev}$$

and the heat of the reaction,

$$CH_3OH+CH_4=C_2H_5OH+2H,$$

$\Delta H°_{291.1}=4.92$ ev[10] give $D(CH_3-H)=4.42$ ev.

[9] C. S. Cummings and W. Bleakney, Phys. Rev. **58**, 787 (1940).

[10] F. R. Bichowsky and F. D. Rossini, *Thermochemistry* (Reinhold, New York, 1936).

The fact that the assumption that propane dissociates to $nC_3H_7^+$ gives a value of $D(CH_3-H)$ considerably larger than the other estimates and well-known relative weakness of secondary C–H bonds[11] leads us to choose b_2 in preference to b_1. A reasonable mean value of these estimates of $D(CH_3-H)$ is $4.3_8\pm 0.2$ ev or 101 ± 4.5 kcal./mole. Corresponding to this choice of $D(CH_3-H)$ we can now write:

$$\begin{aligned} &C_2H_6+2H=2CH_4 \quad \Delta H°_{298.1}=-5.18 \text{ ev} \\ &2CH_4=2CH_3+2H \\ &\quad\quad 2D(CH_3-H)=8.76 \text{ ev} \\ &C_2H_6=2CH_3 \\ &\quad\quad D(CH_3-CH_3)=3.58\pm 0.4 \text{ ev} \\ &\quad\quad\quad\quad =82.6\pm 9 \text{ kcal./mole}. \end{aligned} \tag{C}$$

We have information on but one reaction yielding C_2H_5. From the data on H_2, C_2H_6, and nC_4H_{10} we write;

$$\begin{aligned} &2C_2H_6=nC_4H_{10}+2H \quad \Delta H°_{298.1}=4.96 \text{ ev} \\ &nC_4H_{10}=C_2H_5^++C_2H_5 \quad\quad A_c=14.4_0 \\ &H+C_2H_5^+=C_2H_6 \quad\quad -A_c=15.2_0, \end{aligned} \tag{D}$$

which add to give

$$\begin{aligned} &C_2H_6=C_2H_5+H \\ &\quad\quad D(C_2H_5-H)=4.1_6\pm 0.2 \text{ ev} \\ &\quad\quad\quad\quad =96.2\pm 4.5 \text{ kcal./mole}. \end{aligned}$$

From this we find

$$\begin{aligned} &nC_4H_{10}=2C_2H_5 \\ &\quad\quad D(C_2H_5-C_2H_5)=3.3_6\pm 0.4 \text{ ev} \\ &\quad\quad\quad\quad =77.6\pm 9 \text{ kcal./mole}. \end{aligned}$$

The most recent estimates of $D(H_3C-H)$ are

TABLE I.

Molecule	$\Delta H°_{298.1}$*	$A_c(R_1^*+H)$†	$A_c(R_2^*+CH_3)$	$A_c(R_3^*+C_2H_5)$
CH_4	−0.775 ev			
C_2H_6	−0.876	$15.2_0\pm 0.1$ ev		
C_3H_8	−1.073	$13.9_5\pm 0.1$	$14.5_0\pm 0.1$ ev	
n C_4H_{10}	−1.289		$13.5_0\pm 0.1$	$14.4_0\pm 0.1$ ev
i C_4H_{10}	−1.360		$13.3_0\pm 0.1$	
$H_2=2H$	$\Delta H°_{298.1}=4.502$ ev			

* The heat of formation of the gas from graphite and $H_2(g)$, reference 6 of text. 1 kcal./mole = 0.04338 ev (Herzberg, *Molecular Spectra*, I).

† The apparent critical potentials for the processes indicated in parenthesis. The initial break of the ionization efficiency curve of argon (A^+) occurs at 18.05 ± 0.1 ev on this scale. $I^a(A)=15.69$ ev (Bacher and Goudsmit, *Atomic Energy States* (McGraw-Hill Book Company, New York, 1932).

[11] F. O. Rice and K. K. Rice, *Aliphatic Free Radicals* (Johns Hopkins Press, Baltimore, 1935).

TABLE II.

Molecule	$A_c(R-CH_3^+)$	$A_c(R^+ + CH_3)$	δ
C_3H_8	$13.5_0 \pm 0.1$ ev	$14.5_0 \pm 0.1$ ev	1.0 ev
$n\,C_4H_{10}$	$12.7_0 \pm 0.1$	$13.5_0 \pm 0.1$	0.8
$i\,C_4H_{10}$	$12.7_0 \pm 0.1$	$13.3_0 \pm 0.1$	0.6

those of H. S. Taylor and his co-workers,[12] Burton,[13] and Taylor and Burton.[14] The estimate of H. S. Taylor and co-workers,[12] based on kinetic data on the reactions of methane with deuterium atoms and methyl radicals with *HD* at but one temperature, is 108 kcal./mole. Burton[13] found 94.8 kcal./mole from an interpretation of photochemical data. Taylor and Burton[14] calculated +103 kcal./mole by the methods of Voge.[15] It will be noted that our value is in best agreement with the theoretical estimate and roughly the mean of the kinetic and photochemical estimates.

If we were to assume that the reactions $CH_3 + R^+ \rightarrow R\,CH_3^+$ have activation energies of about 8–9 kcal./mole and the reaction $H + R^+ \rightarrow RH^+$ zero activation energy our results would be brought into agreement with those of Burton. Rice and Herzfeld[16,17] assume 8 kcal./mole as the activation energy of combination of aliphatic free radicals. As was mentioned above, the calculations of Eyring and his co-workers[5] indicate no such activation to be necessary. The failure of theory to account for the barrier restricting rotation in ethane makes one tend to discount the validity of its application to other related problems.[18] Inasmuch as reasonable doubt also exists with respect to Burton's assumptions regarding the interpretation of the onset of diffuseness, predissociation, and the relative position of potential energy surfaces, other sources of information must be tapped before a decision can be reached. It is clear that a sharpening of the theoretical calculations would be highly desirable.

If one ignores the question about the forms of the ionization efficiency curves for dissimilar processes occurring in the same molecule, the electron impact data seem to indicate very small activation energy for the formation of a bond between an aliphatic ion and a methyl radical. In Table II we give a comparison of the apparent critical potentials for the reactions

$$R-CH_3 \rightarrow R\,CH_3^+ \quad \text{and} \quad R\,CH_3 \rightarrow R^+ + CH_3.$$

The difference $A_c(R^+) - A_c(R-CH_3^+)$ gives a measure of the sum, $D(R-CH_3^+)$ + activation energy. If we were to take an activation energy of 9 kcal./mole ($\sim$0.4 ev) we would find $D(R-CH_3^+) \leq 0.6$ ev a limit which seems too low, when compared to the binding energies in the electron deficient molecules B_2H_6 and H_2^+.

In the light of our estimated error and the uncertainties of interpretation, no significance can be attached to the apparent difference between $D(CH_3-H)$ and $D(C_2H_5-H)$ and the associated carbon-carbon bond strengths, even though the differences agree with other estimates.[11]

In conclusion the author would like to acknowledge helpful discussion and criticism by Drs. E. U. Condon and W. Kauzmann of these Laboratories.

[12] N. R. Trenner, K. Morikawa, and H. S. Taylor, J. Chem. Phys. **5**, 203 (1937).
[13] M. Burton, J. Chem. Phys. **6**, 818 (1938).
[14] H. A. Taylor and M. Burton, J. Chem. Phys. **7**, 572 (1939).
[15] H. H. Voge, J. Chem. Phys. **4**, 584 (1936).
[16] F. O. Rice and K. F. Herzfeld, J. Am. Chem. Soc. **56**, 284 (1934).
[17] F. O. Rice and K. F. Herzfeld, J. Chem. Phys. **7**, 671 (1939).
[18] E. Gorin, J. Walter, and H. Eyring, J. Am. Chem. Soc. **61**, 1876 (1939).

Note on Statistical Forces

LOUIS GOLDSTEIN
Physics Department, City College, New York, New York
(Received February 24, 1942)

It is shown that a two-particle force acting in coordinate space represents with a very good approximation the apparent coupling in space between two spinless atoms of ideal symmetrical or antisymmetrical assemblies at all temperatures higher than, or equal to, their transition temperature.

THE equation of state of ideal Bose-Einstein (B.E.) or Fermi-Dirac (F.D.) gases above and at their transition temperature, described by the sum of an infinite series of virial coefficients, corresponds to one of the several aspects of the statistical forces acting between the spinless point atoms forming these gases. In non-ideal classical gases, in whose Hamilton function the kinetic energy is the sum of the individual kinetic energies of the atoms, and the potential energy is the sum of two-particle or two-atom interaction energies, the equation of state is described also[1] by an infinite series of virial coefficients. Assume then for a moment that the virial coefficients of the ideal quantum gases are, from the third one on, all very small in comparison to the first and second virial coefficients. If, moreover, the ratio

$$\rho(T)=|\sum_{k\geq 3}^{\infty}\Phi_k(T)|/|\Phi_2(T)|,$$

where Φ_k denotes the kth virial coefficient at temperature T, were also a small number, then it would appear justified to search for such a two-atom interaction energy which, when introduced into the Hamilton function of a classical ideal gas, would lead to the exact first and second virial coefficients of the ideal quantum gases without leading to exact values of the small negligible virial coefficients of order higher than the second. Such a two-particle interaction taking place in coordinate space could then be regarded as representing, with a very good approximation, the actual forces existing in space between the atoms of these gases by virtue of their respective symmetry in phase space.

These forces have already been derived[2] incidentally by simply identifying the approximate relative probability densities in configuration space of the quantum gases of spinless atoms with that of a classical non-ideal gas having the type of Hamilton function just mentioned, namely, with the total potential energy represented by the sum of two-particle interaction energies depending on the distance of the coupled atoms. It seemed interesting, however, to rediscuss shortly these forces, in particular, in the B.E. case, around the transition temperature of the quantum gases. We should like to show that these statistical forces represent with a good approximation the apparent interaction, in coordinate space, of the atoms of these ideal quantum gases at all temperatures $T\geqslant T_0$, T_0 being the transition temperature of the gases. A rough but reasonable estimate of these forces can also be given for temperatures $T<T_0$.

Indeed, the conditions indicated above concerning the virial coefficients of the gases, and which justify these statistical forces, are fulfilled for both B.E. and F.D. ideal assemblies of spinless atoms at all temperatures $T\geqslant T_0$.

Consider first the B.E. gas. Since the ratio $\rho(T)$ is a smoothly decreasing function of T, it has to be evaluated at T_0, the transition temperature, where it has the largest value. One finds thus,[3]

$$\rho_{\text{B.E.}}(T_0)=0.0537,$$

which is quite small and indicates that it should be possible to represent with a good approximation the forces of statistical origin acting in coordinate space with a two-particle force.

[1] Cf. J. E. Mayer, J. Chem. Phys. **5**, 67 (1937).

[2] Cf. G. E. Uhlenbeck and L. Gropper, Phys. Rev. **41**, 79 (1932).

[3] The first four virial coefficients have been given by Einstein, Ber. d. Berl. Akad. 3 (1925).

In the case of ideal F.D. gases[4] one finds that

$$\rho_{\text{F.D.}}(T_0)=0.0141,$$

the smallness of which, as compared to $\rho_{\text{B.E.}}(T_0)$, is due in part to the alternating signs of the virial coefficients beginning with Φ_2 which is positive. One finds moreover that even the ratio

$$\tilde{\rho}_{\text{F.D.}}(T_0)=\sum_{k\geq 3}^{\infty}|\Phi_k(T_0)|/|\Phi_2(T_0)|$$

is a small number and a generous estimate of its upper limit appears to be less than 0.030. Here, too, therefore, the approximate two-particle statistical force is entirely justified. This force is only approximate since it does not lead to the exact virial coefficients of all order, giving only the first two correctly. This shows that a two-particle force in coordinate space cannot describe correctly the statistical interaction resulting from the imposed symmetry in phase space of these systems.

The physical meaning of the smallness of the ratios $\rho_{\text{B.E.}}$ and $\tilde{\rho}_{\text{F.D.}}$ corresponds to the fact that the atoms of these ideal quantum gases have practically no tendency to form anything but very small clusters, clusters of single atoms and of pairs of atoms.

The forces in question are[2]

$$V_{\substack{\text{B.E.}\\\text{F.D.}}}(r,T)=-kT\log\left(1\pm\exp-[2\pi(r/\lambda)^2]\right),$$

where k is Boltzmann's constant, r is the separation of two atoms, λ is the de Broglie wave-length associated with their average thermal motion, $\lambda=h/(2\pi mkT)^{\frac{1}{2}}$ the positive and negative signs in the argument of the logarithm correspond, respectively, to the symmetrical and antisymmetrical interaction. $V_{\text{B.E.}}(r)_T$ at constant T is a bell shaped potential energy well; $V_{\text{F.D.}}(r)_T$ resembles the usual repulsive interactions. The discussion of these interactions at constant T as well as the interactions $V_{\text{B.E.}}(T)_r$ and $V_{\text{F.D.}}(T)_r$, with the separation r kept constant, leads without difficulty to the determination of the limitations of the validity of these forces. This discussion will be omitted here. These forces cannot be applied directly at temperatures $T<T_0$ because the method used in their derivation is valid only above T_0. A reasonable estimate below T_0 appears to correspond to a temperature independent force, with T_0 substituted for T and λ_0 for λ in the above expression of these forces. The origin of this estimate lies in the fact that the $V(T)_r$ interactions show a tendency to decrease and vanish with temperature below some temperature $T_m(r)$ depending on r. This trend of the statistical forces has no physical meaning and one is led thus to adopt, below T_0, their expression corresponding to T_0, at least at all those larger distances for which $T_m\leqslant T_0$. At those smaller distances for which $T_m>T_0$, it is this temperature T_m which plays the role of T_0.

Having justified the applicability of the ideal statistical two-particle forces, it seems interesting to compare them directly to forces of another nature acting between particles forming a given system. We should like to compare the inter-atomic force between two helium atoms[5] with the symmetrical statistical two-particle force around the transition temperature in the liquid under its saturated vapor pressure at 2.19°K. It is clear that the force $V_{\text{B.E.}}(r,T)$ is rather a lower limit since it has been obtained with the free particle wave functions. It can be shown now that this free particle statistical force is valid for distances extending from well below the position of the minimum in the inter-atomic force—around 3A—to larger distances. One finds thus that the ideal statistical force is roughly twenty times smaller than the inter-atomic force in quite a large interval of separation around the above indicated position of minimum. One might say here that if B.E. statistics were playing an important role in the peculiar transition effect at 2.19°K, then the more exact liquid wave functions could eventually lead to a two-particle non-ideal statistical force whose order of magnitude would be nearer to that of the inter-atomic force. No definite conclusion can naturally be based upon the preceding comparison between the two forces as to their relative importance. Nevertheless, the above ratio of twenty appears quite large. It should be remembered, on the other hand, that no matter how small the statistical

[4] The numerical values of F. D. functions given by J. McDougall and E. C. Stoner, Phil. Trans. **237**, 64 (1938) were used here.

[5] Cf. J. C. Slater and J. G. Kirkwood, Phys. Rev. **37**, 682 (1931).

force is compared to the inter-atomic force it assures an Einstein transition. The preceding comparison seems to indicate that a treatment of the non-ideal helium gas on the basis of the ideal B.E. fluid, where the non-ideal character, i.e., the inter-atomic force, is considered as a perturbation, cannot well be justified. The treatment where the non-ideal classical fluid is taken as the zero-order approximation, and where the symmetry in phase space would be considered as a perturbation, might lead to more plausible results.

Similar results have been obtained recently[6] through detailed and laborious studies on the theory of the second virial coefficient of helium at low temperatures.

[6] Cf. J. De Boer and A. Michels, Physica **9**, 409 (1938) and also B. Kahn, Dissertation, Utrecht (1938).

MAY, 1942 JOURNAL OF CHEMICAL PHYSICS VOLUME 10

The Photolysis of Persulfate*

LAWRENCE J. HEIDT
Research Laboratory of Physical Chemistry, Massachusetts Institute of Technology, Cambridge, Massachusetts

(Received January 13, 1942)

The photochemical efficiency, ϕ, for the decomposition of persulfate by light of $\lambda 254$ mμ is determined by comparison with ϕ for the uranyl oxalate actinometer. The persulfate content was followed by the method of Kurtenacker and Kubina and in representative cases the hydrogen ion produced also was determined. The equation $S_2O_8^{=}+H_2O+h\nu=2HSO_4^{-}+O_2/2$ accounts quantitatively for the data. Evidence is given to show that the main reaction is not the decomposition of SO_4^{-}. Six tenths of a mole of persulfate is decomposed per Einstein absorbed by persulfate in dilute neutral and alkaline solutions when all oxidizable material is absent. Acetic acid increases this yield to unity but non-oxidizable ions have a depressing effect. Many of the observations of Morgan and Crist also are verified. At constant ionic strength, ϕ remains nearly unchanged in alkali, but drops abruptly to less than 0.01 when solutions are acidified suggesting the formation of a weak acid containing photochemically inert persulfate. Absorption spectra and conductivity measurements, however, give no indication that such a weak acid is formed. The explanation offered for these facts is that the hydrogen ion associates with and thereby stabilizes the persulfate ion after the latter absorbs a photon. The stabilizing effects of other ions, except perhaps bisulfate, is much less than hydrogen which is thought to be related, among other things, to their larger size. Hydrogen peroxide was not found in any of the solutions.

ULTRAVIOLET light of $\lambda 254$ mμ decomposes colorless aqueous solutions of persulfate, the reaction $H_2O+S_2O_8^{=}+h\nu=2HSO_4^{-}+O_2/2$ accounting quantitatively for the increase in acidity accompanying the loss of persulfate[1] as found in experiments 9c and 12 summarized in Table I and in the text under H^+ ion yields.

Crist[2] precipitated the liberated sulfate as the barium salt and found it corresponded to the loss of one mole of persulfate per Einstein absorbed at $\lambda\lambda 302$, 265, and 254 mμ by $0.05M$ $K_2S_2O_8$ when the solution undergoing photolysis was alkaline or had not been acidified. The presence of electrolytes decreased[1–4] the photochemical efficiency, ϕ, sulfuric acid being especially effective.

Since this work, Kurtenacker and Kubina[5] have improved greatly the method for determining persulfate. Their method as used in this research gives values for ϕ about 0.6 as large as

* Contribution from the Research Laboratory of Physical Chemistry, Massachusetts Institute of Technology, No. 493.

[1] J. L. R. Morgan and R. H. Crist, J. Am. Chem. Soc. **49**, 960 (1927) mentioned this fact but gave no data.

[2] R. H. Crist, J. Am. Chem. Soc. **54**, 3939 (1932).

[3] J. L. R. Morgan and R. H. Crist, J. Am. Chem. Soc. **49**, 16 (1927).

[4] J. L. R. Morgan and R. H. Crist, J. Am. Chem. Soc. **49**, 338 (1927).

[5] A. Kurtenacker and H. Kubina, Zeits. f. anal. Chemie **83**, 14 (1930).

those published by Crist.[2] Ammonium, potassium, and sodium persulfates give practically the same results. Most of the work was done on the very soluble sodium salt (at least 2 F.W. dissolve per liter at 25°) because solutions could be made concentrated enough to absorb all but a negligible part of λ254 mμ before it could reach the stirrer.

EXPERIMENTAL WORK

The ammonium, potassium, and sodium persulfates were recrystallized specimens of the best commercial products. The crystals were formed usually from alkaline solutions at less than 35° by evaporation of the colorless mother liquors to 50–70 percent solids. The white crystals were stored in the dark in a vacuum over anhydrone. When added to water, they cooled the solution.

The fresh air dried ammonium salt was found to be a dihydrate by analysis for persulfate. Some of it after standing in a vacuum was used in experiment 1 where it still contained 1.6 moles of water per mole of persulfate. The other persulfates were anhydrous even when only air dried.

A blue crust formed on the crystals of sodium persulfate when allowed to dry in air while in contact with alkali. The phenomenon was reversible so that solutions of the material were colorless. However, when all alkali was washed from the colorless sodium persulfate crystals before they were allowed to dry, they remained colorless on drying and did not change on standing out of direct sunlight. The reflection spectrum of the blue compound is being investigated.

Uranyl oxalate and sulfate and the oxalic acid used in the actinometer were air dried, recrystallized specimens stored in the dark. The other chemicals were of analytical reagent or C.P. quality. Solutions were made with distilled water of pH ~6.

The apparatus and part of the *experimental procedure* have been described.[6] A shutter of stainless steel tubing was used as it corroded less in tap water than the aluminum shutter formerly used.[6a]

The actinometric procedure was like that described.[7] The actinometer contained per liter 0.0017 mole of uranyl *oxalate* and 0.0040 mole of oxalic acid. It gave the same value for ϕ at λ254 mμ as the one 0.001M in uranyl *sulfate* and 0.0067M in oxalic acid.[6b] Photolysis in the actinometer was held, by varying the time of photolysis, to correspond to about 2.5 g of permanganate titer for all values of the light intensity.

The volume of the irradiated solution was always 11 ml measured at 26±1°. All the photochemical experiments were conducted at fairly constant temperature in the range 10 to 21°. A variation of 10° was found to be without measurable effect on the results.

Analyses for persulfate were made at 26±1°. They differed in detail somewhat from that published[5] and several additional precautions were taken. All solutions were weighed to 1 mg. Ferrous ion was added only to acid solutions.

The end-point was determined by electrometric titration using apparatus and a procedure described elsewhere.[8] The bulb was omitted from A in Fig. 1c of that article[8] and the water level in the outer beaker F surrounded the inner beaker E up to the cork ring G. The end-point was always accompanied by a change in color, but it did not shift although the color end-point often faded. It was proved in separate experiments that the evaluation of persulfate was not affected by the ammonium, perchlorate, and the other ions sometimes present.

The ferrous solutions were standardized against permanganate each day they were used. Both solutions were stored in the dark. Permanganate solutions were standardized against Bureau of Standards sodium oxalate at the beginning, about the middle, and at the end of the research and the proper factors at other times interpolated. The latter solutions changed less than 2 percent during the course of the research covering a period somewhat less than a year.

The permanganate used for the analyses for oxalate and persulfate contained, respectively, 0.00183 and 0.0197 formula weight $KMnO_4$ per kg of solution. Some entries in Table I have been adjusted up to 1.5 percent to put them on this basis.

End-points were determined to one drop of permanganate titer independent of the persulfate or oxalate content of the solution titrated. This

[6] L. J. Heidt, (a) Science **90**, 473 (1939), and (b) J. Am. Chem. Soc. **61**, 3223 (1939).
[7] Reference 6b, under column II, p. 3225.
[8] L. J. Heidt, J. Am. Chem. Soc. **61**, 3455 (1939).

TABLE I. Quantum yield, ϕ, measurements. The column headings are explained further in the text.

Expt.	Grams of persulfate in 50 cc at 26±1°	Moles of persulfate per liter found in dark sample	Wt. of a cc at 26±1°	Minutes the persulfate was irradiated	Δg of $KMnO_4$ soln ≃ persulfate photolyzed	% persulfate photolyzed	Δg of $KMnO_4$ soln ≃ oxalate photolyzed per min. in the actinometer	ϕ	Persulfate used if not the sodium salt, and other remarks. Concentrations are given in moles/liter
1 a	0.982	0.0854	1.005	31	1.83	9.5	0.85	0.46	ammonium
b		0.0854		31	1.75		.85	.44	salt
c		0.0854		87	4.12	22.	.85	.37	
d		0.0854		87	4.25		.85	.38	
2 abc	1.355	.099	1.012	40	1.55	7.	.52	.48	K salt
d		.10		29	1.6	8.	.66	.57	K with 0.02NaOH
3 abcd	2.513	.186	1.028	32	2.06	5.5	.77	.57	K with 0.02NaOH
4 abcd	1.192	.10	1.011	22.5	1.27	5.7	.80	.47	
ef		.10		69	3.19	14.	.8	.38	
g		.099		30	1.42	6.4	k		
hi		.099		30	1.37	6.4	k		
jk		.099		1056	2.42	11.3	.025	.60	
l		.099		2977	5.00	23.4	.025	.45	
5 ab	2.198	.185	1.023	15	1.13	2.7	.84	.59	
cd		.185		30	2.06	5.0	.80	.57	
e		.185		60.3	3.46	8.3	.80	.47	
fg		.185		180	7.43	17.8	.84	.33	
6 a	5.525	.464	1.064	45	2.08	2.0	.77	.40	
bc		.464		136	5.25	5.	.79	.34	
7 abc	2.201	.186	1.027	31	2.17[b]	5.3	.82	.58	.02NaOH
de		.186		62	4.05[a]	10	.82	.54	.02NaOH
8 a	2.200	.186	1.028	40	2.08[b]	5.0	.65	.53	0.1NaOH
b		.186		90	4.87[b]	11.7	.65	.55	0.1NaOH
cd		.186		1145	2.18[b]	5.3	.020	.64	0.1NaOH
9 ab	13.200	1.12	1.167	144	7.79[b]	3.07	.62	.59	0.1NaOH
c		1.12		963	21.2[a]	8.4	.63	.24	0.1NaOH
10 abc	2.198	.185	1.065	90	5.57[b]	13.5	.76	.51	1.0NaOH
11 ab	2.200	.186	1.136	65	2.44[b]	5.8	.65	.38	.1NaOH + .9Na_2SO_4
12 ab	2.300		1.143	66.8	1.84[a]	4.0	.69	.27	1.0Na_2SO_4
13 abc	2.205	.187	1.036	50	2.35	5.8	.71	.44	0.08Na_2HPO_4
14 abc	3.202	.271	1.156	76	3.27	5.4	.77	.37	.8Na_2HPO_4
15 abc	2.201	.186	1.129	102	4.44	10.7	.76	.38	1PO_4 at pH6.7
16 ab	2.207	.185	1.119	131	5.80[b]	14.1	.70	.42	1Na_2CO_3
17 abc	2.203	.186	1.075	105	3.46	8.3	.82	.27	1H_3PO_4
18 abc	2.201	.186	1.027	79	3.00	7.1	.84	.31	0.02 $NaHSO_4$
19 abc	2.202	.187	1.035	123	2.00	4.8	.87	.12	.1$NaHSO_4$
20 abc	2.203	.186	1.043	423	4.72	11.4	.83	.09	.2$NaHSO_4$
21 abc	2.203	.185	1.110	415	2.38	5.7	.94	.04	1$NaHSO_4$
22 abc	2.199	.186	1.024	100	3.09	7.4	.80	.26	.02H_2SO_4
23 ab	1.191	.10	1.043	629	3.40	15.5	.81	.00ɔ	.5H_2SO_4
24 ab	5.402		1.145	549	4.4	2.7	.77	.007	.5H_2SO_4
25 ab	2.201	.185	1.081	569	5.5	13.2	.73	.009	1.05H_2SO_4
26 ab	2.20	.187	1.113	127	1.2		.78	.008	1$HClO_4$
27 a	2.231	.188	1.032	5.5	.63	1.5	.80	.97	1$HC_2H_3O_2$
b				60	6.78	16.0	.80	.94	
c				180	18.4	44.0	.81	.86	

uncertainty plus all others amounted to less than ±3 percent in ϕ as can be seen by comparing the values for ϕ obtained in experiments 1 and 5 abcd under corresponding conditions.

Extinction coefficients, $\epsilon = [\log_{10}(I_0/I)]/cd$, where c is in moles per liter and d is in cm. ϵ was measured between 300 and 230 mμ in the same way as k on page 3224 of reference 6b. At 254 mμ,

ϵ for 0.186 molar (M) $Na_2S_2O_8$ equaled 22 compared to 20 obtained by Morgan and Crist[4] for the potassium salt at 0.1 and 0.01M. They found ϵ was not affected by 0.02M sulfuric acid, and in this research ϵ was found to be affected less than 5 percent by 0.52M sulfuric acid.

A depth of 2 cm of the colorless 71 percent perchloric acid, used in experiment 26 to acidify the solution, absorbed less than 5 percent of visible and ultraviolet light down to λ230 mμ.

Quantum yields, ϕ, were calculated as moles of persulfate disappearing per Einstein of λ254 mμ absorbed by the system since the persulfate and particles containing it absorbed all but a negligible fraction of this light. The quantum yield data are summarized in Table I.

Averages are given for separate values of ϕ differing within experimental error but averaging over greater differences in ϕ to conserve space would misrepresent the dependence of ϕ upon the fraction photolyzed.

$\phi = 19.7\phi_a$(Δg of $KMnO_4$ soln equal to the persulfate photolyzed)/1.83 (min. the persulfate was irradiated) (Δg of $KMnO_4$ soln equal to the oxalate photolyzed per min. in the actinometer). ϕ_a is the quantum yield for the actinometer, and was taken as 0.63 at 254 mμ and 25° with a positive ten degree temperature coefficient of 1.03.

Moles of persulfate photolyzed $= 2.5 \times 1.97 \times 10^{-5}$ (Δg of $KMnO_4$ soln equal to the persulfate photolyzed).

Einsteins absorbed per min. $= (2.5/\phi_a)(1.83 \times 10^{-6})$($\Delta g$ of $KMnO_4$ soln equal to the oxalate photolyzed per min.).

The volume of stock solution of persulfate was usually 50 cc and contained the weight of persulfate recorded in Table I. The specific gravities also were determined to obtain the volume of the weighed solutions analyzed, and are recorded in Table I since no data were available in the literature from which to calculate them.

Alongside the weights of persulfates in the 50-cc stock solution are listed the moles of persulfate found per liter in the portion kept in the dark. In every case, except experiment 1, these two quantities are equivalent; hence analyses are internally consistent, the dark reaction is negligible and pure materials were used. In experiment 1, the value 0.0854M instead of 0.1 is caused, as noted above, by the presence of 1.6 mole of water of hydration left in the originally dihydrated ammonium persulfate.

The acetic acid in experiment 27 increased ϕ to unity and thus acts as an oxidizable acceptor for persulfate activated by light. Thus more easily oxidized substances like chloride in acid and cellulose also would be likely to increase ϕ. To avoid their presence, the persulfate solutions and crystals during purification and afterward were allowed to contact only themselves and glass, and especial care was taken to avoid introducing material containing copper, manganese, and silver which are known to catalyze the reduction of persulfate in thermal reactions.

Neither acetic acid nor any of its products of oxidation by persulfate activated by light reduce persulfate in the dark under the prevailing conditions because in the photolyzed solutions in experiment 27 the conc. of persulfate was the same immediately after photolyses as it was after they had stood a day in the dark. The dark reaction in the unphotolyzed samples also was negligible.

The perchloric acid in experiment 26 probably contained some chloride for an initial fast reaction occurred during photolysis until the oxidizable impurities were consumed. The data given in Table I for this experiment represent differences between photolyses in which the fast reaction had been extinguished.

Air does not affect the reaction as was found also by Morgan and Crist.[4] In experiments 1b and d and 4 hi, the solutions were photolyzed under their own vapor pressure all air having been pumped off, yet these experiments gave the same results as the corresponding ones in air, namely, experiments 1a, 1c, and 4g, respectively. In experiments 4g and hi, the *k* signifies that the same average light intensity was used although its absolute value was not determined.

Stirring in the solutions photolyzed under their own vapor pressure was accomplished as follows: A horse-shoe Alnico magnet was rotated by a motor and drove an iron bar attached at right angles to the shaft holding the quartz stirrer. The iron bar and shaft were jacketed with gas tight brass and turned freely with graphite as a lubricant. A glass tube connected the jacket and reaction cell and made gas tight connections through rubber joints. The glass tube contained a side arm fitted with a stopcock, through which

TABLE II. Conductivity measurements showing the additivity of the conductances of sulfuric acid and persulfate. Conductances given equal $100/R$ where R is the observed resistance in ohms. The cell constant was 0.296, and the temp., 25.0°. Solution B contained 6.004 g $Na_2S_2O_8$ in 25 ml which weighed 28.880 g. Values in columns D and E are for an equal volume of water instead of 0.04N H_2SO_4 or B, respectively. Conductances are additive when $A=D+E$.

	A	D (Water instead of acid)	E (Water instead of persulfate)	$D+E$
20 ml of 0.04 N H_2SO_4	3.85	6×10^{-5}		
" " +1 ml B	6.75	3.07	3.70	6.77
+2 ml B	9.01	5.44	3.59	9.03
+3 ml B	10.9	7.47	3.45	10.92
+5 ml B	14.0	10.89	2.20	14.09

the system was evacuated and its pressure determined. Care was taken to pump air from the solution only while stirring vigorously. This prevented boiling over.

Efficient stirring was exhibited by the constancy of ϕ in experiments 3 abcd where the rate of stirring was about doubled, trebled, and quadrupled yet ϕ remained at 0.58 ± 0.03. When stirring was slower ϕ dropped to 0.42, varying from 0.35 to 0.44. This drop in ϕ is probably caused in part by the local accumulation of hydrogen ions in the zone absorbing most of the actinic light. The same cause is also at least partly responsible for the low values for ϕ in experiment 6; also the increase in ϕ as the light intensity was decreased as observed in experiments 4 jh and l and possibly even in the otherwise alkaline solution in experiment 8 cd.

Correction for loss of solvent by evaporation was made by determining the loss in weight of the solution during an experiment. In no case, did this exceed 2 percent of the original amount of solvent and was negligible when gas was not pumped from the solution.

The evolution of oxygen during photolysis was exhibited by an increase in the pressure of the colorless vapor in equilibrium with the system when made gas tight. No corresponding increase in pressure occurred in the dark.

Tests for peroxide were made with titanium sulfate and vanadic acid. In experiments 23 and 24 no peroxide was found in the photolyzed or dark samples although positive tests were obtained when a drop of 3 percent hydrogen peroxide was added. Neither could any peroxide be detected by titration with permanganate under conditions where the permanganate would have been bleached by hydrogen peroxide but not by the persulfate.

The H^+ *ion yield* was determined by titration with 0.025N sodium hydroxide and 0.011N sulfuric acid using phenolphthalein as the indicator. In experiment 9 c, 5 ml of the dark and photolyzed samples were neutralized, respectively, with 44 ml of the acid and 16.5 ml of the base. This gives 1.97 milli-equivalents of acid liberated in the photolysis corresponding to the loss of 2.09 milli-equivalents of $Na_2S_2O_8$. The corresponding milli-equivalents in experiment 12 were 0.187 and 0.181.

In experiments 7–12, and 16, the superscripts attached to some of the values in the borderline cases mean that the solution was acidic, a, or basic, b, at the end of the photolysis.

*p*H *measurements* also were made. The glass electrode gave 2.2, 1.9, 1.7, and 1.5 for the final *p*H of the solutions after photolysis in experiments 5 ab, cd, e and fg, respectively, and 2.7 for that of the freshly prepared dark samples for experiments 5 and 6. These *p*H values although showing the correct trend are doubtless too low because bromthymol blue indicated a *p*H of 6.8, about that expected, for 4.79 g $Na_2S_2O_8$ (compared to 2.2 g in experiment 5 and 5.53 g in experiment 6) in enough water to make 50 cc of solution at 25°. *p*H values obtained with the quinhydrone as well as the chloranil (plus its hydroquinone) electrode were even lower than those obtained with the glass electrode, e.g., they indicated negative values for the *p*H of 0.33M sodium persulfate.

Conductivity measurements were made with student type apparatus kindly put at my disposal by Professor Dietrichson of this laboratory. The measurements are summarized in Table II.

DISCUSSION

Ammonium, potassium, and sodium persulfates give practically the same results when conditions are otherwise similar as is evident by comparing experiment 1 a with 2 abc and 4, and experiments 3 abcd with 5 cd. The value of 0.58 ± 0.02 for ϕ is, however, less than the previously reported value of unity[2] for 0.05 formal $K_2S_2O_8$.

The difference cannot be due to the dark reaction for in both researches this was negligible.

The effect of H^+ ion is to smother ϕ in a way similar to that suggested by the kinetic studies of Morgan and Crist.[1,3,4] These ions progressively decreased ϕ in experiments 5 and 17 through 26 from 0.6 in dilute neutral and alkaline solution to less than 0.01 when the total hydrogen ions exceeded those of persulfate. This is the primary reason that ϕ is less than 0.58 in experiments 1, 2, 4, and 5 efg in which experiments no alkali was present to neutralize the hydrogen ions produced by the photolysis; in experiments 5 abcd the fractions decomposed were small so that the effect of hydrogen ion concentration on ϕ was negligible.

The decrease in ϕ as the acidity increases suggests the formation of a weak acid containing photochemically inert persulfate. If the weak acid is $HS_2O_8^-$, the photochemical data give it a dissociation constant about 10^{-4}; however, the conductivity measurements suggest that its presence is improbable. Hydrogen ions furnished by sulfuric acid in experiments 23–25 and by perchloric acid in experiment 26 appear to be equally effective in decreasing ϕ, but the low values for ϕ in experiments 18, 19, and 22 imply also a specific effect of bisulfate; otherwise, e.g., in experiment 18, ϕ could hardly have been halved when there was less than one H^+ for five persulfates unless mixing was inadequate. The effects upon ϕ of $H_2PO_4^-$, $HPO_4^=$, $PO_4^{\equiv}$, $SO_4^=$, $CO_3^=$, and OH^- ions in themselves are much less than that of hydrogen ion because ϕ in experiments 10 through 16 is seen to have remained above half of 0.6, when the *p*H was greater than 5, although the concentrations of some of these ions had been increased to over five times the persulfate. Similar remarks can be made concerning the positive ions Na^+, K^+, and NH_4^+.

MECHANISM

The structure of the persulfate ion revealed by x-ray data[9] suggests a cause for the observations recorded above. The ion consists of two SO_4^- tetrahedrons held together by one single homopolar bond between two oxygen atoms at one corner of each of the two tetrahedrons. This structure is electrically unstable and should be stabilized by a positively charged particle especially if small enough to wedge between its parts and ought then to form a complex such as the weak acid suggested by the photochemical data. This must occur, however, only after the persulfate ion has been opened by the absorption of an actinic photon because neither the absorption spectra cited nor the conductivity measurements given in Table II indicate any association between any positive ion and persulfate in its compact normal or *thermally* excited state. In fact the rate of the thermal reaction is known to be increased by adding acid. On the other hand, the rapid decrease in ϕ is not caused by the onset of the production of hydrogen peroxide for none could be found.

The decomposition of SO_4^-, namely, $H_2O + SO_4^- + h\nu = HSO_4^- + OH$, followed by $OH + OH = H_2O + (O)$ and $(O) + (O) + M = O_2 + M$ where M in any third body cannot be responsible for the main reaction giving the quantum yield of 0.6. If SO_4^- were the initial reactant, ϕ as calculated could not exceed 0.5 unless there were subsequent reactions involving SO_4^- which would have increased ϕ with the persulfate concentration. Such an increase in ϕ does not occur as can be seen by comparing experiments 7 ab and 8 ab with 9. Moreover, the products of the reaction $OH + OH = H_2O + (O)$ should give way to the production of some H_2O_2 in acid solution and thereby lower the measured ϕ but no H_2O_2 was found although ϕ was lower. The near independence of ϕ upon temperature also makes improbable any reactions requiring thermal activation.

The main reactions responsible for the quantum yield of 0.6, therefore, probably are $H_2O + S_2O_8^= + h\nu = 2HSO_4^- + (O)$ followed by $O + O + M = O_2 + M$.

The increase in ϕ to unity by acetic acid in experiment 27 suggests that yields of less than unity are due to reformation of persulfate in the absence of an oxidizable acceptor or the presence of an environment inhibiting the separation of the primary photochemical fragments or both. These hypotheses I plan to test in the near future by a systematic study of the effects upon ϕ of ionic strength and ions like cupric, manganous, and silver which act as positive catalysts when persulfate acts as an oxidizing agent.

[9] R. C. Evans, *Crystal Chemistry* (Cambridge University Press, New York, 1939), p. 253, and R. C. L. Zachariasen and W. H. Mooney, Zeits. f. Krist. **88**, 63 (1934).

Statistical Mechanics of Binary Mixtures

T. ALFREY* AND H. MARK
Brooklyn Polytechnic Institute, Brooklyn, New York
(Received November 12, 1941)

The configurations of a binary mixture are described by specification of the occupants of a reference set of lattice point pairs, rather than by specification of the occupants of each individual lattice point. If the total interaction energy can be expressed as the sum of terms due to nearest neighbor pairs, the configurational partition function can be derived directly.

CONSIDER an N point lattice, filled with N_a molecules of type A, and N_B molecules of type B. Each molecule in the lattice is surrounded by z nearest neighbors, so that altogether, there are $(Nz/2)$ pairs of nearest neighbors in the lattice. The usual assumption is made that the total interaction energy can be expressed as a sum of nearest neighbor contributions.

If M_{AA}, M_{AB}, and M_{BB} represent the number of AA contacts, AB contacts, and BB contacts, respectively, $M_{AA}+M_{AB}+M_{BB}=(Nz/2)$, and the configurational energy can be written, for the configuration c, as

$$E_c=\epsilon_{AA}M_{AA}+\epsilon_{AB}M_{AB}+\epsilon_{BB}M_{BB}. \quad (1)$$

Because of the necessary linear relationship between M_{AA}, M_{AB}, and M_{BB}, this expression can be written simply as:

$$E_c=\epsilon'_{AB}M_{AB}, \quad (2)$$

where the interaction energy is referred to that of the separated components as zero.

The configurational partition function is given by the following expression:

$$\begin{aligned} Z_c&=\sum_c \exp -[E_c/kT] \\ &=\sum_c \exp -[\epsilon'_{AB}M_{AB}/kT] \\ &=\sum_{M_{AB}} \phi(M_{AB}) \exp -[\epsilon'_{AB}M_{AB}/kT], \end{aligned} \quad (3)$$

where $\phi(M_{AB})$ represents the number of distinct configurations which possess M_{AB} contacts of the type $A-B$. The direct evaluation of the function $\phi(M_{AB})$ has presented some difficulty. As a result, the problem of binary mixtures is generally treated in quite another manner—by the use of grand partition functions.

The difficulty of evaluating $\phi(M_{AB})$ lies in the complexity of the relation between the variables used in determining the distinctness of a configuration and those used in calculating the energy of a configuration. In the process of *counting* configurations, each lattice point is considered separately; i.e., the lattice point specifications are the elements of the statistical analysis. However, since the configurational energy is an *interaction* energy, it cannot be expressed as a function of the separate lattice point specifications. The configurational energy is a sum of terms, each of which depends upon the simultaneous specification of two *different* lattice points.

It is, therefore, proposed to describe each configuration by specifying the occupants of a certain set of pairs of lattice points. Such a description must, of course, result merely in a reclassification of the set of $(N!/N_A!N_B!)$ lattice configurations.

Consider the N numbered lattice points to be made up of a set of $(N/2)$ numbered pairs of nearest-neighbor lattice points, in such a way that each lattice point belongs to one and only one pair. If the point lattice is now filled with molecules, the $(N/2)$ pairs will be of three kinds —AA, AB, and BB. We introduce a parameter X, defined as the number of AB pairs among the reference set of $(N/2)$ lattice point pairs.

The number of AA pairs in the reference set is obviously $(N_A/2-X/2)$, and the number of BB pairs is $(N_B/2-X/2)$.

For a particular value of the parameter X, the number of distinct configurations can be obtained in the following way: The number of ways of arranging X indistinguishable elements of one type, $(N_A/2-X/2)$ elements of a second type, and $(N_B/2-X/2)$ elements of a third type, among $(N/2)$ different places, is given by the

* Monsanto Chemical Company Research Fellow.

following expression:

$$\frac{(N/2)!}{X!\left(\frac{N_A}{2}-\frac{X}{2}\right)!\left(\frac{N_B}{2}-\frac{X}{2}\right)!}. \tag{4}$$

However, since there are two distinct ways of arranging each $A-B$ pair within its reference position, the total number of distinguishable molecular configurations corresponding to a given value of X is given by:

$$\phi(X)=\frac{(N/2)!2^X}{X!\left(\frac{N_A}{2}-\frac{X}{2}\right)!\left(\frac{N_B}{2}-\frac{X}{2}\right)!}. \tag{5}$$

The total number of distinct configurations must, of course, be the same, regardless of how they are specified.

$$\sum_X \phi(x)=\frac{N!}{N_A!N_B!}. \tag{6}$$

The assumption is now made that the *total* number of AB contacts in a given configuration is given accurately by zX. This will be true for the overwhelming majority of configurations.

$$E_c=\epsilon'_{AB}\cdot z\cdot X. \tag{7}$$

The configurational partition function Z becomes:

$$Z=\sum_X \frac{(N/2)!2^X \exp -[\epsilon' zX/kT]}{X!\left(\frac{N_A}{2}-\frac{X}{2}\right)!\left(\frac{N_B}{2}-\frac{X}{2}\right)!}. \tag{8}$$

$\bar{X}$, the most probable value of X, can be obtained by maximizing the log of the function within the sum, using Stirling's approximation.

$$0=\frac{\partial}{\partial X}\left[\frac{N}{2}\ln\frac{N}{2}+X\ln 2-\frac{\epsilon'_{AB}\cdot z\cdot X}{kT}-X\ln X-\left(\frac{N_A}{2}-\frac{X}{2}\right)\ln\left(\frac{N_A}{2}-\frac{X}{2}\right)-\left(\frac{N_B}{2}-\frac{X}{2}\right)\ln\left(\frac{N_B}{2}-\frac{X}{2}\right)\right], \tag{9}$$

$$0=\ln 2-\frac{\epsilon'_{AB}z}{kT}-\ln\bar{X}+\frac{1}{2}\ln\left(\frac{N_A}{2}-\frac{\bar{X}}{2}\right)+\frac{1}{2}\left(\frac{N_B}{2}-\frac{X}{2}\right), \tag{10}$$

$$\bar{X}^2=(N_A-\bar{X})(N_B-\bar{X})\exp -[2\epsilon_{AB}z/kT]. \tag{11}$$

Solving for $\bar{X}$, we obtain:

$$\bar{X}=(N_A+N_B)\cdot\frac{-1+\left[1+\frac{4N_AN_B}{(N_A+N_B)^2}\cdot\exp\left[2\epsilon'_{AB}z/kT\right]\right]^{\frac{1}{2}}}{2(\exp\left[\epsilon'_{AB}z/kT\right]-1)}. \tag{12}$$

This is similar in form to the value reported by Rushbrooke.[1] If we assume that the sum in (8) can be replaced by its maximum term, the following expression for ΔF_{mixing} results:

$$\Delta F_{\text{mixing}}=-kT\left[\frac{N}{2}\ln\frac{N}{2}+\bar{X}\ln 2-\bar{X}\cdot\frac{\epsilon'_{AB}z}{kT}-\bar{X}\ln\bar{X}-\left(\frac{N_A}{2}-\frac{\bar{X}}{2}\right)\ln\left(\frac{N_A}{2}-\frac{\bar{X}}{2}\right)-\left(\frac{N_B}{2}-\frac{\bar{X}}{2}\right)\ln\left(\frac{N_B}{2}-\frac{\bar{X}}{2}\right)\right]. \tag{13}$$

The authors hope to treat other nearest-neighbor problems by the same general method.

[1] G. S. Rushbrooke, Proc. Roy. Soc. **A166**, 296 (1938).

Letters to the Editor

THIS section will accept reports of new work, provided these are terse and contain few figures, and especially few halftone cuts. The Editorial Board will not hold itself responsible for opinions expressed by the correspondents. Contributions to this section should not exceed 600 words in length and must reach the office of the Managing Editor not later than the 15th of the month preceding that of the issue in which the letter is to appear. No proof will be sent to the authors. The usual publication charge ($3.00 per page) will not be made and no reprints will be furnished free.

The Carbon-Hydrogen Bond Strengths in Methane and Ethane

HOLGER G. ANDERSEN, C. B. KISTIAKOWSKY, AND E. R. VAN ARTSDALEN*
The Department of Chemistry, Harvard University, Cambridge, Massachusetts
April 8, 1942

WE have determined, from the kinetics of the photochemical methane-bromine and ethane-bromine reactions, the activation energies of simple steps which can be used to calculate the upper limits of the binding energies of the systems CH_3–H and C_2H_5–H. Additional research, coupled with highly probable analogies, establishes the absolute bond strength with considerable certainty in the case of methane, and an uncertainty of not more than 2 kcal. for ethane.

The dependence of the photochemical rate of bromination of methane on concentrations, light intensity, and total pressure establishes the following mechanism:

$$\begin{aligned}
&(1)\ Br_2+h\nu &&= 2Br\\
&(2)\ Br+CH_4 &&= CH_3+HBr\\
&(3)\ CH_3+Br_2 &&= CH_3Br+Br\\
&(4)\ CH_3+HBr &&= CH_4+Br\\
&(5)\ Br+Br+M &&= Br_2+M.
\end{aligned}$$

The over-all reaction rate derivable from this chain, and agreeing with the experimental facts, is

$$\frac{d(CH_3Br)}{dt}=\frac{k_2k'I^{\frac{1}{2}}(CH_4)(Br_2)^{\frac{1}{2}}(1/C_{tot})^{\frac{1}{2}}}{1+k_4(HBr)/k_3(Br_2)},$$

where I is the incident light intensity, k' a non-temperature-dependent apparatus constant, and C_{tot} the total concentration of all gases. The exact similarity with the hydrogen-bromine reactions, investigated by the Bodenstein school, will be noted; indeed, the bond strength derivation is modeled after that of the H−H bond, as described in detail by Bodenstein and Jung.[1]

The temperature dependence of the over-all rate, which is clearly ascribable to reaction (2), is such that E_2, the activation energy, is 17.8 kcal. Since the energy change in a simple reaction is equal to the difference in activation energies, we have

$$\begin{aligned}
CH_4+Br=CH_3+HBr \quad & -(17.8-E_4)\text{ kcal.}\\
HBr=H+Br \quad & -85.8\\
\hline
CH_4=CH_3+H \quad & -(103.6-E_4).
\end{aligned}$$

The energy of dissociation of hydrogen bromide is from the best available thermal and spectroscopic data.[2, 3]

The activation energy of (4) is believed to be very small, since it is similar to the reaction of hydrogen atoms with hydrogen bromide, whose activation energy is only about 1 kcal.[4] Its magnitude was nonetheless determined in two independent ways: (a) The temperature variation of inhibition by hydrogen bromide—through step (4)—showed that E_4-E_3 was about 2 kcal., with some uncertainty because the rate is rather insensitive to changes in k_4/k_3. (b) The yield of methane in the photolysis of methyl iodide-hydrogen bromide mixtures, which is attributable to reaction (4), shows that E_4 is about 0.8 kcal. greater than the activation energy of

$$CH_3+I_2=CH_3I+I,$$

which a considerable body of evidence indicates as proceeding on practically every collision. We choose $E_4=1.5\pm1$ kcal. as a sufficiently conservative estimate from these experiments.

Combining this quantity with the maximum, the bond strength becomes 102 ± 1 kcal.

A similar study of the photochemical bromination of ethane gave an activation energy of 13.8 kcal., so that the maximum value here is 13.8+85.8=99.6 kcal. The difference in the activation energies of the corresponding reactions (4) and (5) was zero in this case. No experiments of the type described under (b) were performed, but it is reasonable to assume that E_3 is not much more than 2 kcal. If this is done, the bond strength is, in round numbers, 98 ± 2 kcal. in ethane.

The experimental details, as well as additional theoretical aspects, will be published in a series of papers as soon as the pressure of other work permits.

* Now at Department of Chemistry, Lafayette College, Easton, Pennsylvania.
[1] Bodenstein and Jung, Zeits. f. physik. Chemie **121**, 127 (1926).
[2] Beutler, Zeits. f. physik. Chemie **B29**, 315 (1935).
[3] A. R. Gordon and C. Barnes, J. Chem. Phys. **1**, 692 (1933).
[4] J. C. Morris and R. N. Pease, J. Chem. Phys. **3**, 796 (1935).

Raman Line of Cyanide Ion

GEORGE GLOCKLER AND H. T. BAKER
Department of Chemistry, State University of Iowa, Iowa City, Iowa
April 4, 1942

IN a study involving the force constant of the cyanide ion, we noticed incidentally two lines (838 and 2080 cm^{-1}) mentioned by Hibben.[1] The original experiments were carried out by Pal and Sen Gupta[2] on potassium cyanide solutions. For a diatomic ion only one Raman line should be found. From other compounds containing the cyanide group 2080 cm^{-1} evidently is its frequency. The lower vibration must, therefore, be spurious, either because of the use of an improper excitation line or because of the presence of an impurity. We determined the Raman spectrum of sodium cyanide solutions (Hilger E(2) spectro-

graph, Eastman I-J spectrographic plates, 4358A Hg lines for excitation). We find one line only corresponding to a frequency of 2086.7 ± 2.7 cm^{-1}, as the average of six different measurements. No trace of the lower frequency appears on any of our plates. Further study convinced us that the low vibration is caused by a line of the cyanate ion.[2] Its presence as an impurity in cyanide because of oxidation of the initial material by atmospheric oxygen is readily understood. The force constant of cyanide ion is 1.65 megadynes per cm.

[1] J. H. Hibben, *The Raman Effect and Its Chemical Applications* (Reinhold Publishing Corporation, New York, 1939), Table 90, p. 453.
[2] N. N. Pal and P. N. Sen Gupta, Ind. J. Phys. **5**, 13, (1930).

On the Heat of Sublimation of Carbon

G. Herzberg
Department of Physics, University of Saskatchewan, Saskatoon, Saskatchewan
April 13, 1942

On the basis of a theoretical interpretation of the absorption spectra of benzene, butadiene, and hexatriene, Kynch and Penney[1] in a recent paper come to the conclusion that "the weight of evidence in favor of L (heat of sublimation of carbon) = 170 kcal./mole is overwhelming." Accordingly, they conclude that there is no discrepancy between the dynamically and statically determined heat of sublimation and that the explanation of this discrepancy suggested by Herzberg, Herzfeld, and Teller[2] is unnecessary and unsound. Kynch and Penney have, however, overlooked important published work which, in the writer's opinion, eliminates definitely the value $L = 170$ kcal./mole and only permits values of $L \leqslant 135$ kcal./mole.

A value $L = 170$ kcal./mole would imply, as Kynch and Penney realize, that the heat of dissociation of carbon monoxide $D(CO)$ is 11.111 ev (256.1 kcal./mole).[3] However, Faltings, Groth, and Harteck[4] have shown that carbon monoxide is dissociated by absorption of light of wave-length 1295A (but not of light of wave-length 1470A) with a quantum yield one. This experiment seems to prove that $D(CO) \leqslant 9.57$ ev and therefore that $L \leqslant 135$ kcal./mole. It would at any rate require rather artificial assumptions to account for this photolysis on the basis of $D(CO) = 11.111$ ev. Accordingly, the apparent agreement obtained by Kynch and Penney between the long wave-length limits of the observed absorption spectra of benzene, butadiene, and hexatriene with those calculated on the basis of $L = 170$ kcal./mole seems to be due to a chance coincidence.

In addition to this apparent agreement, Kynch and Penney give some further evidence which, in their opinion, supports $L = 170$ kcal./mole. They say that the old Birge-Sponer extrapolation of the vibrational levels of the ground state of CO leads to 11.34 ev for $D(CO)$ in good agreement with their adopted value (11.054 ev). However, it is now well known that for almost all diatomic molecules in their ground states the linear extrapolation of the first vibrational quanta gives a value for D_0 that is 20–40 percent too high. If anything, therefore, the vibrational levels are in favor of the lower $D(CO)$ value.

Furthermore, Kynch and Penney refer to the work of White[5] who found the heat of dissociation of C_2N_2 into 2CN to be 6.33 ev by measuring the equilibrium concentration of CN in C_2N_2. This value for $D(C_2N_2)$, on the basis of thermochemical equations and with $D(CO) = 11.111$ and 9.144 ev, leads to $D(CN) = 6.43$ and 4.46 ev, respectively. The smallness of the latter value is taken as evidence against $D(CO) = 9.144$ and $L = 170$ kcal./mole. However, White's $D(C_2N_2)$ value seems to be open to serious objection since it is about equal to or larger than $D(CN)$. Even considering the resonance between the single and triple bonds in C_2N_2 one would certainly expect that the energy required to break the C−C bond in C_2N_2 is appreciably smaller than the energy required to break the C≡N bond. If one accepts White's value for $D(C_2N_2)$, that is, admits a failure of valence theory for as simple a molecule as C_2N_2, it seems one could not expect a quantitative agreement of calculations based on this theory with experiment for such complicated molecules as butadiene, hexatriene, and benzene. If any such agreement is obtained it would appear to be fortuitous.

It may be mentioned that White's results disagree strongly with the earlier low dispersion work of Kistiakowsky and Gershinowitz[6] who obtained the very reasonable value $D(C_2N_2) = 77$ kcal./mole. At any rate it appears that White's determination of $D(C_2N_2)$ is much less direct and more subject to errors than the determination of an upper limit of $D(CO)$ by observing its photo-dissociation.

Finally, Kynch and Penney refer to the considerations of Baughan[7] who considers the difference between the heat of removal of the first H atom from CH_4 (103.6 kcal.) and the average C−H bond strength (87.3 kcal.), as obtained from $L = 124$ kcal. and the heat of formation of CH_4, as evidence against the low value of L. He finds that with $L = 169$ kcal. one obtains an average C−H bond energy of 98.6 kcal. which is almost equal to the heat of removal of the first H atom. However, the energy of dissociation of CH is known to be 80.0 kcal.[8] showing that considerable differences between the heats of removal exist (as it does also for H_2O). Hence there does not appear to be any difficulty from this angle in adopting a low value for L. Rather the opposite is the case.

The discussion of the mechanism of the sublimation of graphite by Herzfeld, Herzberg, and Teller[2] was meant as a possible explanation, not (as Kynch and Penney seem to think) as supporting evidence for the discrepancy between Marshall and Norton's L (obtained from rates of evaporation of carbon in vacuum) and the equilibrium L obtained from the spectrum. But later unpublished work by Johnston and Marshall[9] seems to confirm this explanation since an exceedingly small accommodation coefficient was found for carbon atoms on graphite. Johnston and Marshall have also shown that Bassett's[10] determination of the triple point of carbon is only compatible with a low (equilibrium) value for the heat of sublimation.

A great deal of work on the ionization and dissociation of CO, CH_4, and other molecules by Tate and his coworkers also seems to rule out $D(CO) = 11.144$ ev and favor $D(CO) \sim 9.6$ ev [see, for example, Hagstrum and Tate].[11]

From all this it seems to follow that the weight of

evidence is strongly *against* $L=170$ kcal./mole. The heat of dissociation of CO is in all probability smaller than 9.57 ev and therefore the heat of sublimation of carbon is smaller than 135 kcal./mole. Which of the various values compatible with this conclusion is the correct one is not as yet certain, but the writer still feels that the values suggested in his review:[3] $D(\mathrm{CO})=9.144$ ev, $L=124.8$ kcal./mole are the most likely ones.

[1] G. J. Kynch and W. G. Penney, Proc. Roy. Soc. **A179**, 214 (1941).
[2] G. Herzberg, K. F. Herzfeld, and E. Teller, J. Phys. Chem. **41**, 325 (1937).
[3] Kynch and Penney give the value 11.054 ev which is the value given in the author's review [Chem. Rev. **20**, 145 (1937)] based on the old conversion factors. They state erroneously that the possibility of this value was not considered by the writer.
[4] K. Faltings, W. Groth, and P. Harteck, Zeits. f. physik. Chemie **B41**, 15 (1938).
[5] J. U. White, J. Chem. Phys. **8**, 459 (1940).
[6] G. B. Kistiakowsky and H. Gershinowitz, J. Chem. Phys. **1**, 432 (1932).
[7] E. C. Baughan, Nature **147**, 542 (1941).
[8] See G. Herzberg, *Molecular Spectra and Molecular Structure* I. *Diatomic Molecules* (New York, 1939).
[9] I am greatly indebted to Professor H. L. Johnston for informing me of these results in advance of publication.
[10] J. Bassett, Comptes rendus **208**, 267 (1939); J. de phys. et rad. **10**, 217 (1939).
[11] H. D. Hagstrum and J. T. Tate, Phys. Rev. **59**, 354 (1941).

Note on the Theory of Fusion

JOHN G. KIRKWOOD AND ELIZABETH M. BOGGS
Department of Chemistry, Cornell University, Ithaca, New York
April 1, 1942

IN conversations with some of our colleagues concerning the theory of fusion, the question has arisen whether the distribution function $\rho_1(\mathbf{R})$, defined by us in a recent article,[1] can represent a non-uniform density distribution with the period of a specified space lattice or whether, even in a crystalline phase, it must have the constant value unity everywhere. The arguments for the latter alternative, can, we believe, be disposed of by imposing several rather trivial restraints on the system of molecules comprising the crystalline phase. Although these restraints were not explicitly stated in our definition of $\rho_1(\mathbf{R})$, they are implicit in our solution of the integral equation satisfied by this distribution function. It is the purpose of this note to state them in explicit form.

It is true that the partition function of a system of N molecules subject only to intermolecular forces fails to converge. Convergence is realized only when the system is subjected to external forces from the walls of a closed envelope. The potential barriers at the envelope surface are implicit in all calculations of the classical partition function in which the configuration space accessible to each molecule is limited to the finite volume v of a containing vessel. If not only the volume of the envelope, but also its form, position, and orientation are prescribed, the question of the coordinate system to which $\rho_1(\mathbf{R})$ is referred to is relieved of any ambiguity. It is to be a coordinate system fixed in orientation and position relative to the envelope.

If only the volume v of the envelope is prescribed, there is at first glance a certain ambiguity in the definition of $\rho_1(\mathbf{R})$ arising from the invariance of the potential of intermolecular force to translations and rotations of the system of molecules as a whole, and, therefore, an invariance under these operations of the phase integrals defining $\rho_1(\mathbf{R})$. There are thus six coordinates, which are given a random distribution in configuration when we calculate the partition function by statistical mechanics. We may conveniently choose these coordinates as the position $\mathbf{R}_0$ of the center of gravity of the system of molecules, and the angles specifying the orientation of the principal axes of the moment of inertia tensor $\mathbf{I}$.

$$\mathbf{R}_0=\frac{1}{M}\sum_{i=1}^{N} m_i\mathbf{R}_i$$
$$\mathbf{I}=\sum_{i=1}^{N} m_i\mathbf{R}_i\mathbf{R}_i \qquad (1)$$
$$M=\sum_{i=1}^{N} m_i.$$

If we impose the trivial restraints of constancy of the position $\mathbf{R}_0$ of the center of gravity and constancy of the moment of inertia tensor $\mathbf{I}$ relative to a conveniently chosen external coordinate system, all ambiguity in the definition of $\rho_1(\mathbf{R})$ in this system of coordinates appears to be removed. In physical terms, these restraints mean that we fix the position and orientation of the crystal by imposing suitable external forces. If such forces are not imposed, the periodic density distribution of a perfect crystal would, of course, be blurred into a uniform density distribution by rotatory and translatory Brownian motion of the crystal as a whole. To say that for this reason an equilibrium crystal cannot have a periodic density distribution relative to an exterior corrdinate system is a quibble which results from blindly carrying out all operations of summation in the partition function without taking proper account of their physical significance. Except for the limitations of the indeterminism principle, which are not important here, rotatory and translational Brownian motion of the crystal could in principle be suppressed completely by suitable external forces, and this is all that is necessary for our purposes. The use of the impermeable envelope could be avoided by applying the methods of the grand ensemble to a finite portion of an infinite crystal, without, however, changing the physical content of our conclusions.

A theory of fusion could, of course, be based entirely on an investigation of the distribution function $\rho_2(\mathbf{R}, \mathbf{R}')$ in the space of molecular pairs, leading, in the crystalline phase, to a distribution function $\rho_1(\mathbf{R})$ periodic or uniform depending upon whether the restraint (1) is imposed or not. Such a theory does not appear to be as convenient or satisfactory as that based upon the direct investigation of $\rho_1(\mathbf{R})$. A similar situation arises in the investigation of crystal structure by the x-ray diffraction technique. The intensity distribution in the x-ray photograph of a crystal is actually determined by $\rho_2(\mathbf{R}, \mathbf{R}')$, the distribution function in pair space. However, in analyzing crystal structure with the neglect of thermal disorder, it is customary to factor $\rho_2(\mathbf{R}, \mathbf{R}')$ into $\rho_1(\mathbf{R})\rho_1(\mathbf{R}')$ and to discuss the properties of $\rho_1(\mathbf{R})$. The existence of $\rho_1(\mathbf{R})$ is implied in the operations of the theory of space groups. The utility of the concept of a periodic $\rho_1(\mathbf{R})$ is never questioned here, although its existence in a perfect crystal in equilibrium is subject to restraints of the type of Eq. (1).

[1] J. G. Kirkwood and E. Monroe, J. Chem. Phys. **9**, 514 (1941).